

University of Alberta

**Geology of the Nicola Group in the vicinity of the Iron Mask batholith,
Kamloops, British Columbia**

by

Shawna Elizabeth White

A thesis submitted to the Faculty of Graduate Studies and Research
in partial fulfillment of the requirements for the degree of

Master of Science

Department of Earth and Atmospheric Sciences

©Shawna Elizabeth White

Spring 2010

Edmonton, Alberta

Permission is hereby granted to the University of Alberta Libraries to reproduce single copies of this thesis and to lend or sell such copies for private, scholarly or scientific research purposes only. Where the thesis is converted to, or otherwise made available in digital form, the University of Alberta will advise potential users of the thesis of these terms.

The author reserves all other publication and other rights in association with the copyright in the thesis and, except as herein before provided, neither the thesis nor any substantial portion thereof may be printed or otherwise reproduced in any material form whatsoever without the author's prior written permission.

Examining Committee

Dr. Philippe Erdmer, Earth and Atmospheric Sciences

Dr. Tom Chacko, Earth and Atmospheric Sciences

Dr. Claire Currie, Physics

Abstract

Two regional scale deformation events are observed in the Kamloops region. A Late Triassic-Early Jurassic southwest directed compressional event and a later Tertiary extensional deformation episode, manifested in the uplift of the Nicola horst.

The Nicola horst is bounded to the northeast by the Cherry Creek Tectonic Zone, a northwest striking fault zone that separates schistose footwall rocks of the Nicola horst from relatively undeformed Nicola Group rocks in the hanging wall. The fault is interpreted to have accommodated multiple episodes of movement associated with both compressional and extensional tectonics.

A pervasive metamorphic fabric, exposed in the horst and cross-cut by the 144.8 ± 5.9 Ma LeJeune granodiorite, is interpreted to represent a broad, Middle Jurassic shear zone, formed by east-directed translation of the Nicola arc during contractional tectonics inboard of an east dipping subduction zone. Variations in orientation of the fabric suggest subsequent east-directed compression during post-Jurassic, pre-Eocene deformation.

Acknowledgments

Foremost, I would like to thank my supervisor, Dr. Philippe Erdmer, for providing me with guidance and valuable comments, financial support and an environment in which to work. Thanks is also extended to Dr. Tom Chacko for various valuable discussions in metamorphic petrology and offering words of encouragement toward the completion of the thesis.

Thanks to the employees of Abacus Mining and Exploration for showing us the geology of the AJAX property. A special thanks to Rob Falls of Abacus, for allowing us access to the Ajax property, showing us various cross-sections and company core and for many an interesting discussion on the mysteries of the Kamloops region picrite.

My sincere thanks to the cattle ranchers in the Kamloops region, in particular, George Little, Jacko Ranch and Sugarloaf Ranch for allowing us access to their private properties during the field season. I'd also like to extend a special thanks to Nadia Brummer for her valuable assistance and friendship during the 2007 field season.

I'd like acknowledge Mitch Mihalynuk of the British Columbia Geological Survey for introducing me to the project and offering his expertise in the field.

Dr. Tony Simonetti is acknowledged, having helped a great deal with running the laser ablation system and discussing/interpreting the data I collected.

Andrew Locock is thanked for his helpful discussion on the interpretation of microprobe data and its use in mineral identification. Dr. Murray Gingras and Dr. Brian Jones are acknowledged for their assistance in the interpretation of microfossils and trace fossils. A special thanks to John Waldron for his guidance, support and helpful comments during the final writing stages of my thesis.

I would specially like to thank Jamie Kraft. I cannot thank him enough for the countless discussions and positive support towards the completion of this thesis. Throughout the past 3 years Jamie has become one of my best friends.

Thanks to Mark Labbe, Donny Resultay and David Pirie for going out of their way on multiple occasions in order to rush a section or make sure my sections were polished for the probe. Thanks is also extended to Sergei Matveev for helping me to collect quantitative mineral compositional data and teaching me how to operate the electron microprobe.

I'd also like to acknowledge all the amazing people I have met during my time at the U of A. I'd like to mention in particular: Hilary Corlett, Faye Wyatt, Jamie Kraft, JF Gagnon, Walter Loogman, Micheal Moroskat and Suzy Byron, without whom I would not have had such an amazing graduate student experience. You guys make me smile and constantly remind me just how important good friends are. I'd also like to thank my sister and best friend Diana.

Finally I'd like to thank my parents. There really isn't words that can express how much they mean to me and what they have done for me to help out during my time at the University of Alberta. I therefore feel it most appropriate to just say thank you mom and dad. You know how much I love and appreciate you.

Table of Contents

Chapter 1: Introduction	1
1.1 Introduction	1
1.2 Regional Geology	3
1.3 Location, Access and Topography	8
1.4 Previous Work	8
1.5 Present Work- Methods	12
1.6 References	14
Chapter 2: Stratified and Intrusive Rocks	21
2.1 Introduction	21
2.2 Stratigraphy of Nicola Group Rocks	21
2.2.1 Stratified Rocks	22
Plagioclase > Augite Lithic Tuff and Augite Porphyritic Lapilli Tuff: LTrNfat (1)	22
Plagioclase Porphyritic Flows: LtrNfp (2)	26
Plagioclase Tuff and Lapilli Tuff: LTrNft (3)	27
Heterolithic Augite – Plagioclase Porphyritic Lapilli Tuff and Volcanic Breccia: LTrNafb (4)	29
Interlayered Volcaniclastic and Pyroclastic Rocks: LTrNaps (5)	31
Coarse Augite Porphyritic Flows and Breccia: LTrNap (6)	39
Coarse Augite-Plagioclase Porphyritic Flows and Breccia: LTrNafp (7)	39
Picritic Volcanic Breccia: LTrNop (8)	41
Augite Porphyritic Volcanic Breccias and Laharic Deposits: LTrNvl (9)	44
Nicola Group Sedimentary Facies: LTrNs (10)	46
Undivided Volcanic and Sedimentary Rocks: LTrNu (11)	49
Eocene Kamloops Group: EKav (12)	49

Miocene Basalts: Mivb (13)	52
2.3 Intrusive Rocks Exposed in the Nicola Horst	52
Late Jurassic- Early Cretaceous LeJeune Biotite Granodiorite: ECLgd	53
Hornblende-Biotite Granodiorite (Frogmoore Granodiorite): PFgd	55
2.4 Volcanic Facies and Depositional Environment	55
Intermediate-Source Facies	56
Transitional Aerial to Marine Depositional Environment	57
Distant-Source Facies	58
Marine Depositional Environment	59
2.5 References	60
Chapter 3: Metamorphism	63
3.1 Introduction	63
3.2 Analytical Methods	64
3.3 Rocks South of the Cherry Creek Tectonic Zone: Domain [3]*	64
3.4 Rocks North of the Iron Mask Batholith: Domain [2]*	69
3.5 References	73
Chapter 4: Geochronology of LeJeune Granodiorite	75
4.1 Introduction	75
4.2 Methods and Analytical Techniques	75
4.3 Results	77
4.4 References	80
Chapter 5: Structural Geology	81
5.1 Introduction	81
5.2 Folds and Associated Foliations	81

5.3 Foliated Rocks: South of the Cherry Creek Fault Zone	86
5.3.1 Nicola Group Rocks	86
5.3.2 Foliated Zones within the Frogmoore Granodiorite	93
5.4 Faults and Shear Zones	96
5.4.1 Northwest Striking Fault Zones	96
Cherry Creek Tectonic Zone	96
The Iron Mask Batholith	96
5.4.2 North Striking Fault Zone	97
Clapperton Fault	97
5.4.3 Northeast Trending Faults	97
5.5 Discussion: Three Structural Domains	98
5.5.1 Domain [1] and Domain [2]	98
Boundary Between Domain [1] and Domain [2]	103
5.5.2 Domain [3]	103
Folds	104
5.5.3 Bounding Faults of the Ductily Deformed Footwall	104
5.5.4 Reactivation of the Cherry Creek Tectonic Zone	106
5.6 References	107
Chapter 6: Discussion of Tectonic History	109
6.1 Basement of Quesnellia	109
6.2 Backfolds and Associated Backthrusts	110
6.2.1 Introduction	110
6.2.2 Latest Triassic - Earliest Jurassic Deformation	111
Southwest Vergent Structures: Kamloops Region	112
Sub Jurassic Unconformity	113

Plutonism: Pre-, Syn-, or Post-Deformational?	113
6.2.3 Southwest Vergent Structures: Omineca Belt	117
6.3 Tertiary Deformation	119
Fabrics within the Nicola Horst: A Tectonic Window	124
6.4 References	129
Chapter 7: Conclusions	134
Appendix 1	137

List of Tables

Chapter 2 Tables

Table 2.2.1: Representative microprobe analyses for augite phenocrysts in units LTrNap and LTrNafp.	42
---	----

Chapter 3 Tables

Table 3.3.1a: Representative microprobe analyses of amphibole grains in biotite-amphibole schist unit: Domain [3].	66
--	----

Table 3.3.1b: Representative microprobe analyses of plagioclase grains in biotite-amphibole schist unit: Domain [3].	67
--	----

Table 3.4.1a: Representative microprobe analyses of amphibole grains in meta-sediments of the Dome Hills succession: Domain [2].	71
--	----

Table 3.4.1b: Representative microprobe analyses of plagioclase grains in meta-sediments of the Dome Hills succession: Domain [2].	71
--	----

Chapter 4 Tables

Table 4.3.1: Summary of data collected from 6 analyses on 4 zircon grains in a sample of unit ECLgd.	78
--	----

List of Figures

Chapter 1 Figures

- Figure 1.1.1: Location of the Iron Mask batholith and associated porphyry deposits . 2
- Figure 1.2.1: Terrane map of the Canadian Cordillera. 4
- Figure 1.4.1: Location of study areas from previous work. 13

Chapter 2 Figures

- Figure 2.1.1: Geological map of the Nicola Group in the vicinity of the Iron Mask batholith (map inset: back of thesis) 138
- Figure: 2.2.1: Cross-section A-A' (on Figure 2.1.1) 23

Chapter 3 Figures

- Figure 3.3.1: P-T diagram showing principle metamorphic facies for metabasite rocks. 68

Chapter 4 Figures

- Figure 4.3.1: Tera-Wasserburg diagram displaying concordia age of unit ECLgd. 79

Chapter 5 Figures

- Figure 5.2.1: Stereonet showing pole-to-bedding measurements within Nicola Group rocks: Domain [1]. 82
- Figure 5.2.2: Stereonet showing density plot of pole-to-bedding measurements within Nicola Group rocks: Domain [1]. 82
- Figure 5.2.3: Stereonet showing poles-to-bedding measurements within rocks of the Dome Hills succession of the Nicola Group: Domain [2]. 84
- Figure 5.2.4: Stereonet showing cleavage orientation within rocks of the Dome Hills succession of the Nicola Group: Domain [2]. 85
- Figure 5.3.1: Vertical gradient aeromagnetic map of the Iron Mask batholith. 87
- Figure 5.3.2 Stereonet displaying west-northwest striking tectonic fabric: Domain [2]. 87
- Figure 5.3.3: Stereonet showing southeast trending mineral lineations along west-northwest striking foliations: Domain [3]. 89
- Figure 5.3.4: Stereonet showing northwest plunging, tilted folds formed within meta-Nicola Group rocks: Domain [3]. 94

Figure 5.5.1: Location map depicting three northwest trending domains. 99

Chapter 6 Figures

Figure 6.2.1a: Schematic section A-A' depicting latest Triassic-earliest Jurassic deformation. Deformation is post intrusion. Section A-A' on Figure 3.5.1. 115

Figure 6.2.1b: Schematic section A-A' depicting latest Triassic-earliest Jurassic deformation. IMB is intruded pre- or syn-deformation. Section A-A' on Figure 3.5.1. 116

Figure 6.3.1: Geological map of the Nicola horst. 120

Figure 6.3.2: Stereonet displaying a best fit girdle through poles-to-foliation. Data displayed is from this study and that of Moore and Pettipas (1990): Domain [3]. 123

Figure 6.3.3: Stereonet displaying restoration of mineral lineations: Domain [3]. 123

Figure 6.3.4 a,b: (a): Schematic section running east-west through the Nicola horst. 125

List of Photos

Chapter 2 Photos

Photo 2.2.1: Planar laminated, plagioclase bearing tuffaceous sandstone. Unit LTrNfat (1)	25
Photo 2.2.2: Plagioclase lapilli tuff. Unit LTrNft (3)	28
Photo 2.2.3: Augite porphyritic lapilli tuff. Unit LTrNaftb (4)	32
Photo 2.2.4: Mudclasts within volcanoclastic rocks of the Nicola Group. Unit LTrNaps (5)	34
Photo 2.2.5: Picritic basalt. Unit LTrNop (8)	43
Photo 2.2.6: Augite porphyritic volcanic breccia. Unit LTrNvl (9)	45
Photo 2.2.7: Red coloured, plagioclase rich, fine to coarse grained sandstone and siltstone interbedded with volcanic breccia and conglomerate.	45
Photo 2.2.8: Planar laminated mudstone and siltstone of the Dome Hills succession of the Nicola Group. Unit LTrNs (10).	47
Photo 2.2.9: Tectonized augite porphyry.	50
Photo 2.2.10: Tectonized fragmental volcanoclastic rocks.	51
Photo 2.2.11: Miocene vesicular basalt.	51
Photo 2.2.12: Feldspar megacryst within unit ECLgd	54
Photo 2.2.13: Foliation formed in Frogmoore granodiorite phase of the Nicola batholith.	54

Chapter 5 Photos

Photo 5.2.1: Small cm-scale southeast plunging folds formed within the Nicola Group sedimentary rocks: Domain [2].	84
Photo 5.2.2: Cleaved Nicola Group rocks: Domain [2].	85
Photo 5.3.1: Strong stretching lineation defined by stretched augite porphyritic fragments: Domain [3].	89
Photo 5.3.2: Tension gashes formed in deformed Nicola Group footwall rocks south of the Afton tailings pond.	90
Photo 5.3.3: Schistose fabric deflected by ridged aggregates of quartz: Domain [3].	90
Photo 5.3.4: Asymmetric folded veinlets of quartz: Domain [3].	92
Photo 5.3.5: Northwest trending folds located south of the Afton tailings pond.	92

Photo 5.3.6: Northwest trending, chevron folds located south of Rush Lake.	94
Photo 5.3.7: Crenulated tectonic fabric formed in meta-Nicola Group rocks: Domain [3].	95
Photo 5.3.8: Small, meter-wide shear zone within the Frogmoore granodiorite phase of the Nicola batholith.	95

List of Plates

Plate 2.2.1: Augite + plagioclase tuff.	25
Plate 2.2.2: Plagioclase > augite porphyry displaying trachytic texture.	28
Plate 2.2.3: Volcanogenic mudstone and siltstone interbedded with coarser grained, tuffaceous fragments and individual broken crystals of augite.	32
Plate 2.2.4: Coarse grained, heterolithic volcanoclastic.	34
Plate 2.2.5: Small, rounded spheres of diameter ~0.1 mm observed within volcanogenic mudstone and siltstone. Their consistent size and shape suggests a biological origin.	36
Plates 2.2.6 a,b: Adhesive meniscate burrows (AMB).	38
Plate 2.2.7: Hornfelsed augite porphyry. The plate shows augite having been pseudomorphed by actinolite.	40
Plate 2.2.8: Augite + plagioclase porphyry.	40
Plate 2.2.9: Picritic basalt. Note that olivine has been completely replaced by serpentine.	43
Plate 2.2.10: Meta-sediments of the Dome Hills succession of the Nicola Group. The mineral assemblage is indicative of greenschist-amphibolite facies metamorphism.	47
Plate 2.2.11: Volcanic fragments displaying a shape-defined foliation south of the Cherry Creek Tectonic Zone.	50
Plate 3.3.1: Photo displaying amphibolite grade mineral assemblage and metamorphic fabric in hornblende-biotite schist (Sample sw-827).	68
Plate 3.4.1: Photo displaying low-grade metamorphic, mineral assemblage of the Dome Hills succession, Nicola Group (Sample sw-164).	72

Chapter 1: Introduction

1.1 Introduction

The following work investigates the deformation history of Nicola Group rocks in the Kamloops area. The Nicola Group comprises a diverse assemblage of Late Triassic (Preto, 1979; Monger and McMillan, 1984) submarine to subaerial (Lefebure, 1976; Preto, 1979) volcanic, volcanoclastic and sedimentary rocks. The Kamloops region is of particular geological interest due to a strong economic history in mining. The Iron Mask batholith (IMB), located approximately 10 km southwest of Kamloops, is a Late Triassic (Mortensen et al., 1995), composite alkalic intrusion (ie: Lang and Stanley, 1995) and is a source of Cu, Au, and Ag produced from various porphyry deposits (Figure 1.1.1). Late Triassic volcanic rocks of the Nicola Group are host to the various intrusive phases of the IMB, and as such, a detailed structural analysis of these host rocks can lead to not only a better understanding of the structural elements within and tectonic history of the Nicola arc, but also structure within the batholith, and therefore may aid in future mineral exploration.

A two and one-half month field season was completed in the summer of 2007, when detailed geological mapping and sample collection was carried out. Structural and geologic data were collected and compiled with pre-existing data to generate an improved geologic map of the area (Figure 2.1.1: map inset).

The Kamloops region was affected by at least two regional scale deformation events: (1) A Late Triassic-Early Jurassic compressional episode, generating the dominant, northwest trending structural panels that control the map pattern and (2) an Early Tertiary deformation event involving uplift of the Nicola horst in an extensional environment. A pervasive tectonic fabric formed within meta-Nicola Group rocks exposed in the Nicola horst may represent a broad Middle Jurassic shear zone that has

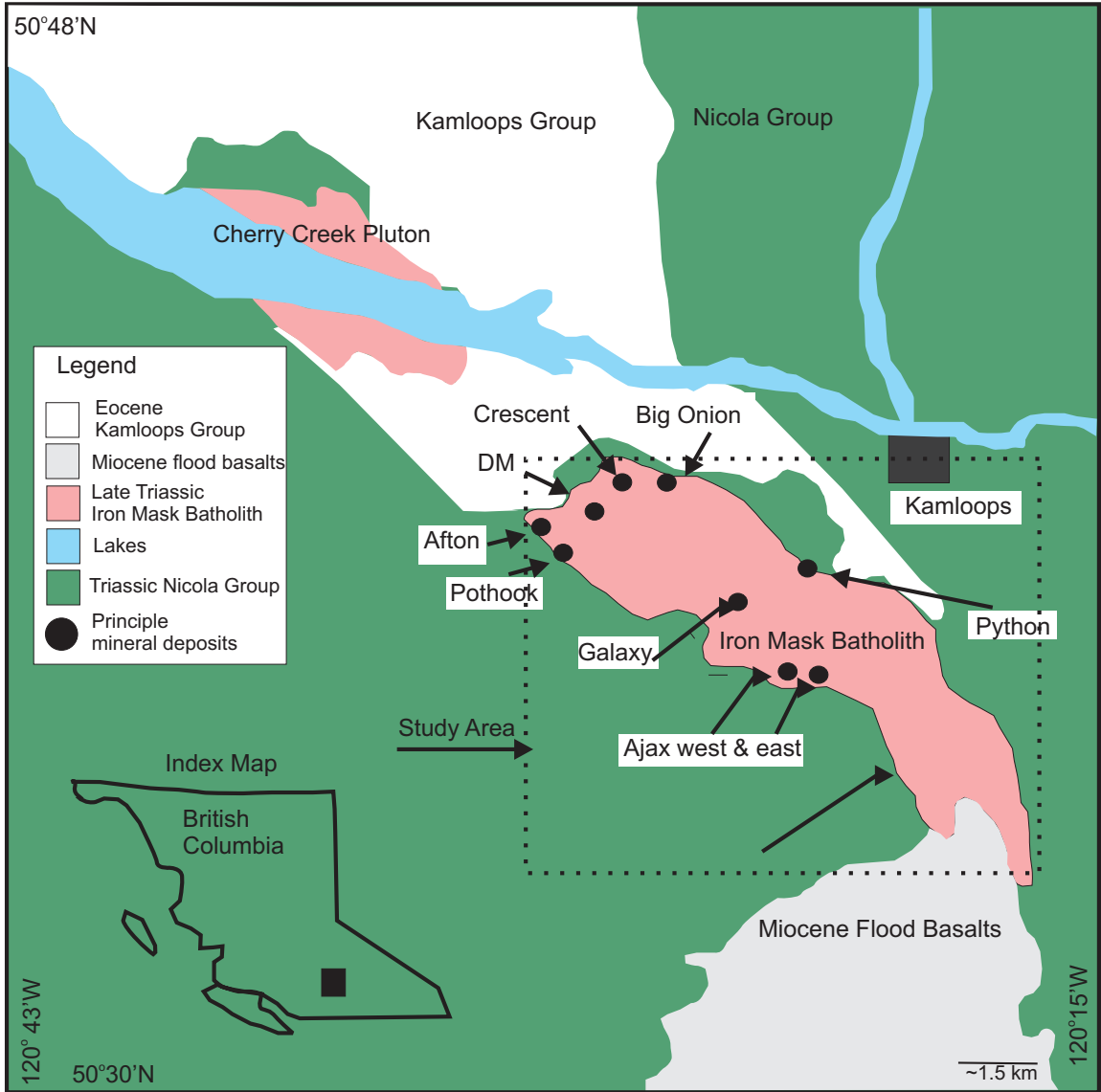


Figure 1.1.1: Location of the Iron Mask batholith and associated porphyry deposits (Modified from Kwong, 1977).

subsequently been gently folded by protracted east-directed compression during Jurassic-Paleocene deformation.

By constraining the timing of deformation episodes that have generated the dominant structural features within Nicola Group rocks, it is possible to discuss whether these “events” may have imparted observable strain on the Iron Mask batholith.

1.2 Regional Geology

The study area is located within the Intermontane Belt, one of the five morphogeological belts of the Canadian Cordillera (Figure 1.2.1; e.g. Wheeler and Gabrielse, 1972). The belt is bounded by the Omineca Belt to the east and the Coast Belt to the west, and in contrast to these adjacent belts, the Intermontane Belt has relatively low relief and rocks are rarely metamorphosed as high as greenschist facies. The area of this study is situated ten kilometres southwest of the city of Kamloops, British Columbia, at the eastern margin of the Intermontane Belt, where underlying rocks consist mainly of arc volcanic, sedimentary and plutonic rocks of the Nicola Group. This Late Triassic arc succession comprises primarily flow, pyroclastic, and volcanoclastic rocks ranging in composition from rhyolite to basalt and is, for the most part, largely unmetamorphosed or low grade metamorphic, except near the margins of plutons where contact metamorphism occurred (Preto, 1977). The Nicola arc is approximately 40 km wide and extends from near the international border ~180 km northward to Kamloops Lake. The Nicola Group continues northward, beneath extensive cover of Tertiary strata, and extends into northern British Columbia and Yukon where the rocks are known as the Takla and Stuhini volcanic assemblages.

The Nicola Group can be divided into four north striking regional facies belts, each approximately 10-15 kilometres wide (Preto, 1979; Monger, 1985; Monger and McMillan, 1989). The western belt consists principally of flow, pyroclastic and

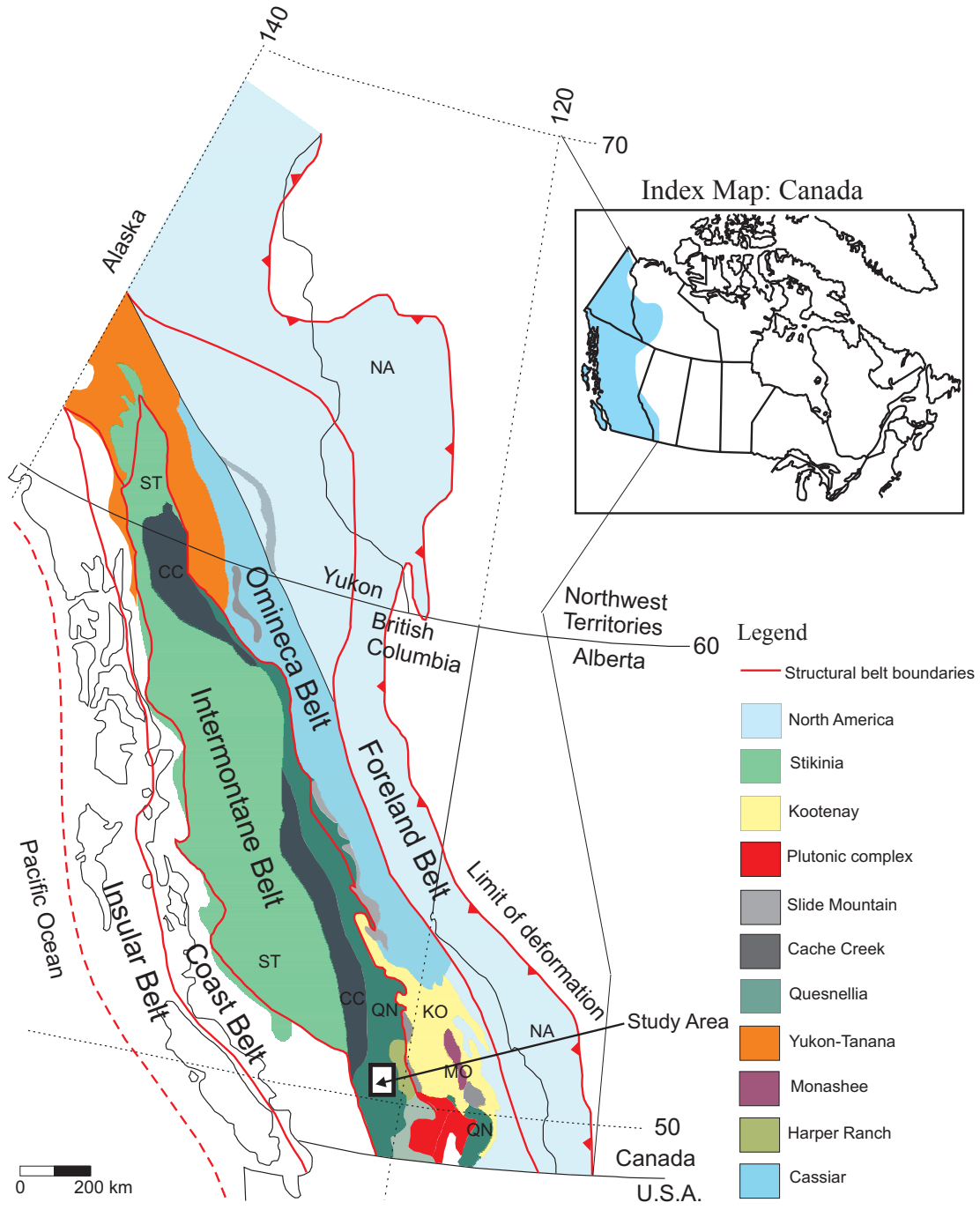


Figure 1.2.1: Map of the Canadian Cordillera depicting the five morphogeological belts. Included for reference are the various terranes discussed in the above section and the location of the thesis study area (modified from Wheeler et al., 1991).

volcaniclastic rocks ranging in composition from basalt to rhyolite, with interbedded argillite and reefoid limestone. A central belt is characterized by augite porphyritic basaltic and andesitic flows, volcanic breccia and lahar deposits, with minor interbedded crystal-lithic tuff. An eastern volcanic facies defines a belt of similar composition to rocks in the central zone but represents a transition to a dominantly epiclastic and volcaniclastic facies. The easternmost belt is dominated by a sedimentary facies composed of laminated mudstone and siltstone, volcanic sandstone, minor carbonates, and lesser basalts. The study area straddles the boundary between the eastern volcanic facies and the easternmost sedimentary facies.

The Nicola Group underlies much of Quesnellia*, where other assemblages, considered also to be part of a “Quesnel terrane,” range in age from latest Devonian through early Jurassic. Within the southern Canadian Cordillera, the Late Triassic Nicola Group and the Early Jurassic Rossland Group are representative of a magmatic arc complex which formed above an east-dipping subduction zone (Mortimer, 1987). This complex mix of Late Triassic to Early Jurassic arc assemblages and related igneous intrusions unconformably overlap Paleozoic subterrane that have been formed in at least two different tectonic settings: the oceanic Okanagan subterrane and the arc related Harper Ranch subterrane (Monger, 1977; Wheeler et al., 1991). These Devonian to Permian assemblages are the oldest known rocks within Quesnellia, and as such, have been interpreted to form the terrane’s primitive basement (Monger et al., 1991). The upper Paleozoic Harper Ranch Group is the type stratigraphy for the Harper Ranch subterrane (Monger et al., 1991), and in the Kamloops region it represents the oldest known strata in Quesnellia (Monger and McMillan, 1984). There is, however, some debate with respect to the nature of Quesnellia’s basement rocks, as some authors report evidence that Nicola Group rocks may be stratigraphically rather than structurally emplaced onto the ancient North American craton. (Erdmer et al., 1999; Erdmer et al., 2002; Unterschutz et al., 2002; Thompson et al., 2006).

Volcanic and sedimentary rocks of the Lower Jurassic Rossland Group form a discontinuous belt running along the southeastern margin of Quesnellia. In the Kamloops, Clearwater and Nelson areas, Rossland Group rocks or correlative assemblages are observed to unconformably overlie Triassic and older strata (Roback, 1993; Schiarizza et al., 2002; Beatty, 2003; Beatty et al., 2006). Eocene volcanic rocks of the Kamloops Group unconformably overlie the Nicola Group and Iron Mask rocks. Jurassic strata of the Ashcroft Formation are restricted to scattered outcrops of shale, sandstone and conglomerate, however Jurassic strata are absent from the study area. Rocks of the Kamloops Group form a graben, separating the Iron Mask pluton from the satellite Cherry Creek pluton, which surfaces northwest of the study area (Figure 1.1.1). Flat lying Miocene flood basalts blanket large portions of the region and unconformably overlie Nicola Group and Iron Mask rocks in the southeastern portion of the map area.

West of the study area lie rocks of the Cache Creek terrane. Ranging in age from Lower Carboniferous to Middle Jurassic, the Cache Creek terrane includes shallow-water carbonate, bedded radiolarian chert, argillite, basalt and gabbro (Monger et al., 1991). These rocks are interpreted to represent the remnants of an east-dipping subduction-accretionary complex in the Late Triassic (Travers, 1978). The Omineca Belt lies east of the study area and includes metamorphosed Peri-Laurentian strata such as Upper Paleozoic oceanic rocks of the Slide Mountain terrane and rocks of the Kootenay Arc, Proterozoic to Paleozoic strata that developed either on or beside the continental margin of the North American craton (Klepacki, 1985; Colpron and Price, 1995). The Slide Mountain terrane, a narrow belt of siliciclastic rocks and mafic and ultramafic volcanic rocks, has been considered to represent an oceanic basin of unknown width, having opened in the Carboniferous and/or Permian (Klepacki, 1985; Roback et al., 1994). The basin would have separated the Kootenay arc and Quesnel terrane at this time (Tempelman-Kluit, 1979). In this interpretation, amalgamation of the Intermontane Belt (Cache Creek, Quesnel, Stikine and Slide Mountain terranes) began with the closure of

the Slide Mountain ocean basin. This closure is thought to have begun in the Paleozoic, and completed by Middle Jurassic. In the southern Canadian Cordillera however, Thompson et al., (2006) suggested that strata of the Slide Mountain terrane were not deposited in a basin floored by oceanic crust but rather on shallow water sandstone and carbonate platform strata. In that interpretation, Late Paleozoic extension initiated crustal cracking but failed to produce oceanic lithosphere beneath the Slide Mountain basin (Thompson et al., 2006). There is consensus, however, that there is ample evidence to support a Slide Mountain ocean farther north (Struik, 1987; Nelson, 1993; Ferri, 1997).

There is a complex history of deformation within and adjacent to Quesnellia at the latitude of the study area. Multiple episodes of crustal thickening are inferred and at least one phase of extension. Fabrics observed in latest Triassic granodioritic plutons indicate Late Triassic-Early Jurassic deformation, interpreted to result from accretion of Quesnellia onto the continental margin (Friedman et al., 2002) or possibly the eastward migration of Nicola magmatism (Parrish and Monger, 1992; Beatty et al., 2006). Early to Middle Jurassic deformation has been attributed to east-directed thrusting of Quesnellia above eastern pericratonic rocks (e.g. Brown et al., 1986). The deformation episode generated regional-scale, southwest verging folds and associated thrust faults (Brown et al., 1986). Thompson et al. (2006) alternatively suggested that Jurassic through Paleogene deformation resulted from a trapping of the continental margin prism, and underlying weaker crust, between thicker and stronger crust to the east and a block or ribbon of North American crust, the Okanagan High, onto which Quesnel and Slide Mountain strata were stratigraphically emplaced. Extensional and strike-slip Eocene faults have been reported both south (Ewing, 1980; Fyles, 1990) and north of the study area (Schiarizza and Israel, 2001), and Tertiary faults within the study area largely influence map patterns (Monger and McMillan, 1984). The Nicola horst, occupying the southern portion of the study area, is largely a manifestation of this Tertiary extension (Ewing, 1980; Moore and Pettipas, 1990).

1.3 Location, Access and Topography

The study area lies approximately 10 km southwest of Kamloops (Figure 1.4.1). The area mapped occupies a block bounded by latitude 50° 41' to the north and latitude 50° 29' to the south, and by longitude 120° 15' to the east and 120° 33' to the west, covering a total area of approximately 400 km². The Coquihalla and Lac le Jeune roads are the main access routes in the area, while numerous secondary roads, mainly used for forestry, allowed for easier accessibility in heavily treed areas.

Private property, mainly used for cattle farming, spans a large portion of the region. Accessing these areas required permission from various land owners.

The geomorphology is primarily a result of the last glaciation, where ridges are aligned in a series of northwest trending drumlins. The drumlins are defined by a blunt, stoss side which faces up-glacier and a gently sloping lee side, interpreted to be oriented in the ice flow direction (e.g. Benn and Evans, 1997). Bedrock outcrops are generally exposed on steeper northwest facing stoss sides, where the lee sides are generally covered by vegetation. Exposures generally follow this northwest trend.

1.4 Previous Work

Rocks of the Late Triassic Nicola Group are exposed in a belt that extends from Kamloops Lake south to the International Boundary, underlying much of the Intermontane belt in south-central British Columbia (Figure 1.2.1). Dawson carried out the earliest geological work on these volcanic rocks in 1877 in the vicinity of Nicola Lake (Dawson, 1879). During this study the author was the first to name and describe the Nicola Group. The author's initial description of the Nicola Group is as follows:

“East of the inner ranges of the coast system of mountains great areas are covered by rocks which may be correlated with little doubt with the green series of the upper part of the Whipsaw Creek, and assigned with probability to the Triassic age. As being a characteristic exhibition of these rocks, the

section found on the south side of Nicola Lake, from which it is proposed to designate these rocks as the Nicola series, will be first noticed.

These rocks are exposed between the mouth of McDonald's River, and the bridge across the Nicola at the outlet of the lake, a distance of seven and one-half miles. With the exception of the limestone, they appear to be entirely of volcanic origin, consisting of agglomerates, with beds made up of fine volcanic debris, and others which have originally been sheets of molten matter. All these have been indurated, perhaps in some cases recrystallized by metamorphism, and have since suffered a greater or less amount of that alteration by decomposition of original constituent minerals, so common in the older volcanic rocks. Taken as a whole, the series is now distinctly feldspathic, and in colour, green of various shades." (Dawson, 1879)

Dawson (1985) later defined the type locality of the Nicola Group just south of Nicola Lake.

Rice (1947) and Cockfield (1948) mapped the Princeton and Nicola map sheets between 1939 and 1944, and provided the first comprehensive geological reports for the region. Duffell and McTaggart carried out field work during 1945 and 1946 in the Ashcroft region producing a detailed regional report and map of the area (Duffell and McTaggart, 1952). In 1960 and 1961, Vancouver based mining companies conducted studies of the Nicola Group rocks between the International Boundary and Stump Lake in an attempt to subdivide the volcanic rocks and determine their structure (Fahrni, 1962; cited in Preto 1979). Schau (1968) presented a detailed description of the Nicola Group, where the author mapped a 1200 km² area south of Nicola Lake. His contributions aided in understanding the geologic history of the Nicola Group by subdividing volcanic units, determining their structure, and understanding the environments in which volcanic and sedimentary units were deposited (Preto 1979).

A study of the south-central Cordillera by Campbell (1966) led to the interpretation that in late Upper Triassic time a central zone of volcanism was flanked on the east and west by basins of sedimentary accumulation. Detailed mapping by Schau (1968) south of Nicola Lake supported Campbell's observations.

The Nicola Project, which aimed at regional mapping of Nicola Group rocks in

southern British Columbia, did not commence until 1972, when P. A. Christopher mapped the area of Fairweather Hills, near Aspen Grove. This mapping led to the production of a preliminary map of the region at a scale of 1:15840 (Christopher, 1973). In this study, Christopher (1973) documented a well-exposed volcanic center that was known to contain numerous copper prospects. A more detailed study of the volcanic rocks exposed in the Fairweather Hills vicinity was carried out by Lefebure in 1974 (Lefebure, 1976). The study focused on describing Nicola Group stratigraphy in greater detail in an attempt to recognize its relation to the distribution and type of copper occurrences (Lefebure, 1976). The Nicola Project mapping was expanded by Preto in 1973, 1974 and 1975, when Preto mapped an extensive portion of the central Nicola Group between Merritt and Princeton (Preto, 1974, 1975, 1976). In these studies Preto (1974; 1975; 1976) recognized three regional facies belts within the Nicola Group (see Section 1.2).

Monger and McMillan (1984; 1989) produced a revised map of the Ashcroft area. In the accompanying map notes Monger and McMillan (1984) described the structural geology of the Ashcroft map area as being dominated by Tertiary faults which largely govern the map pattern. These faults have been ascribed by Price (1979) and Ewing (1980) to be related to right-lateral transform motions and crustal extension. As a result of this crustal extension, Ewing (1980) suggested that the Nicola batholith and associated metamorphic rocks, appear to form a block that rose from deeper in the crust, becoming exposed in the early Tertiary, consequently re-setting a number of its isotopic systems. K-Ar work carried out by Preto et al. (1979) on biotites and hornblendes from the Nicola batholith suggested a Paleocene age while revised Rb-Sr isotopic data from McMillan et al. (1981) suggested that at least some of the deformed plutonic rocks in the batholith are Early Jurassic or older.

Further work on the Nicola Batholith, now recognized as the Nicola horst (e.g. Ewing, 1980; Moore and Pettipas, 1990), was carried out in 1988 and 1989, when mapping was done at a scale of 1:50 000 (Moore and Pettipas, 1990). The authors

recognized the horst as a major structure bounded by Tertiary faults, where these faults are part of the regional system of Eocene extensional features proposed by Ewing (1980) and elaborated on by Monger and McMillan (1989). Moore and Pettipas (1990) studied the internal structure of the horst, noting that a strong flattening and mixed shear senses was consistent with a compressional regime. The authors interpreted the fabric in the horst to be related to accretion of the Nicola arc and later Tertiary extension has exposed these early strain features.

The study area is dominated by north to northwest striking high- and moderate-angle faults thought to have been active as early as mid-Triassic (Campbell and Tipper, 1970; Preto, 1977). Preto (1977) suggested that the distribution and extent of the Nicola Group were controlled by and are focused along these deep-seated faults, and considered them to be an ancient, long lived rift system. Mortimer (1987) suggested, using geochemical evidence and petrology from flow rocks across the entirety of the Nicola arc, that the Nicola Group resulted from early Mesozoic volcanism above an east-dipping subduction zone.

Directly northeast of Kamloops, strata of Quesnellia have been mapped at reconnaissance scale by Smith (1979) and Monger and McMillan (1984, 1989). Southwest verging structures were recognized within Nicola Group sedimentary rocks and were interpreted to be Middle Jurassic in age (Monger and McMillan, 1989). More recently Beatty (2003) completed a detailed study of the area northeast of Kamloops and provided detailed descriptions of the Upper Paleozoic Harper Ranch Group and Upper Triassic Nicola Group, new paleontological data, geologic field relationships, and regional correlations to better constrain the tectonic history of Quesnellia in the Kamloops region. In this study, Beatty (2003) suggested that deformation of the Nicola Group and underlying Harper Ranch Group is Late Triassic-Early Jurassic in age.

A study by Erdmer et al., (1999) demonstrated that the basement of Quesnellia stratigraphy may be much older than previously thought (e.g. older than the Upper

Paleozoic Harper Ranch Group). A 560 Ma granite clast was discovered within the Nicola horst, which implies crust at least as old as latest Proterozoic was present beneath the horst. Erdmer et al. (2002) and Unterschutz et al. (2002) offered compelling geochemical and Nd isotopic data from Triassic clastic rocks of the Quesnel terrane that showed detritus has been partially derived from evolved (old continental) sources, which supports the hypothesis that the Nicola Group may have been deposited at the ancient continental margin.

Logan and Mihalynuk (2005) studied Nicola Group rocks in the vicinity of the Iron Mask batholith. Most of the study focused on intrusive phases, however the stratigraphy and structure of the Nicola Group was also described. In this study, an abrupt transition from massive to strongly schistose Nicola Group rocks, over a strike-normal distance of approximately 100 m, was recognized just south of the Iron Mask batholith. Logan and Mihalynuk (2005) refer to this area of strongly foliated rocks as the Cherry Creek Tectonic Zone (CCTZ), which is depicted on their geological map of the Iron Mask region (Logan and Mihalynuk, 2006). Figure 1.4.1 shows locations of study areas from previous work described above.

1.5 Present Work- Methods

Mapping of the area was carried out at a scale of approximately 1: 16000 and presented in this thesis at a 1:25 000 scale (Figure 2.1.1). Field mapping was conducted in the summer of 2007, during a two and one-half month field season. The main focus of this study was the acquisition of detailed field information including: outcrop distributions, geologic unit descriptions and structural data. From these data, a detailed geological map of the region was generated. Examination of thin sections for petrographic analysis aided in the descriptions of the mineral assemblages for the various rock units identified in the field. Microscopic primary and secondary fabrics were also examined from these thin sections.

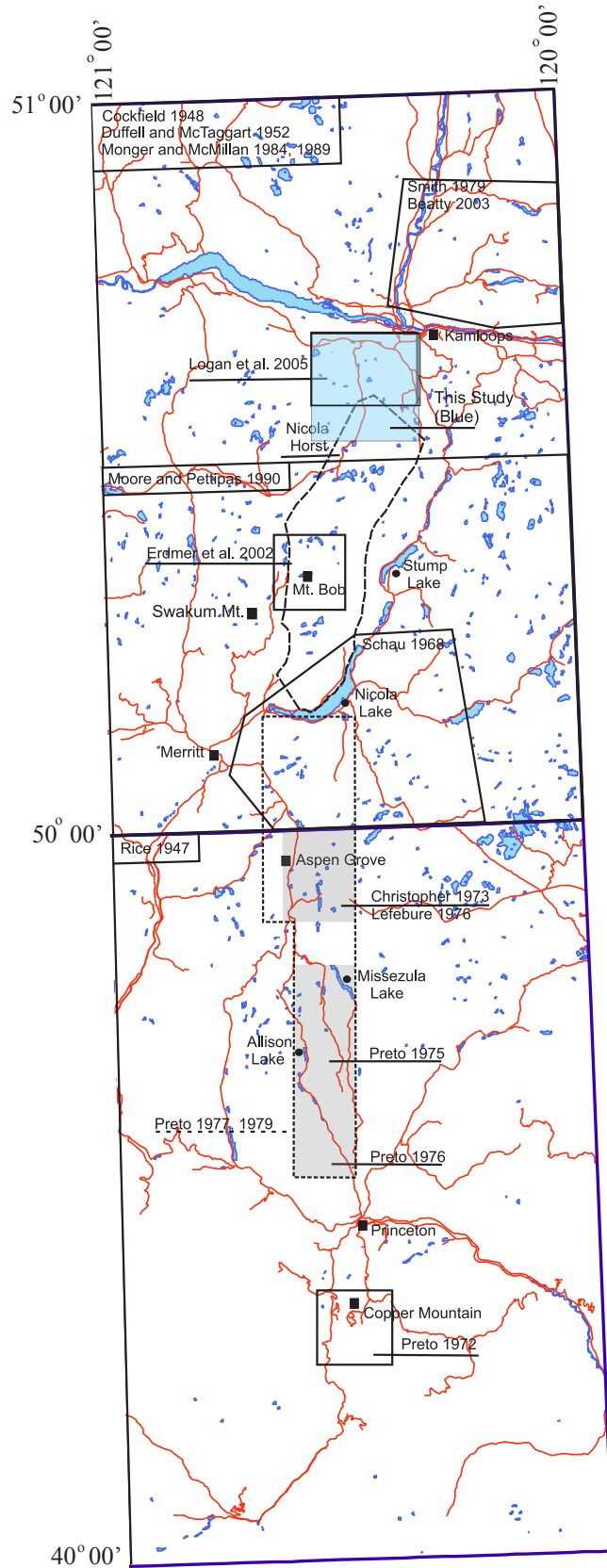


Figure 1.4.1: Location of study areas from previous work on Nicola Group rocks between the Kamloops region and Copper Mountain

1.6 References

- Beatty, T.W. 2003. Stratigraphy of the Harper Ranch Group and tectonic history of the Quesnel terrane in the area of Kamloops, British Columbia. M.Sc. thesis, Simon Fraser University, Burnaby, B.C. 213 p.
- Beatty, T.W., M.J. Orchard, and P.S. Mustard. 2006. Geology and tectonic history of the Quesnel terrane in the area of Kamloops, British Columbia. In: M. Colpron, J. Nelson (Editors), Paleozoic Evolution and Metallogeny of Pericratonic Terranes at the Ancient Pacific Margin of North America. *Geological Association of Canada, Special Paper 45*: 483-504.
- Benn, D. and D.J.A. Evans. 1997. *Glaciers and Glaciation*. 1st Ed. Arnold, London, UK.
- Brown, R. L., J.M. Journeay, L.S. Lane, D.C Murphy, and C.J. Rees. 1986. Obduction, backfolding and piggyback thrusting in the metamorphic hinterland of the southeastern Canadian Cordillera. *Journal of Structural Geology* 8, no. 3/4: 255-268.
- Campbell, R.B. 1966. Tectonics of the south central cordillera of British Columbia: in Tectonic History and Mineral Deposits of the Western Cordillera. *Geological Survey of Canada special Vol. 8*: 61-72.
- Campbell, R.B., and H.W. Tipper. 1970. Geology and mineral exploration potential of the Quesnel Trough, British Columbia. *British Columbia Institute of Mining and Metallurgy Bulletin* 63: 785-790.
- Christopher, P.A. 1973. Preliminary geological map of the Aspen Grove area, British Columbia. British Columbia Department of Mines and Petroleum Resources, Preliminary Map No. 10.
- Cockfield, W.E. 1948. *Geology and Mineral Deposits of Nicola Map-Area, British Columbia*. Mem, 249. Geological Survey of Canada.
- Colpron, M., and R.A. Price. 1995. Tectonic significance of the Kootenay terrane, southeastern Canadian Cordillera; An alternative model. *Geology* 23: 25-28.

- Dawson, G.M. 1879. Preliminary report on the physical and geological features of the southern portion of the interior of British Columbia. *Geologic Survey of Canada, Rept. of progress, 1877-78.*
- . 1895. Report on the area of the Kamloops map-sheet, British Columbia. *Geologic Survey of Canada VII*, pt. B, no. Annual Rept., 1894: 3B-427B.
- Duffell, S., and K.C. McTaggart. 1952. *Ashcroft Map-Area, British Columbia*. Mem, 262. Geological Survey of Canada.
- Erdmer, P., Moore, J.M., L. Heaman, R.I. Thompson, K.L. Daughtry, and R.A. Creaser. 2002. Extending the ancient margin outboard in the Canadian Cordillera: record of Proterozoic crust and Paleocene regional metamorphism in the Nicola horst, southern British Columbia. *Canadian Journal of Earth Sciences* 39: 1605-1623.
- Erdmer, P., R.I. Thompson, and K.L. Daughtry. 1999. Pericratonic Paleozoic succession in Vernon and Ashcroft map areas, British Columbia; in Current research 1999-A. *Geologic Survey of Canada*: 205-213.
- Ewing, T.E. 1980. Paleogene tectonic evolution of the Pacific Northwest. *Journal of Geology* 88: 619-638.
- Fahmi, K.C. 1962. Aspen Joint Venture, Study of Nicola Rocks, Princeton and Merritt Districts, British Columbia, private report.
- Ferri, F. 1997. Nina Creek Group and Lay range assemblage, north-central British Columbia: remnants of Late Paleozoic oceanic and arc terranes. *Canadian Journal of Earth Sciences* 34: 854-874.
- Friedman, R., G. Ray, and I. Webster. 2002. U-Pb zircon and titanite dating of intrusive rocks in the Heffley Lake area, south-central British Columbia, in Geological Fieldwork. *B.C. Ministry of Energy and Mines, Paper 2002-1*: 109-118.
- Fyles, J.T. 1990. Geology of the Greenwood-Grandforks area, British Columbia, NTS 82E/1,2. *B.C. Ministry of Energy, Mines and Petroleum Resources, Open File 1990-25.*

- Klepacki, D.W. 1985. Stratigraphy and structural geology of the Goat ranges area, southeastern British Columbia. Ph.D thesis, Massachusetts Institute of Technology, Boston, Massachusetts.
- Kwong, Y.T.J. 1987. Evolution of the Iron Mask Batholith and Associated Copper Mineralization; B.C. Ministry of Energy, Mines and Petroleum Resources, Bulletin 77. *British Columbia Ministry of Energy, Mines and Petroleum Resources Bulletin 77.*
- Lang, J.R. and Stanley, C.R. 1995. Geology of the Crescent alkali Cu-Au porphyry deposit, Afton Mining Camp, British Columbia (92I/9); In Porphyry Deposits of the Northwestern Cordillera of North America, Schroeter, T.G., Editor. *Canadian Institute of Mining, Metallurgy and Petroleum Special Volume 46: 581-592.*
- Lefebure, D.V. 1976. Geology of the Nicola Group in the Fairweather Hills, B.C. Queen's University.
- Logan, J.M., and M.G. Mihalynuk. 2005. Porphyry Cu-Au Deposits of the Iron Mask Batholith Southeastern British Columbia: In Geological Fieldwork 2004. *British Columbia Geological Survey Branch, Paper 2005-1.*
- . 2006. Geology of the Iron Mask Batholith. Open File Map 2006-11. British Columbia Geologic Survey Branch.
- McMillan, W.J., Armstrong, R.L. Harakal, J. 1981. Age of the Coldwater Stock and Nicola Batholith, near Merritt (92H). *British Columbia Department of Mines and Petroleum Resources, Geological Fieldwork: 102-105.*
- Monger, J.W.H. 1977. Upper Paleozoic rocks of western Canadian Cordillera and their bearing on Cordilleran evolution. *Canadian Journal of Earth Sciences 14: 1832-1859.*
- . 1985. Structural evolution of the southwestern Intermontane belt, Ashcroft and Hope map areas, British Columbia; in Current Research, Part A. *Geologic Survey of Canada, Paper 85-1A: 349-358.*

- Monger, J.W.H., and W.J. McMillan. 1984. Bedrock geology, Ashcroft, British Columbia (92 I). Geological Survey of Canada.
- . 1989. Bedrock geology, Ashcroft, British Columbia (92 I). Geological Survey of Canada, Map 42.
- Mortensen, J.K., D.K. Ghosh, and F. Ferri. 1995. U-Pb geochronology of intrusive rocks associated with copper-gold porphyry deposits in the Canadian Cordillera; In Porphyry Deposits of the Northwestern Cordillera of North America, Schroeter, T.G., Editor. *Canadian Institute of Mining, Metallurgy and Petroleum Special Volume 46*: 142-158.
- Mortimer, N. 1987. The Nicola Group: Late Triassic and Early Jurassic subduction-related volcanism in British Columbia. *Canadian Journal of Earth Sciences* 24: 2521-2536.
- Preto, V.A.. 1974. Geology of the Allison Lake-Missezula Lake area (92 H/15E). *British Columbia Department of Mines and Petroleum Resources, Geological Fieldwork*: 9-13.
- . 1975. Geology of the Allison Lake-Missezula Lake Area, British Columbia, *British Columbia Department of Mines and Petroleum Resources, Preliminary map No.* 17.
- . 1976. Geology of the Nicola Group south of Allison Lake (92H/10E). *British Columbia Department of Mines and Petroleum Resources, Geological Fieldwork*: 55-58.
- . 1977. The Nicola Group: Mesozoic volcanism related to rifting in Southern British Columbia. *Geological Association of Canada*, no. Special Paper 16: 39-57.
- . 1979. Geology of the Nicola Group between Merritt and Princeton, British Columbia. *British Columbia Ministry of Energy, Mines and Petroleum Resources*, no. Bulletin 69: 90.
- Monger, J.W.H., J.O. Wheeler, H.W. Tipper, H. Gabrieleise, T. Harms, L.C. Struik, R.B.

- Campbell, C.J. Dodds, G.E. Gehrels, and J. O'Brian. 1991. Part B: Cordilleran terranes (Chapter 8), in H. Gabrielse and C.J. Yorath Editors, *Geology of the Cordilleran Orogen in Canada: Geologic Survey of Canada, Geology of Canada*, no. 4 (Also Geological Society of America, *The Geology of North America*, Vol. G-2): 281-327.
- Moore, and A.R. Pettipas. 1990. Geological studies in the Nicola Lake region (92 I/SE); Part A. In Nicola Lake region geology and mineral deposits. *British Columbia Geological Survey Branch, Open File 1990-29*.
- Nelson, J.L. 1993. The Sylvester allochthon: upper Paleozoic marginal basin and island arc terranes in northern British Columbia. *Canadian Journal of Earth Sciences* 30: 631-643.
- Parrish, R.R., and J.W.H. Monger. 1992. New U-Pb dates from southwestern British Columbia: in Radiogenic age and isotopic studies; Report 5. *Geologic Survey of Canada, Paper 91-2*: 87-108.
- Price, R.A. 1979. Intracontinental ductile spreading linking the Fraser River and Northern Rocky Mountain Trench transform fault zones, south-central British Columbia and northeast Washington. *Geologic Society of America, Abstracts with Programs* 11: 499.
- Rice, H.M.A. 1947. *Geology and Mineral Deposits of the Princeton Map-Area, British Columbia*. Mem, 243. Geological Survey of Canada.
- Roback, R.C. 1993. Late Paleozoic to middle Mesozoic tectonic evolution of the Kootenay arc, northeastern Washington and southeastern British Columbia. PhD thesis, University of Texas, Austin, Texas.
- Roback, R.C., J.H. Sevigny, and N.W. Walker. 1994. Tectonic setting of the Slide Mountain terrane, southern British Columbia. *Tectonics* 13: 1242-1258.
- Schau, M.P. 1968. Geology of the Upper Triassic Nicola Group in south-central British Columbia. University of British Columbia; Unpubl. Ph.D. thesis.

- Schiarizza, P., S. Heffernan, and J. Zubar. 2002. Geology of the Quesnel and Slide Mountain terranes west of Clearwater, south-central British Columbia (92P/9, 10, 15, 16), in Geological Fieldwork 2001. *B.C. Ministry of Energy, Mines, Paper 2002-1*: 83-108.
- Schiarizza, P., and S. Israel. 2001. Geology and mineral occurrences of the Nehalliston Plateau, south-central British Columbia (92P/7,8,9,10), in Geologic Fieldwork 2000. *B.C. Ministry of Energy and Mines, Paper 2001-1*: 83-108.
- Smith, R. 1979. Geology of the Harper Ranch Group and Nicola Group northeast of Kamloops, British Columbia. University of British Columbia; M. Sc. thesis.
- Struik, L.C. 1987. The ancient western North America margin: An alpine rift model for the east-central Canadian Cordillera. *Geologic Survey of Canada, Paper 87-15*: 19.
- Tempelman-Kluit, D.J. 1979. Transported cataclastic, ophiolite and granodiorite in Yukon; evidence of arc-continent collision. *Geologic Survey of Canada, paper 79-14*: 27.
- Thompson, R.I., P. Glombick, P. Erdmer, L. Heaman, and Y. Lemieux. 2006. Evolution of the ancestral Pacific margin, southern Canadian Cordillera: Insights from new geologic maps. In: M. Colpron, J. Nelson (Editors), *Paleozoic Evolution and Metallogeny of Pericratonic Terranes at the Ancient Pacific Margin of North America. Geologic Association of Canada, Special Paper 45*: 433-482.
- Travers, W.B. 1978. Overturned Nicola and Ashcroft strata and their relations to the Cache Creek Group, southwestern Intermontane Belt, British Columbia. *Canadian Journal of Earth Sciences 15*: 99-116.
- Unterschutz, J., R.A. Creaser, P. Erdmer, R.I. Thompson, and K.L. Daughtry. 2002. North America margin origin of Quesnel terrane strata in the southern Canadian Cordillera: inferences from geochemical and Nd isotopic characteristics of Triassic metasedimentary rocks. *Geological Society of America Bulletin 114*: 462-

475.

Wheeler, J.O., A.J. Brookfield, H. Gabrielse, J.W.H. Monger, H.W. Tipper, and G.J.

Woodsworth. 1991. Terrane map of the Canadian Cordillera. Geological Survey of Canada, Map 1713A.

Wheeler, J.O. and Gabrielse, H. 1972. The Cordilleran structural province; In Variations in Tectonic Styles in Canada, Price, R.A. and Douglas, R.J.W., Editors.

Geological Association of Canada Special Paper 11: 1-81.

Chapter 2: Stratified and Intrusive Rocks

2.1 Introduction

Within the study area, the stratigraphy of Nicola Group rocks is difficult to unravel because lateral and strike-normal facies changes occur rapidly, as can be expected where volcanic rocks are deposited in a proximal, geologically active depositional environment. Map units are laterally discontinuous such that individual layers cannot be traced along strike for more than a few hundred metres. The present study has led to revision of the British Columbia Geological Survey Open File 2006-11 map (Logan and Mihalynuk, 2006) and the local Nicola Group stratigraphy is interpreted to be more complex than depicted on the existing map of the study area (Figure 2.1.1: map inset). Outcrop exposure is poor in many portions of the study area, particularly so south of the Cherry Creek Tectonic Zone (CCTZ). Stratigraphic linkages are therefore difficult to establish south of the CCTZ and rocks underlying this portion of the map area remain undivided (Figure 2.1.1: Section 1.4, 5.4.1).

2.2 Stratigraphy of Nicola Group Rocks

Nicola Group rocks in the area strike northwest and dip steeply toward the northeast. Bedding tops indicators are scarce, but the few observed indicate that the strata are, for the most part, upright (Figure 2.2.1). Steeply dipping strata can locally be slightly overturned.

South of the Iron Mask batholith (IMB), Nicola Group rocks include thick (500 m-1 km) sequences of pyroclastic rocks which show minor sedimentary reworking. The pyroclastic rocks are defined below according to the recommendations of the International Union of Geological Sciences (IUGS) subcommission on the systematics of igneous rocks as outlined by Schmid (1981). The volcanic deposits in the map area include augite-plagioclase tuff, lapilli tuff, and coarse volcanic breccia. The deposits are interbedded with thin sequences of reworked volcanoclastic rocks, including

sandstone and siltstone. Moving up stratigraphy (to the northeast in map view), there is a gradational change to more fragmental volcanoclastic rocks, lahar debris flows (Logan and Mihalynuk, 2005) and reworked equivalents. Lesser basaltic flows and even rarer andesitic flows are discontinuous and interlayered with the volcanoclastic and pyroclastic deposits. Volcanic flows are augite or augite-plagioclase porphyritic. Augite and augite-plagioclase porphyritic fragments are the primary constituent of all fragmental units. Primary volcanic textures and sedimentary structures are well preserved.

The Nicola Group has been interpreted to range in age from late Carnian to late Norian on the basis of fossil data collected from limestone units in western, central and eastern portions of the Nicola arc (Preto, 1979; Monger and McMillan, 1984). A general younging of the Nicola Group from west to east is interpreted from the data, whereby rocks underlying the Kamloops region are, in general, late Norian in age (Monger and McMillan, 1984). In the study area, limestone was not observed, hence fossils were not found. Absolute ages of rock units underlying the Iron Mask region were not determined in this study however relative ages for Nicola Group rocks in the Iron Mask region are interpreted on the basis of stratigraphic relationships.

2.2.1 Stratified Rocks

Augite - Plagioclase Lithic Tuff and Augite Porphyritic Lapilli Tuff: LTrNfat (1)

A large portion of the map area is underlain by plagioclase > augite tuff and augite porphyritic lapilli tuff. This unit forms the basal portion of the stratigraphic succession that is bounded by the CCTZ to the southwest and the Iron Mask batholith to the northeast (Figure 2.1.1). The unit ranges in thickness from about 800 m up to approximately 1200 m. Exposures are generally green in colour; however colour can range from a grey-green to a deep bluish-green. The unit is generally fresh, but weathered surfaces can be light pink in colour. Plagioclase is the most abundant mineral with lesser augite. The unit is fragmental; with fragments being of predominantly tuffaceous size (<

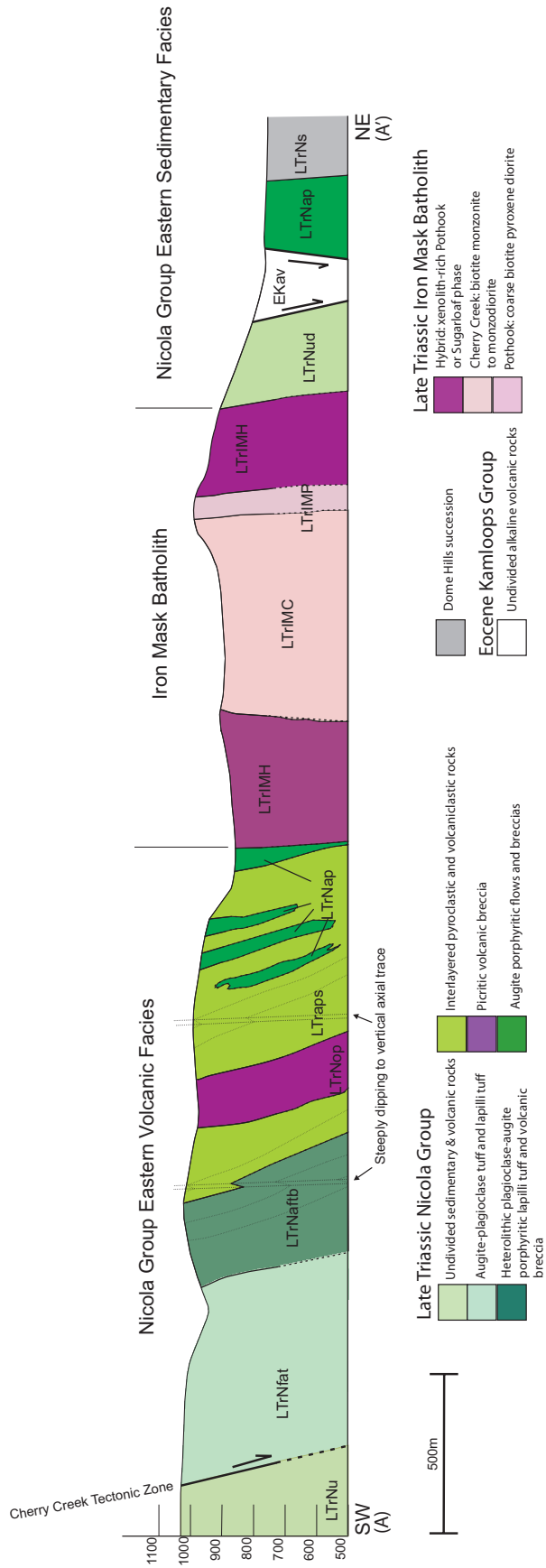


Figure: 2.2.1: Cross-section A-A' (on Figure 2.1.2) showing steeply tilted succession of Nicola Group rocks and intrusive phases of the Iron Mask batholith. Note minor folds within the volcanoclastic unit of the Nicola Group. LTrNfat, LTrNfatb, ...etc.. refers to map units on Figure 2.1.2.

2mm) in finer grained portions of the unit. Fragments can be larger, ranging from 5-7 mm and are commonly plagioclase + augite and augite porphyritic lithics, with lesser isolated crystals. Individual crystals are generally euhedral and are commonly broken. Both fragments and individual crystals show little evidence of sedimentary transport; fragment boundaries are subangular to subrounded and cusped (Plate 2.2.1). For the most part the unit is massive, with no visible layering. There are, however, a few localities where thin interlayering (centimetres to 10's of centimetres) of planar laminated rocks is observed. These layers can be traced along strike for up to 2.5 km, but commonly form lenses less than a kilometre in length. Within these finely laminated zones, soft sediment deformation features such as load casts and flame structures were observed. Dewatering features cross-cut thin laminations and appear to originate along layers of pressure dissolution that have been formed parallel to sedimentary laminations. These interbedded units are therefore interpreted to be sedimentary in origin and include laminated sandstone and siltstone (Photo 2.2.1). These layers are important from a structural mapping point of view as they allow measurement of bedding orientation of otherwise massive strata. Joint surfaces of fine grained, massive portions of the unit display plumose structure.

Coarse grained fragmental rocks define the massive portions of this unit and are interpreted to represent pyroclastic material according to the recommendations of the IUGS subcommission on the systematics of igneous rocks (Schmid, 1981). According to these recommendations, it is stated that

“ *Pyroclasts* are individual crystals, crystal fragments, glass fragments and rock fragments generated by disruption as a direct result of volcanic action. The shapes they assumed during disruption or during subsequent transport to the primary deposit must not have been altered by later redeposition processes.” (Schmid, 1981)

Volcanic derived pyroclasts show evidence of deposition with no reworking by later sedimentary processes. Sizes of individual lithic fragments and crystals indicate that the unit is dominantly tuffaceous (\leq 2mm), with coarser grained portions (fragments ranging from 5-7 mm) representing a lapilli tuff. Thin layers of finely laminated

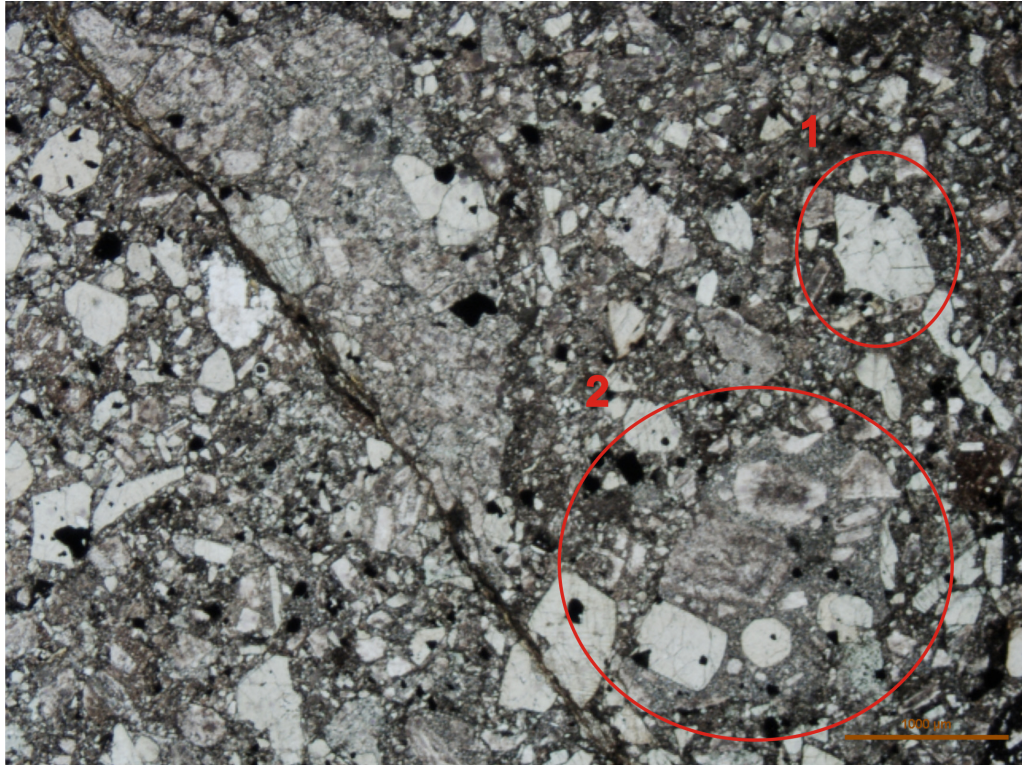


Plate 2.2.1: Augite + plagioclase tuff. (1) Broken CPX crystal. (2) Porphyritic pyroclastic fragments of tuffaceous size. Note cusped boundaries.



Photo 2.2.1: Planar laminated, plagioclase bearing tuffaceous sandstone interbedded within plagioclase-augite tuff and lapilli tuff.

tuffaceous sandstone, interbedded within the massive pyroclastic material, may have been derived from reworking of proximal volcanic rocks and are interpreted to have formed during periods of erosion and redeposition between episodes of volcanism. According to Schmid (1981) fine grained volcanogenic material within laminated sandstone and siltstone should be referred to as “reworked pyroclasts” or “epiclasts.”

Plagioclase Porphyritic Flows: LtrNfp (2)

Interlayered within the plagioclase > augite tuff described above are plagioclase > augite porphyries. The unit is relatively thin, with a thickness ranging from approximately 75-200 metres, with individual flows being approximately 10 m in thickness. The unit forms small lenses, extending along strike (northwest) for no more than a kilometre. Exposures are generally fresh and range in colour from deep green to dark purple. Plagioclase constitutes at least 80% of the total rock, with augite constituting approximately 20%. The unit is porphyritic with phenocrysts of both plagioclase and augite being euhedral. Phenocrysts are consistent in size (~ 1mm), with augite being slightly smaller than plagioclase. Augite phenocrysts commonly display igneous zoning. In most cases, plagioclase displays trachytic texture that is observable both in outcrop and thin section (Plate 2.2.2). The unit is generally massive with no measurable fabric, however the distribution of outcrops on the geological map (Figure 2.1.1) suggests that the unit is interlayered with the plagioclase-augite tuff and lapilli tuff and does not cross-cut stratigraphy. As such the unit is interpreted as a porphyritic flow, and the alignment of plagioclase laths is interpreted as the flow direction. The flows are thin and form discontinuous bodies interlayered within plagioclase > augite tuff and augite porphyritic lapilli tuff. An absolute age for the unit was not determined, but its map distribution suggests that it is coeval with plagioclase > augite tuff and augite porphyritic lapilli tuff, where flows were most likely being generated during deposition of the pyroclastic material.

Plagioclase Tuff and Lapilli Tuff: LTrNft (3)

Plagioclase crystal tuff and lapilli tuff define a unit that stratigraphically lies above plagioclase > augite tuff and augite porphyritic lapilli tuff. The unit is extensive, extending along strike for more than 5 km and having a thickness of approximately 500 m at its thickest point. When fresh, exposures are generally grey in colour and the fragmental nature of the unit is not obvious, however when weathered pink lapilli-sized fragments (2-8mm), weather in positive relief (Photo 2.2.2). Plagioclase is the dominant mineral, constituting greater than 90% of the unit, with augite being minor or absent. Plagioclase crystals show lamellar twinning, are generally euhedral, and can have broken or rounded edges. The unit is moderately to poorly sorted with plagioclase ranging in size from 0.1-1 mm. Strong alteration is evident in thin section and sericitic alteration is strongest in the cores of plagioclase crystals. Minor anhedral magnetite crystals speckle the unit and are relatively smaller than plagioclase (~ 0.1mm). The matrix is crystal supported and larger fragments (0.5-6 cm) contain an abundance of plagioclase that form interlocking networks of the crystal laths. This is in contrast to the underlying lithic tuff unit in which tuffaceous and lapilli sized fragments are dominantly porphyritic. Grain size variations are not observed in outcrop and there is no measurable layering. In thin section however, grading is observed. Sedimentary structures are not observed and reworking is not evident. The unit lies just above augite porphyritic lapilli tuff. The plagioclase tuff unit does not interlayer with the underlying unit; rather it is an abrupt but conformable lithologic boundary. The absolute age of this unit has not been determined; however from stratigraphic relationships it is interpreted to be younger than the underlying porphyritic tuff and lapilli tuff. Because of the crystal supported nature of this unit, the absence of sedimentary structures and lack of evidence to support reworking (e.g. crystals are euhedral), the unit is interpreted to represent a pyroclastic deposit, following the recommendations of Schmid (1981). Small variations in grading observed in thin section are most likely a reflection of preferential fall out during air fall

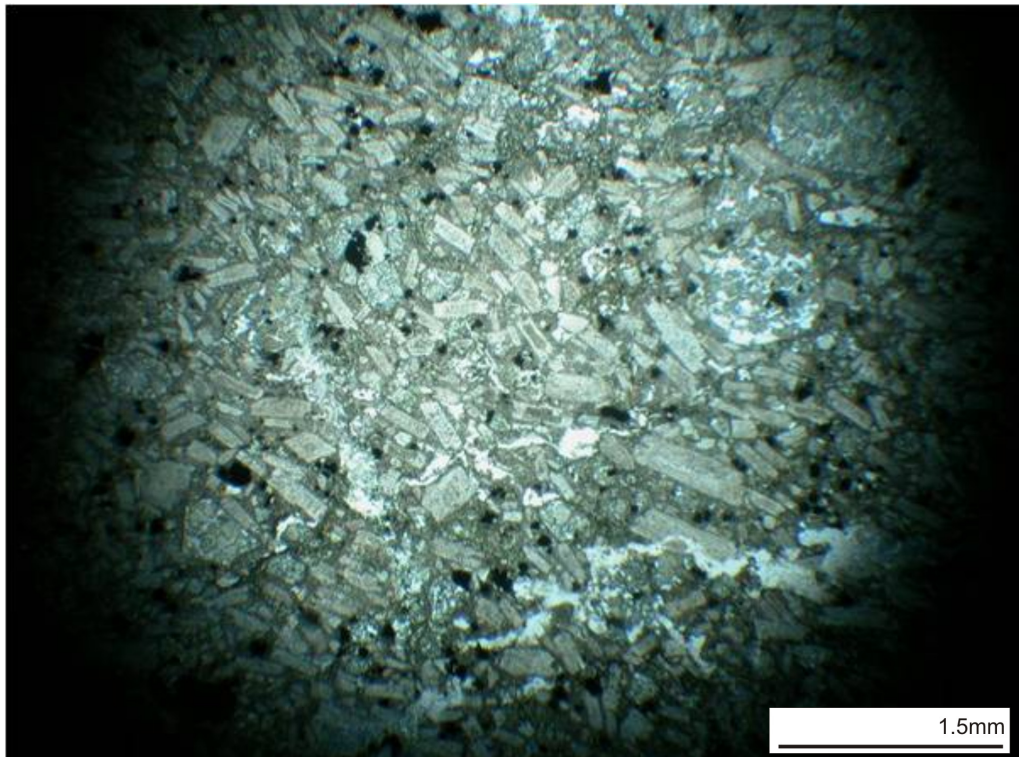


Plate 2.2.2: Plagioclase > augite porphyry. Note trachytic texture. Alignment is interpreted to represent flow direction.



Photo 2.2.2: Plagioclase lapilli tuff. Lapilli size fragments weather with high relief

deposition. Finer grained portions (0.1-2 mm) of this unit are interpreted as crystal tuff and coarser portions (fragments ranging from 2 mm-6 cm) are considered a plagioclase rich lapilli tuff.

**Heterolithic Augite – Plagioclase Porphyritic Lapilli Tuff and Volcanic Breccia:
LTrNaftb (4)**

Lying stratigraphically atop dominantly plagioclase-bearing tuff and its reworked equivalents are augite-rich porphyritic tuff, lapilli tuff and volcanic breccia. The unit forms a succession approximately 350-500 m thick and extends along strike across the entirety of the map area. Exposures range from deep green to maroon in colour, and weathered surfaces make the fragmental nature of this unit apparent. Fragments of varying compositions and textures weather grey, green and maroon. Augite and plagioclase are the dominant minerals of the unit and fragments are dominantly augite porphyritic. Mineralogically, all fragments are similar but the ratio of augite to plagioclase within separate fragments can vary. Fragments also display varying igneous textures such as porphyritic textures, trachytic textures and interlocking crystal laths. Most fragments are augite or augite and plagioclase phyric, with phenocrysts encased in an aphanitic matrix. The proportion of matrix to phenocrysts can vary from about 60:40 to ~ 15:85. Phenocrysts can range in size from 0.5- 2 mm on average; however augite crystals are generally larger than plagioclase and can reach up to 5 mm. Augite phenocrysts are observed to be either floating in an aphanitic matrix or within a groundmass defined by an interlocking network of plagioclase laths. In the later case, plagioclase is generally larger (1-2 mm) and more abundant, constituting ~80% of total rock while augite phenocrysts (~1-1.5 mm) make up approximately 20% of the total rock. When plagioclase is the dominant phenocryst, the texture is generally trachytic, with phenocrysts ranging in size from 0.3 – 2 mm.

There is little evidence of reworking in these deposits. The fragments can range in

shape from sub-angular to sub-rounded, but the majority maintain cusped, sub-rounded boundaries. There is also an absence of definitive sedimentary structures and there is no significant amount of epiclastic material found within the unit. Generally, sorting is poor but increases to moderate within the finer grained portions of the unit (≤ 3 mm). Larger fragments (6- 30 cm) are matrix supported, where the matrix is comprised of porphyritic fragments and individual, whole or broken crystals of plagioclase and augite. Fragments can show varying degrees of alteration, but typically exposures of the unit are fresh and original mineralogy and volcanic textures are preserved. No absolute age for the unit has been determined; however the unit rests stratigraphically atop and is interlayered with plagioclase tuff and augite porphyritic lapilli tuff, suggesting that lower portions (interlayered within the underlying plagioclase tuff) are as old as the plagioclase tuff and the upper portions are relatively younger.

On the basis of the observations above, it is interpreted that the unit is dominantly pyroclastic. Individual fragments, for the most part, range in size from 2-60 mm and following recommendations outlined in Schmid (1981), the term lapilli tuff is used to describe this pyroclastic unit. Where fragment size ranges from 15 to 30 cm in size, this unit can be characterized as a pyroclastic breccia, containing block-sized, sub-angular fragments (Schmid, 1981). Some fragments have characteristic shapes which are commonly observed throughout the unit. For example, tear-drop shaped fragments are common. They are interpreted to have been molten during flight (Photo 2.2.3). The wide (stoss) side would represent the front side of the bomb and the tapered (lee) side was most likely produced by frictional air resistance dragging the plastic wall or skin of the bomb toward the rear. Where observed in fragments greater than 64 mm, the term agglomerate would be appropriate.

Interlayered Volcaniclastic and Pyroclastic Rocks: LTrNaps (5)

Augite ± plagioclase porphyritic volcaniclastic rocks underlie a relatively large portion of the map area, extending along strike from the northwest corner of the map sheet (where it is structurally juxtaposed with a down-faulted block of Eocene Kamloops Group volcanic rocks) for over 20 kilometres to the southeast where the unit is unconformably overlain by Miocene flood basalts (Figure 2.1.1). Only a minimum thickness can be estimated because the upper portion of the unit is intruded by various phases of the Iron Mask batholith (Figure 2.1.1). At its thickest point the volcaniclastic succession is at least 2.5 km thick. Fine grained portions (grain size < 2 mm) of the unit are deep green in colour and weathered surfaces are pink. Individual fragments within coarser portions of the unit (grain size > 2 mm) weather with a range of colours (purple, maroon, red, pink, grey, light green) which is largely a reflection of mineralogical differences between fragments.

The composition of this unit is similar to underlying pyroclastic rocks, containing predominantly augite and plagioclase. The unit is defined on the basis of grain size variations, reworked volcanic textures and sedimentary structures.

Fine to medium grained portions (0.1-0.5 mm) of this unit contain predominantly plagioclase crystals. Minor amounts (< 5%) of mafic minerals, including augite and actinolite, are observed in thin section. These mafic crystals are relatively small (~0.2 mm) and are generally broken off pieces of crystals. These crystals are tightly packed together generating a crystal supported texture. The unit is well sorted and crystals show minor degrees of rounding at crystal corners. Coarse grained portions (1-2 mm) contain plagioclase and augite porphyritic fragments. Fragments are subangular to subrounded and sorting is moderate.

Sedimentary structures were observed in the fine-medium grained portions of the unit. Load features, flame structures and convolute bedding are common and useful in determining way up for these beds. These structures indicate rapid deposition. Sediments



Photo 2.2.3: Augite porphyritic lapilli tuff. Note tear drop shape of outlined lapilli fragment. This shape is commonly observed within the pyroclastic unit of the Nicola Group and is interpreted to be indicative of molten transport.

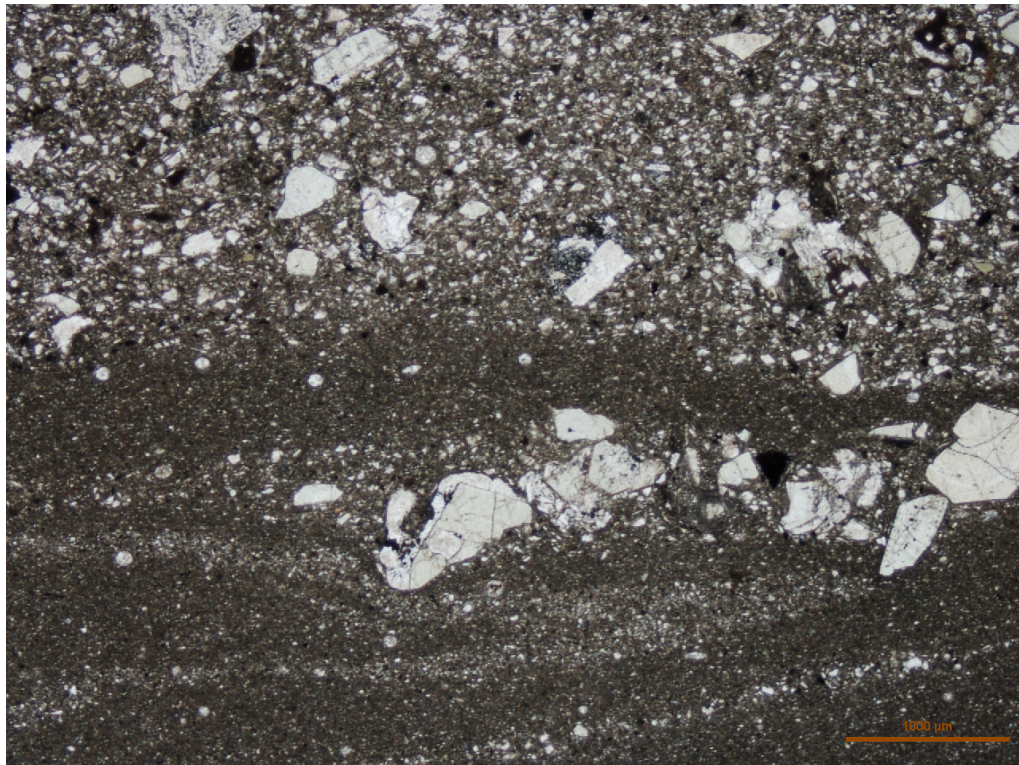


Plate 2.2.3: Volcanogenic mudstone and siltstone interbedded with coarser grained tuffaceous fragments and individual broken crystals of augite. Note rounded spheres ($\sim 0.1\text{mm}$). These are interpreted to have a biological origin and are indicative of a marine depositional environment.

commonly show evidence of compaction where water escape structures and pressure solution are observed in thin section. Cross-laminations were also observed and used to identify way up. These features are clear indicators that this unit represents reworked volcanoclastic material and not primary pyroclastic debris. Well rounded fragments and crystals are only rarely observed in sedimentary material therefore their absence should not preclude interpretation as a volcanoclastic deposit in the Nicola Group (Plate 2.2.3).

In the coarser grained fragmental units (>2 mm), clasts are mainly augite ± plagioclase porphyritic but can vary in texture and modal abundance (Plate 2.2.4). The matrix of these porphyritic fragments can be aphanitic or can contain an interlocking network of plagioclase crystals. Crystal size between individual fragments also varies and plagioclase generally ranges in size from about 0.2-1 mm and is generally euhedral. Porphyritic augite ranges in size from 0.2-2.5 mm. Modal abundances of minerals also vary between individual fragments, and where plagioclase is more abundant than augite (> 60%) fragments generally display trachytic textures. Individual crystals are also grains within the unit. Augite crystals are generally larger than plagioclase (augite size 0.5-2.5 mm: plagioclase size 0.2-1mm). Individual crystals may show minor rounding at corners. Non volcanic or epiclastic fragments are also observed within the unit (e.g. laminated mud clasts (Photo 2.2.4)). Individual fragments also show evidence of independent alteration histories. Phenocrysts of amphibole (pseudomorphing augite) are present in some porphyritic fragments, and some fragments contain chlorite and epidote in the matrix. Plagioclase in these samples is strongly saussuritized at the cores. These fragments occur in the same hand sample as fresh, non-altered fragments containing fresh, igneous zoned augite and twinned plagioclase (not altered at core). The volcanic fragments can be subangular to subrounded, where laminated mud fragments are generally rounded. These coarser portions of the unit are massive and poorly sorted, with fragments ranging in size from ~ 2mm - 15cm. The mineralogical and textural heterogeneities and the varying alteration histories of the fragments suggest

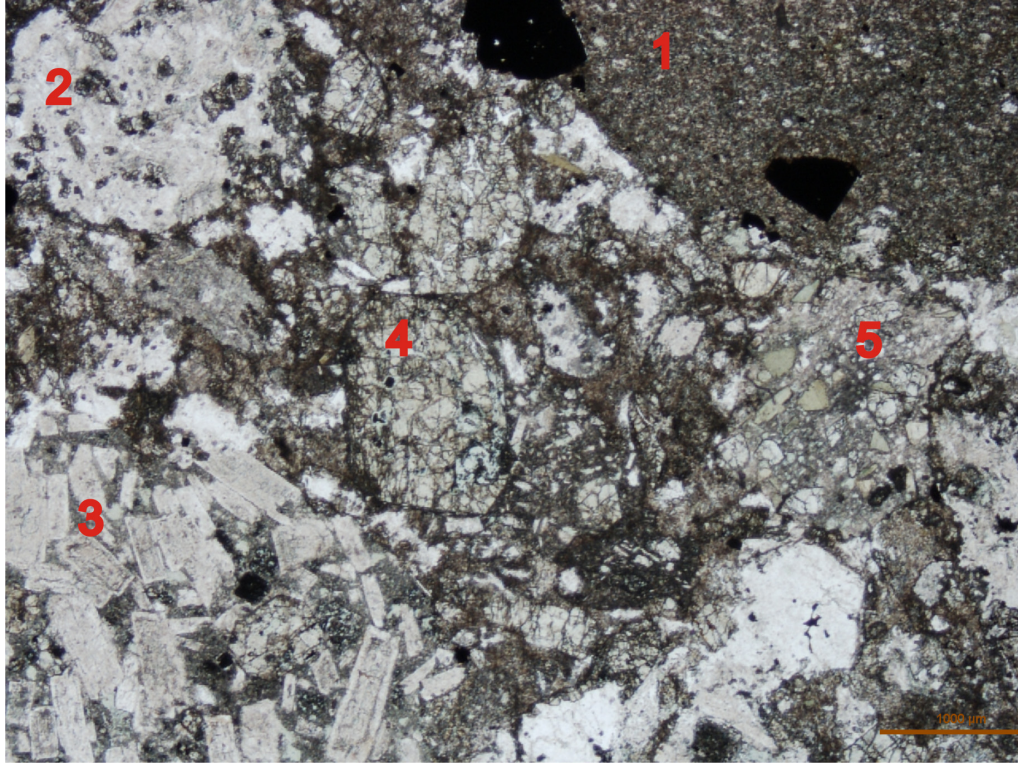


Plate 2.2.4: Coarse grained, heterolithic volcaniclastic. Fragments include: (1) rounded mud clast, (2) clast displaying interlocking plagioclase crystals, (3) plagioclase - augite porphyritic fragment, (4) Individual augite crystal and (5) an augite porphyry fragment.



Photo 2.2.4: Mudclasts within volcaniclastic rocks of the Nicola Group.

that the coarser portions of the unit are volcaniclastic and may be termed a volcanic conglomerate. These conglomerates are interlayered within fine grained sandstone and siltstone that display obvious sedimentary structures (see above text for details).

Unlike the underlying pyroclastic deposits, rocks of this unit (including fine grained and coarse fragmental portions) are not massive, such that changes in average grain and fragment size occur over strike-normal distances of approximately 0.5- 10 m. Within sand and silt sized portions of the unit grain size variations define millimetre - centimetre scale laminations. Deep green exposures of fine- to coarse-grained tuffaceous sandstone, siltstone, and coarser conglomerate are interbedded with less reworked pyroclastic material such as augite \pm plagioclase lapilli tuff. Lateral discontinuity of individual layers and beds is apparent, and no suitable marker horizon within this unit could be distinguished.

Compositional similarities between volcaniclastic rocks and underlying lapilli tuff and volcanic breccia are interpreted to indicate that the volcaniclastic unit represents reworked equivalents of the underlying lithologies. As such, moving up stratigraphy from southwest to the northeast, a transition to increasingly reworked volcaniclastic strata occurs. The contact zone between the underlying lapilli tuff unit and the overlying volcaniclastic rocks is gradational, whereby the stratigraphic contact is defined by the interruption of massive pyroclastic deposits by thin laminations of mudstone and siltstone interbedded with the underlying pyroclastic unit. The first appearance of the mudstone marks the unit's basal contact. Its upper limit is the intrusive contact with the Iron Mask batholith. As such thicknesses recorded are minimum values.

Small spheres of \sim 0.1 mm diameter are found at numerous locations within volcanogenic mudstone and siltstone of unit LTrNaps (Plate 2.2.5). These spheres have been silicified and are observed to have no internal structure. A few of these structures are infilled with carbonate and in rare cases vestiges of a rim or wall type material remains. The relatively larger (than matrix) spheres are matrix supported, suspended within the

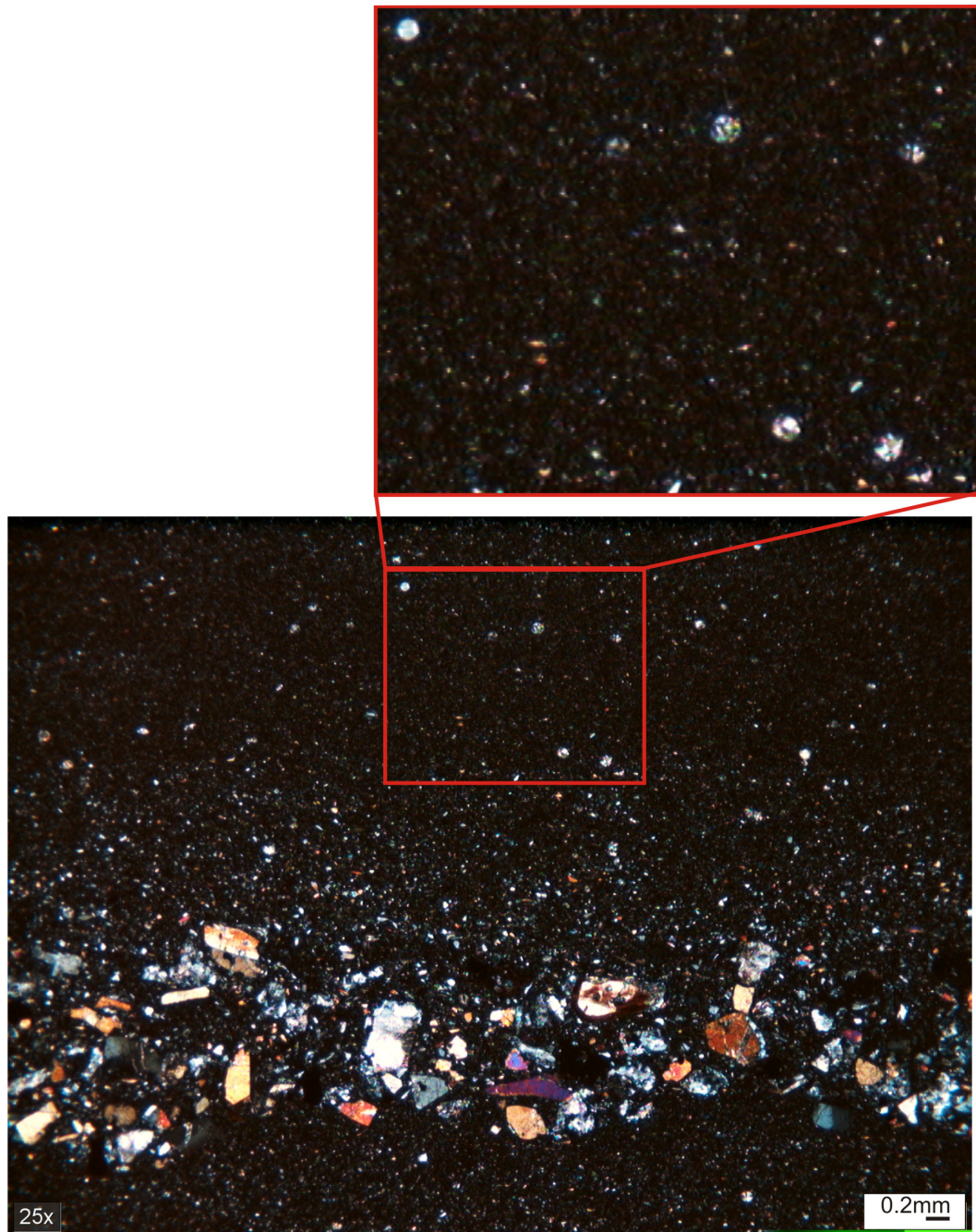
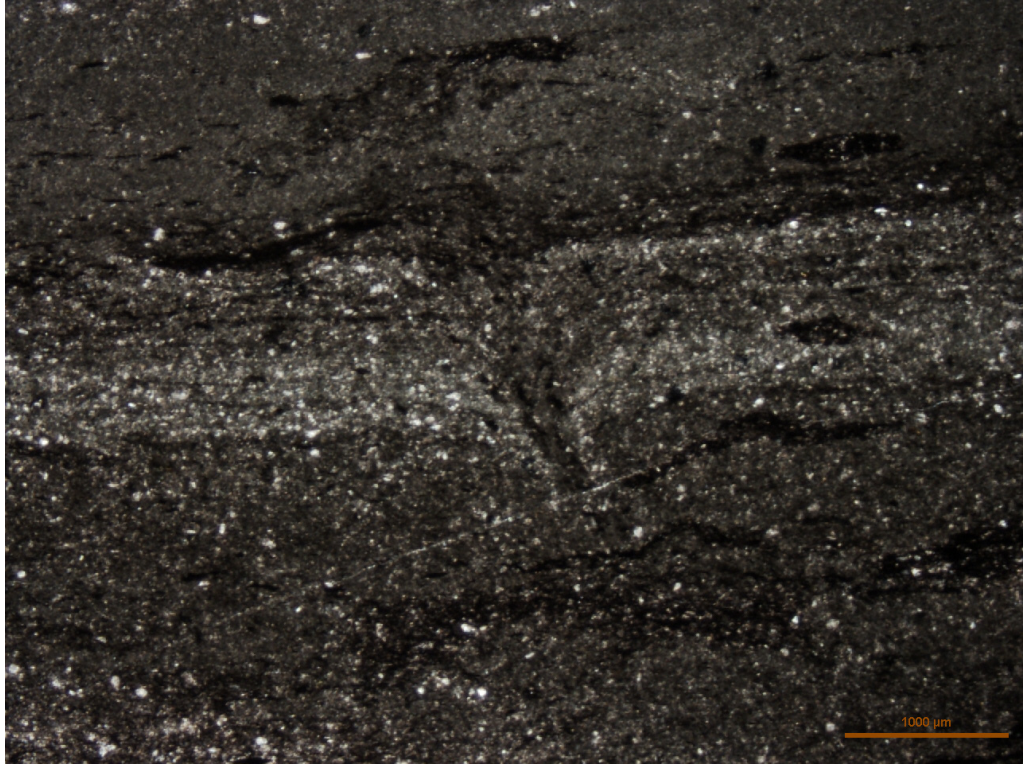


Plate 2.2.5: Small, rounded spheres of diameter ~ 0.1 mm observed within volcanogenic mudstone and siltstone. Their consistent size and shape suggests a biological origin. They are interpreted to indicate that the sediment was deposited in a marine environment.

volcanogenic mud. An igneous origin (e.g. melt origin) can be ruled out due to complete absence of these structures in all igneous and volcanic units within the map area. The consistent size and shape of the structures indicates that the spheres are most likely of biological origin; however, due to the lack of internal structure it is difficult to place a definitive label on the biological structures. The size and shape is consistent with such forms as calcispheres, which are hollow, typically spherical, calcareous nanofossils believed to be algal cysts. Another possibility would be coccoliths, which are calcium carbonate platelets secreted from planktonic organisms called coccolithophores. From the above observations the structures are most likely of marine origin and as such sandstone and mudstone containing the species can be interpreted to have been deposited in a marine environment. Any interpretations beyond this would be completely speculative.

Trace fossils were discovered within finely laminated rocks of the Nicola Group. These fossils are interpreted to be adhesive meniscate burrows (AMB) which are horizontal to vertical burrows characterized by backfill menisci (Plate 2.2.6 a,b.) (M. Gingras pers. comm., 2008). The trace represents the locomotion and feeding behavior of insect larvae moving through the substrate. This behavior is distinctive of soil bugs (Insecta: Hemiptera) and beetles (Insecta: Coleoptera) (Willis and Roth, 1962; Villani et al., 1999). These traces first appear in the rock record in the Permian and can be found today in terrestrial settings, in particular alluvial and marginal- lacustrine environments. The presence of these trace fossils in strata that are interlayered with marine strata suggests that this sequence of Nicola Group rocks was most likely deposited in a transitional marine-terrestrial environment. This idea is further discussed in Section 2.4.



a.)



b.)

Plates 2.2.6 a,b: Adhesive meniscate burrows (AMB). These trace fossils are interpreted to represent locomotion and feeding of soil bugs or beetles. See text for details.

Coarse Augite Porphyritic Flows and Breccia: LTrNap (6)

Augite porphyritic flows and associated breccias occur immediately southwest of the IMB. The unit can range in thickness from 100-700 m, but is most likely thicker, as the upper limit of the unit has been truncated by the Iron Mask batholith (IMB). The unit extends along strike for upwards to 5 kilometres, but its full extent is not evident because it has been interrupted along strike by intrusions (phases of the IMB). Exposures are dark green in colour. Small (~0.2) laths of euhedral plagioclase are in the groundmass with larger euhedral augite phenocrysts ranging in size from 0.5 to 4 mm. Augite is pseudomorphed by actinolite in samples that have been hornfelsed near the margin of the batholith (Plate 2.2.7) (Location 1*). Brecciated portions consist entirely of augite porphyritic fragments. Fragments are angular to subrounded and can range in size from 10 cm to over 50 cm. The unit is massive, however outcrop distributions suggest that the unit strikes northwest, parallel to the regional stratigraphic trend, and therefore it does not cross-cut Nicola Group strata. As such the unit is interpreted to be a porphyritic basaltic flow, interlayered within volcanoclastic and pyroclastic units of the Nicola Group and is therefore part of the Nicola Group stratigraphic sequence. Interlayering indicates that deposition of volcanoclastic strata in the basin was punctuated by periodic emplacement of volcanic flows of similar texture and composition. Absolute ages for the unit were not obtained, but from stratigraphic relationships it is clear that deposition of flows was coeval with deposition of volcanoclastic material. Representative augite compositions are displayed in table 2.2.1 (sample 334-sw).

Coarse Augite-Plagioclase Porphyritic Flows and Breccia: LTrNafp (7)

Augite - plagioclase porphyritic rocks are interlayered within volcanoclastic and pyroclastic strata of the Nicola Group. The unit is relatively thin, with an average thickness of approximately 100 m and it is discontinuous along strike, extending for a maximum length of 1.2 km. The colour is maroon to purple, which may reflect deposition

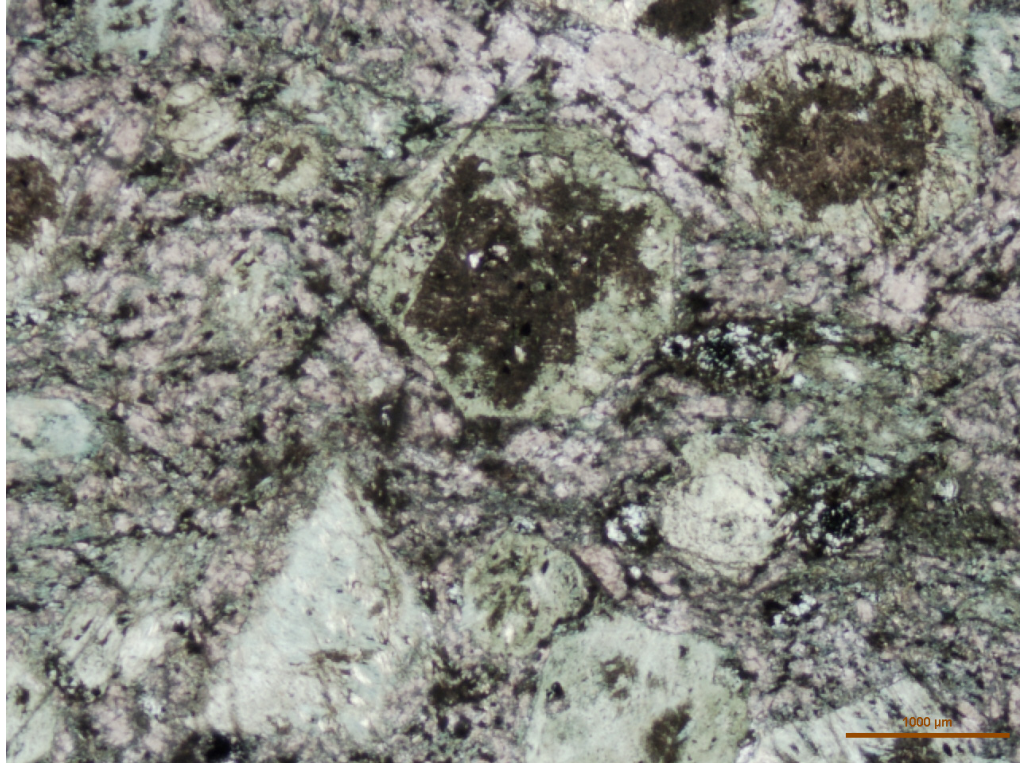


Plate 2.2.7: Near the margin of the batholith volcanic rocks of the Nicola Group are hornfelsed. The plate shows augite having been pseudomorphed by actinolite.

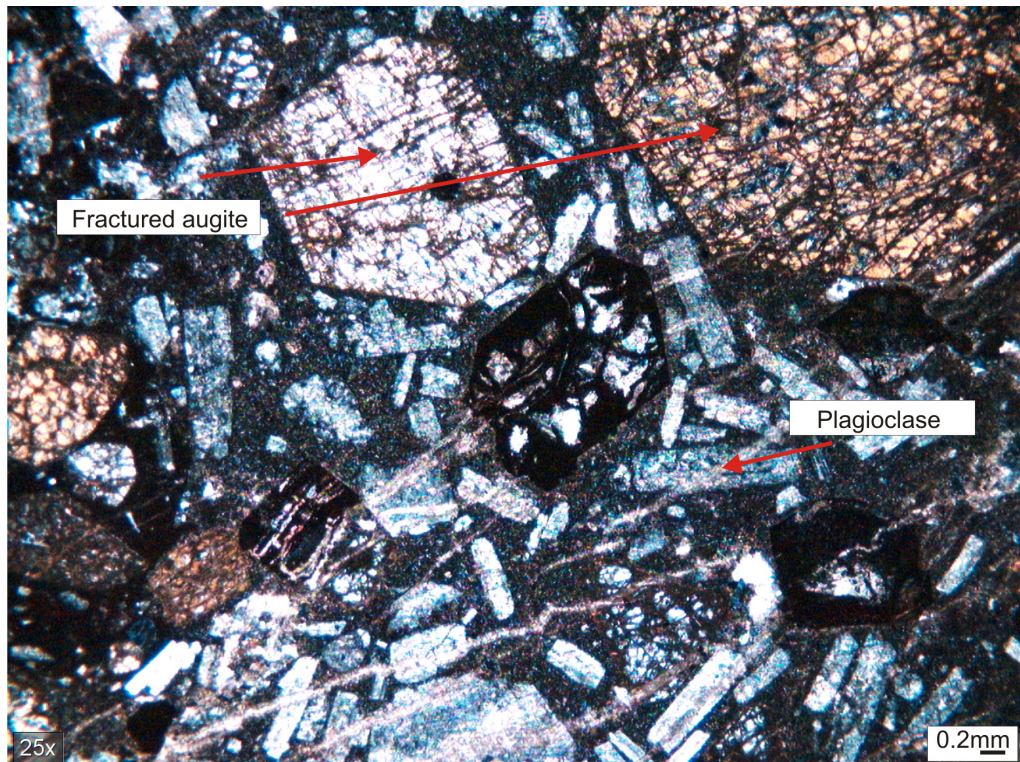


Plate 2.2.8: Augite + plagioclase porphyry. In hand sample, augite displays a creamy white colour which may be the result of a relatively lower Fe/Mg ratio. See text for details.

in a subaerial environment. In weathered outcrops, a brecciated texture is often more readily observed. The unit is pyroxene and plagioclase porphyritic with crystals occurring in roughly equal modal abundance. Pyroxene phenocrysts are much coarser in size (~0.5 cm) with euhedral plagioclase laths being < 1 mm. The pyroxenes (sample 234-sw, Table 2.2.1) display a creamy white colour, which is perhaps the result of an overall lower Fe/Mg ratio (relative to augite compositions of unit LTrNap, sample 334-sw: Table 2.2.1). The matrix is aphanitic in hand sample (Plate 2.2.8). In general, the unit lacks measurable layering. These porphyries are interpreted to be an extrusive phase on the basis of the unit's concordant map pattern and interlayering with volcanoclastic and pyroclastic rocks of the Nicola Group. These porphyritic flows and volcanic breccias however, are discontinuous and individual flows cannot be followed along strike for more than a few 10's of metres. It is interpreted that these discontinuous flows were extruded intermittently during deposition of Nicola Group volcanoclastic strata and are therefore coeval with this unit.

Picritic Volcanic Breccia: LTrNop (8)

Augite-olivine porphyries are found in close proximity to the Iron Mask batholith (IMB), interlayered within the upper portions of the volcanoclastic rocks of the Nicola Group (LTrNaps). These porphyries occur as small, poorly exposed, lenticular bodies generally 100-300 m in thickness and extend northwest, along strike, for approximately 0.5 - 2 km. Exposures are generally deep green to black and weathering can give outcrops a red to orange colour. The unit is a coarse, olivine-augite bearing porphyry with olivine phenocrysts being subhedral to euhedral and ranging in size from approximately 1-4 mm. Augite is generally euhedral, smaller (~0.5mm) and displays distinct igneous zoning in fresh samples. Olivine phenocrysts range in abundance from 25-30 % and augite abundance is approximately 35-40 %. Olivine was preserved in one sample, but most samples generally display phenocrysts of serpentine, which is interpreted to have

Sample 234 Pyroxene analysis												Sample 334 Pyroxene analysis																	
Weight %						Augite						Augite																	
SiO2	48.88	51.50	51.58	51.05	52.25	52.40	50.15	51.09	CaO	21.51	21.64	21.90	21.72	21.61	SiO2	48.88	51.50	51.58	51.05	52.25	52.40	50.15	51.09	CaO	21.51	21.64	21.90	21.72	21.61
TiO2	0.77	0.41	0.42	0.40	0.22	0.23	0.52	0.44	TiO2	0.36	0.43	0.36	0.43	0.41	TiO2	0.77	0.41	0.42	0.40	0.22	0.23	0.52	0.44	TiO2	0.36	0.43	0.36	0.43	0.41
Al2O3	5.42	2.77	2.84	3.14	2.25	2.24	4.44	3.25	Al2O3	3.94	4.29	3.45	3.72	5.42	Al2O3	5.42	2.77	2.84	3.14	2.25	2.24	4.44	3.25	Al2O3	3.94	4.29	3.45	3.72	5.42
FeO	8.26	7.25	7.34	8.16	5.80	5.90	7.80	7.26	FeO	8.41	8.69	8.01	8.29	9.20	FeO	8.26	7.25	7.34	8.16	5.80	5.90	7.80	7.26	FeO	8.41	8.69	8.01	8.29	9.20
MnO	0.23	0.27	0.29	0.32	0.16	0.15	0.22	0.26	MnO	0.65	0.75	0.72	0.63	0.83	MnO	0.23	0.27	0.29	0.32	0.16	0.15	0.22	0.26	MnO	0.65	0.75	0.72	0.63	0.83
MgO	13.72	15.23	15.30	14.94	16.42	16.43	14.42	15.16	MgO	14.15	14.14	14.66	14.59	13.59	MgO	13.72	15.23	15.30	14.94	16.42	16.43	14.42	15.16	MgO	14.15	14.14	14.66	14.59	13.59
CaO	21.99	22.01	21.74	21.02	22.19	21.73	21.88	22.23	CaO	0.00	0.00	0.00	0.00	0.03	CaO	21.99	22.01	21.74	21.02	22.19	21.73	21.88	22.23	CaO	0.00	0.00	0.00	0.00	0.03
Na2O	0.40	0.31	0.32	0.41	0.23	0.27	0.38	0.34	Na2O	49.59	49.51	50.31	50.45	48.47	Na2O	0.40	0.31	0.32	0.41	0.23	0.27	0.38	0.34	Na2O	49.59	49.51	50.31	50.45	48.47
K2O	0.00	0.00	0.02	0.01	0.01	0.01	0.00	0.00	K2O	0.23	0.20	0.22	0.19	0.24	K2O	0.00	0.00	0.02	0.01	0.01	0.01	0.00	0.00	K2O	0.23	0.20	0.22	0.19	0.24
Total	99.71	99.76	99.85	99.45	99.53	99.36	99.84	99.80	Total	98.87	99.65	99.66	100.01	99.80	Total	99.71	99.76	99.85	99.45	99.53	99.36	99.84	99.80	Total	98.87	99.65	99.66	100.01	99.80
Number of ions based on 6 oxygen												Number of ions based on 6 oxygen																	
Si	1.832	1.915	1.915	1.908	1.932	1.938	1.869	1.899	Si	1.873	1.858	1.882	1.881	1.823	Si	1.832	1.915	1.915	1.908	1.932	1.938	1.869	1.899	Si	1.873	1.858	1.882	1.881	1.823
Ti	0.022	0.011	0.012	0.011	0.006	0.006	0.014	0.012	Ti	0.018	0.021	0.020	0.018	0.024	Ti	0.022	0.011	0.012	0.011	0.006	0.006	0.014	0.012	Ti	0.018	0.021	0.020	0.018	0.024
Al	0.239	0.121	0.124	0.138	0.098	0.098	0.195	0.142	Al	0.175	0.190	0.152	0.163	0.240	Al	0.239	0.121	0.124	0.138	0.098	0.098	0.195	0.142	Al	0.175	0.190	0.152	0.163	0.240
Fe	0.259	0.225	0.228	0.255	0.179	0.182	0.243	0.226	Fe	0.266	0.273	0.251	0.258	0.289	Fe	0.259	0.225	0.228	0.255	0.179	0.182	0.243	0.226	Fe	0.266	0.273	0.251	0.258	0.289
Mn	0.007	0.009	0.009	0.010	0.005	0.005	0.007	0.008	Mn	0.007	0.006	0.007	0.006	0.008	Mn	0.007	0.009	0.009	0.010	0.005	0.005	0.007	0.008	Mn	0.007	0.006	0.007	0.006	0.008
Mg	0.767	0.844	0.847	0.832	0.905	0.906	0.801	0.840	Mg	0.796	0.791	0.818	0.811	0.762	Mg	0.767	0.844	0.847	0.832	0.905	0.906	0.801	0.840	Mg	0.796	0.791	0.818	0.811	0.762
Ca	0.883	0.877	0.864	0.842	0.879	0.861	0.873	0.876	Ca	0.870	0.870	0.878	0.867	0.871	Ca	0.883	0.877	0.864	0.842	0.879	0.861	0.873	0.876	Ca	0.870	0.870	0.878	0.867	0.871
Na	0.029	0.022	0.023	0.030	0.016	0.019	0.028	0.025	Na	0.026	0.031	0.026	0.031	0.030	Na	0.029	0.022	0.023	0.030	0.016	0.019	0.028	0.025	Na	0.026	0.031	0.026	0.031	0.030
K	0.000	0.000	0.001	0.000	0.000	0.000	0.000	0.000	K	0.000	0.000	0.000	0.000	0.001	K	0.000	0.000	0.001	0.000	0.000	0.000	0.000	0.000	K	0.000	0.000	0.000	0.000	0.001
Total	4.039	4.025	4.023	4.027	4.021	4.016	4.032	4.030	Total	4.034	4.041	4.034	4.036	4.049	Total	4.039	4.025	4.023	4.027	4.021	4.016	4.032	4.030	Total	4.034	4.041	4.034	4.036	4.049
Mg/(Mg+Fe)	0.748	0.789	0.788	0.765	0.835	0.832	0.767	0.788	Mg/(Mg+Fe)	0.750	0.744	0.765	0.758	0.725	Mg/(Mg+Fe)	0.748	0.789	0.788	0.765	0.835	0.832	0.767	0.788	Mg/(Mg+Fe)	0.750	0.744	0.765	0.758	0.725

Table 2.2.1: Representative microprobe analyses for augite phenocrysts in units LTrNap and LTrNapf. Note overall higher Fe/Mg ratios for sample 334 (unit LTrNap).

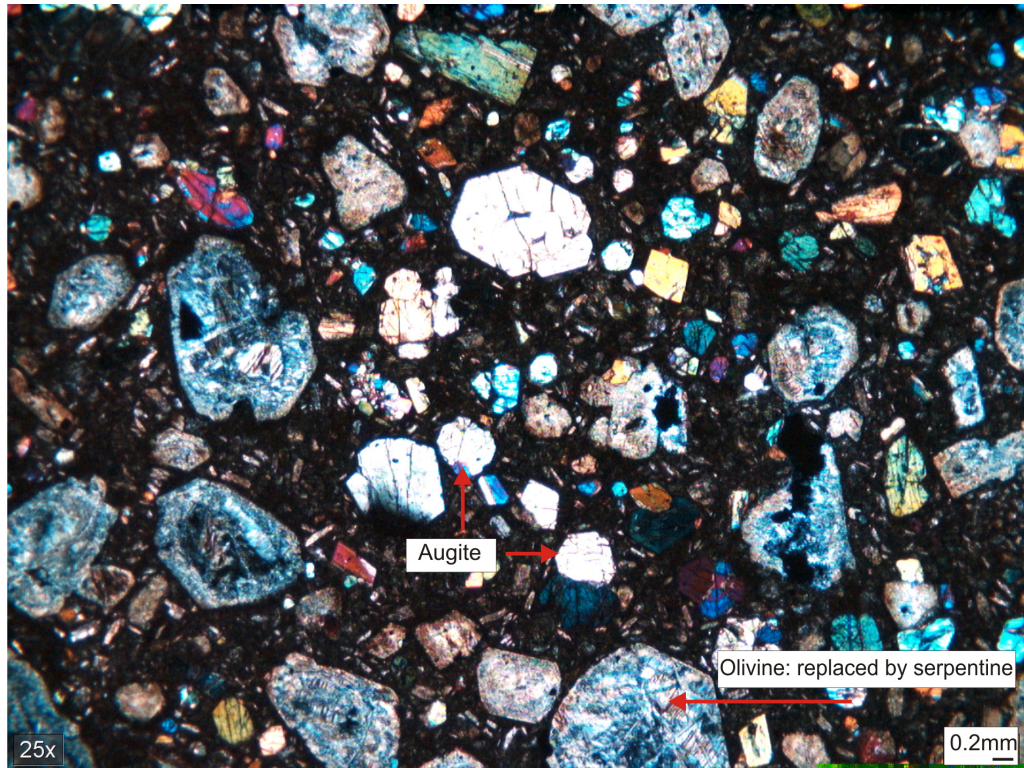


Plate 2.2.9: Picritic basalt. Note that olivine has been completely replaced by serpentine.



Photo 2.2.5: Outcrop exposure of picritic basalt. Note that fragments weather with high relief, giving the outcrop a "knobby" appearance. Fragments are defined by groupings of olivine + augite phenocrysts.

replaced olivine (Plate 2.2.9). The groundmass is typically fine grained and altered to serpentine or talc. Because of the abundance of olivine, the unit has previously been labeled picrite (e.g. Snyder and Russell, 1993, 1994). Whole rock geochemical data from this unit is available in Snyder and Russell (1994). In many exposures, the picrite displays a brecciated texture defined by groupings or clusters of crystals and when weathered these groupings retain a high relief, giving the outcrop a knobby appearance (Photo 2.2.5). These fragments were observed to range, on average, from approximately 5 to 15 cm but can be smaller (1-5cm). Because the picrite is observed to be interlayered within volcaniclastic strata of the Nicola Group (Figure 2.1.1) it is interpreted to represent discontinuous flows, and the brecciated texture is interpreted as a volcanic flow texture. Previous authors have also interpreted the picrite as an extrusive phase (e.g. Snyder and Russell, 1993, 1994) and Logan and Mihalynuk (2005) observed a similar stratigraphic relationship (e.g. the picrite being part of the Nicola Group stratigraphy).

Where the picrite is in fault contact with the IMB, the picrite is completely serpentinized, displaying light to dark green slick surfaces in outcrop. Picrite is intruded by phases of the IMB locally, such as in the south wall of the Ajax West pit (Figure 2.1.1), where serpentinized picrite is intruded by the Sugarloaf phase (e.g. Stanley, 1994; Stanley et al., 1994) of the IMB. Weathered outcrops are rubbly and some have partially been reduced to a bright green-bluish picritic regolith.

Augite Porphyritic Volcanic Breccias and Laharic Deposits: LTrNvl (9)

Augite porphyritic volcanic breccias and laharic deposits occur both north and south of the Iron Mask batholith and underlie a relatively minor portion of the map area (Figure 2.1.1). South of the Iron Mask batholith, augite porphyritic breccias form a relatively narrow lens, interlayered within augite porphyritic tuff and lapilli tuff, with an approximate thickness of 200 m and a lateral extent of ~1 km along strike. The unit can vary in colour from green to maroon or purple. Green exposures consist mainly of blocks



Photo 2.2.6: Augite porphyritic volcanic breccia.

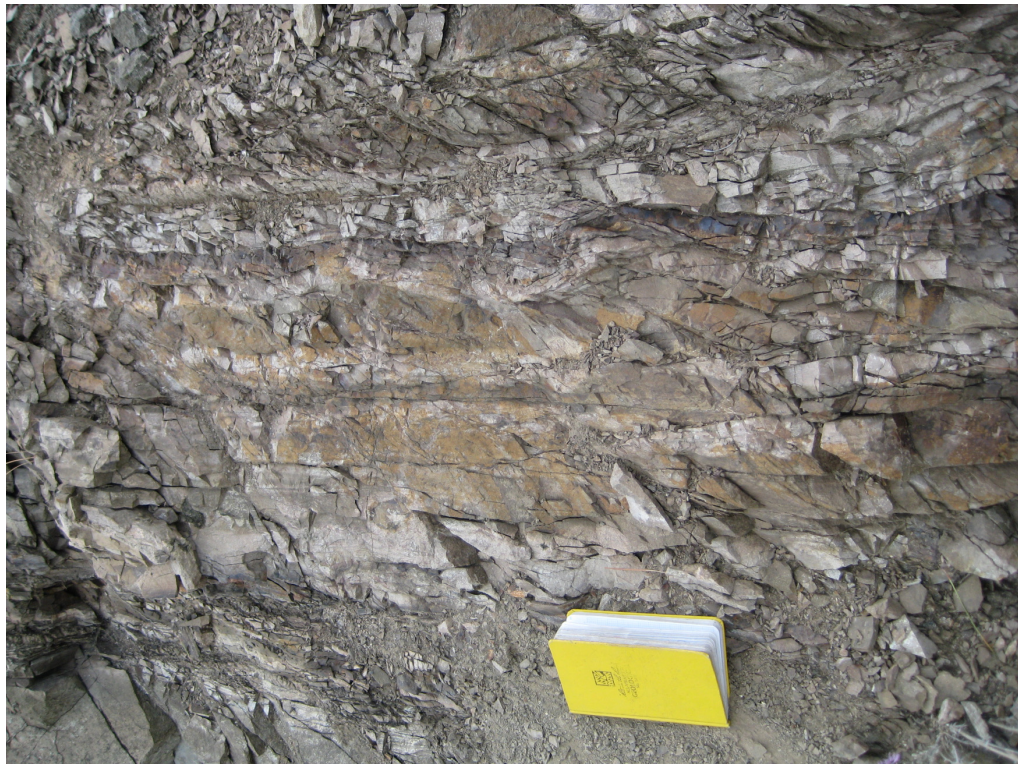


Photo 2.2.7: Red coloured, plagioclase rich, fine to coarse grained sandstone and siltstone interbedded with volcanic breccia and conglomerate.

of augite porphyritic volcanic material and are found south of the Iron Mask batholith (Photo 2.2.6). North of the IMB, the deposits are maroon or purple in colour and contain more intrusive material with clasts of monzonite to monzodiorite, many of which display alteration halos with epidote and potassium feldspar. Volcanic clasts within these portions of the unit include plagioclase-augite porphyry and augite porphyry.

South of the Iron Mask batholith the breccias are massive, poorly sorted and fragments are mainly sub-angular. The clasts are matrix supported, with the ratio of matrix to fragments being 1:1. The fragments range in size from about 0.5 mm to over 0.5 m. North of the Iron Mask batholith, the unit displays layering, is better sorted in finer (pebble to cobble size) facies and has less matrix. Smaller volcanic fragments (10-20 cm) show rounding and clasts are smaller on average (5-20 cm). These features suggest that north of the IMB the unit has been reworked by sedimentary processes. Red, fine to coarse grained sandstone and siltstone and pebble conglomerate are interlayered within coarse (10-20 cm), reworked, fragmental rocks (Photo 2.2.7).

North of the IMB, the unit has been interpreted as a lahar (Logan and Mihalynuk, 2005). The observations above, however, suggest portions of the lahar unit have been re-sedimented and are more correctly referred to as either volcanic conglomerate or breccia. Layering can be observed in lahar deposits of the Nicola Group, however it is generally more subtle in coarse grained portions (>2mm). South of the IMB there is no clear evidence to suggest that these augite porphyritic breccias were the result of volcanic debris being transported by water and the term volcanic breccia (rather than lahar) is therefore preferred. These breccias appear to represent coarser equivalents of the augite porphyritic tuff and lapilli tuff. The breccias are interlayered within augite porphyritic tuff and lapilli tuff and as such are interpreted to be coeval with this unit.

Nicola Group Sedimentary Facies: LTrNs (10)

Occupying the northeast corner of the map sheet, bounded to the southwest by the

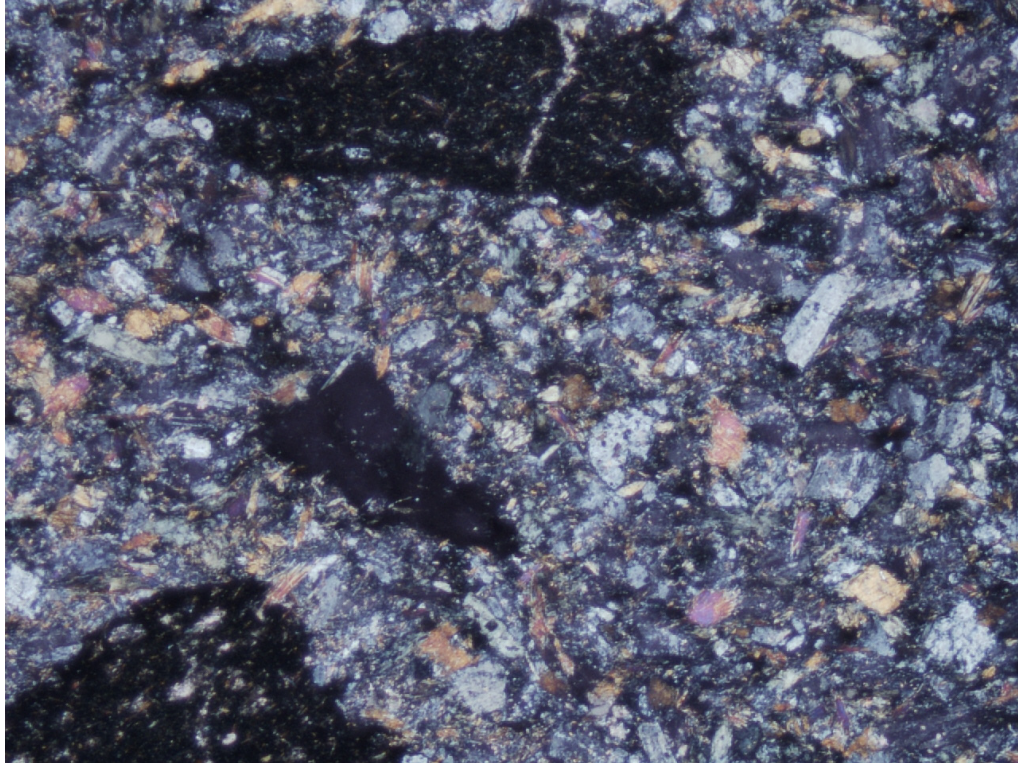


Plate 2.2.10: Meta-sediments of the Dome Hills succession of the Nicola Group. The mineral assemblage is indicative of greenschist-amphibolite facies metamorphism. See text (Section 3.4) for details.



Photo 2.2.8: Planar laminated mudstone and siltstone of the Dome Hills succession of the Nicola Group.

IMB and extending northeast beyond the limit of mapping, are metasedimentary rocks of the Nicola Group. The unit strikes north-northwest and exposures are dominantly grey to dark grey in colour. From thin section, a metamorphic mineral assemblage of amphibole-plagioclase-epidote-quartz \pm carbonate is observed. The assemblage is indicative of upper greenschist or lower amphibolite facies metamorphism (see Chapter 3: Plate 2.2.10). The unit is planar laminated in areas, with laminations being of mm-scale thicknesses. The laminations are defined by grain size variations and the corresponding shade of grey colouration. The laminations are interpreted to be primary sedimentary features that have been preserved during regional metamorphism (Photo 2.2.8). The laminated portion of the unit is dominantly mudstone and siltstone, and is interlayered with fine grained sandstone. Grey, massive, fine grained sandstone, with little to no variation in composition or grain size, form intervals up to 30 metres thick. Within these massive units are mudstone intraclasts, which appear to be flattened, possibly due to compaction. Porphyritic units are interlayered within sedimentary strata and form lenses approximately 500 m thick and about 3 km in length. These porphyritic units, containing phenocrysts altered to chlorite, follow stratigraphy and as such are interpreted as volcanic flows, although a sill origin cannot be ruled out. Individual flows are no more than 20 m in thickness. From lithological similarity, this unit is correlated with the Dome Hills succession mapped by Beatty (2003) approximately 5 km northeast of Kamloops. The Dome Hills succession has been interpreted to young to the east (M.J. Orchard Pers. Comm., 2002, in Beatty, 2003), which is similar to the interpretation of facing direction for the volcanic and volcanoclastic succession just south of the IMB. Fossil collections from massive micritic and bioclastic limestone within the Dome Hills succession 5 km northeast of the study area indicate a late Carnian to early Norian age for the unit (Beatty, 2003).

Undivided Volcanic and Sedimentary Rocks: LTrNu (11)

Underlying an area directly south of the Cherry Creek Tectonic Zone are metamorphosed Nicola Group rocks. The metamorphic rocks continue south for approximately 3-4 km where they are intruded by the LeJeune granodiorite (Figure 2.1.1, Section 2.3). Exposures of these rocks are generally light or dark grey to green. Rocks are observed to have the mineral assemblage plagioclase-hornblende-biotite-epidote-clinozoisite, indicating that rocks south of the CCTZ have undergone amphibolite grade metamorphism (Chapter 3). Hornblende-biotite schist underlies an extensive portion of the area and is interlayered with coarse tectonized porphyry (Photo 2.2.9). Phenocrysts are hornblende pseudomorphing augite, and as such the unit is interpreted to represent a metamorphosed equivalent of augite porphyries, similar to those north of the CCTZ (e.g. Unit LTrNap). Hornblende-biotite schist could be derived from fine grained volcanoclastic material similar to volcanoclastic sediments to the north of the CCTZ (e.g. unit LTrNaps). In some outcrops, the fragmental nature of the unit has been preserved, and a shape-defined foliation is observed. Porphyritic fragments and rounded clasts of epiclastic material, such as mud or clay, have been flattened into the plane of schistosity (Plate 2.2.11) (Photo 2.2.10). These units are interpreted to represent metamorphosed equivalents of coarser fragmental volcanoclastic rocks (e.g. unit LTrNaps) observed north of the CCTZ. Schistose rocks weather recessively; hence exposure in the southern map region is especially poor and subdivision of the Nicola Group in this zone was not possible.

Eocene Kamloops Group: EKav (12)

Unconformably overlying Nicola Group rocks are Middle Eocene volcanic and sedimentary rocks of the Kamloops Group (Ewing, 1981). Rocks of the Kamloops Group occur in scattered localities throughout the map area, occurring as both kilometre-wide outliers and in large (tens of kilometres in length) down-dropped fault blocks along



Photo 2.2.9: Tectonized augite porphyry of the Nicola Group observed south of the Cherry Creek Tectonic Zone.



Plate 2.2.11: Volcanic fragments displaying a shape-defined foliation south of the Cherry Creek Tectonic Zone. A weak schistosity, defined by mica (biotite) is formed within micaceous matrix and wraps around deformed volcanic fragments.



Photo 2.2.10: Flattened mudstone clasts define the foliation in fragmental volcaniclastic portions of the Nicola Group.



Photo 2.2.11: Miocene vesicular basalt.

the northwest, north, and northeast portions of the IMB (Figure 2.1.1). Sedimentary rocks include tuffaceous sandstone, siltstone and shale with lesser conglomerate. The volcanic rocks are predominantly basalt and andesite, but can be rhyolitic (Ewing, 1981). Outcrops are observed to be purple and red in colour. In the north wall of the Afton pit, the Kamloops Group is observed to be dropped down along steeply dipping faults and is structurally juxtaposed alongside Nicola Group rocks (e.g. Logan and Mihalynuk, 2006; Figure 2.1.1).

Miocene Basalts: Mivb (13)

The youngest rocks in the area are Miocene alkaline flood basalts (Logan and Mihalynuk, 2005) which unconformably overlie all volcanic and intrusive rocks in the map area. These flat-lying basalts occupy an extensive region of approximately 50 km² in the southeast corner of the map sheet (Figure 2.1.1). The basalts also occur as small, 0.5-0.25 km² outliers in the southern portion of the study area, unconformably overlying undivided Nicola Group rocks and intrusive phases of the Nicola batholith (Figure 2.1.1). The basalts are brown to dark grey in colour, aphanitic and are commonly vesicular (Photo 2.2.11).

2.3 Intrusive Rocks Exposed in the Nicola Horst

In the south-central portion of the study area, plutonic rocks of the Nicola batholith are exposed in the Nicola horst (e.g. Ewing, 1980; Moore and Pettipas, 1990) (Figure 2.1.1). From outcrop distribution it is estimated that these intrusive phases underlie an area of approximately 20 km² within the map region. Earlier authors (e.g. Preto et al., 1979; McMillan et al., 1981) referred to these intrusive phases as the Nicola batholith, however subsequent radiometric dating of plutonic rocks has led to the interpretation that the batholith is part of a crustal block that rose from deeper levels in the crust in Cenozoic time (Ewing, 1980; Monger and McMillan, 1984). Studies by

Moore et al. (2000) and Ghosh (2003) recognized that there are at least 6 distinct plutonic phases (Figure 6.3.1). Two of these phases have been identified and mapped in this study. They are the Paleocene Frogmoore granodiorite and the Late Jurassic - Early Cretaceous LeJeune granodiorite described below.

Late Jurassic- Early Cretaceous LeJeune Biotite Granodiorite: ECLgd

The LeJeune granodiorite is exposed in the northernmost part of the Nicola horst. It is a medium to coarse grained biotite granodiorite, with biotite constituting 5-7% of the total rock. Feldspars constitute up to 50% of the rock, with plagioclase being much more abundant than potassic feldspar, which comprises no more than 10%. The feldspars occur as phenocrysts and within the equigranular groundmass along with quartz, which constitutes approximately 25 – 30%. Concentrically zoned, igneous titanite also occurs as an accessory mineral, and can reach up to 2 mm in length. A distinguishing feature of this rock is the feldspar megacrysts, which have been observed to range from 1 to 5 cm in length (Photo 2.2.12). They display simple twins visible in outcrop. A very weak planar fabric defined by coarse biotite grains can be identified in many outcrops. Biotite can be altered to epidote and chlorite.

An absolute age for the LeJeune granodiorite has been determined using radiometric dating techniques. A U/Pb date from titanite yielded a date of 144 +/- 1.6 Ma (Moore et al., 2000). In this study, a sample collected from the LeJeune granodiorite yielded a U/Pb zircon age of 144.8 +/- 5.9 Ma (Chapter 4), in agreement with previous results.

Another intrusive phase, the Bush Lake granodiorite, has been identified just north of the LeJeune granodiorite (Ghosh, 2003). Ghosh (2003) indicated that the units were difficult to distinguish from each other but stated that, in general, the Bush Lake granodiorite has more prominent (biotite-defined) foliation and smaller K-feldspar megacrysts (1-3 cm), as opposed to the 5-9 cm K-feldspars found in the LeJeune



Photo 2.2.12: Feldspar megacryst within LeJeune biotite granodiorite phase of the Nicola batholith.



Photo 2.2.13: Well developed foliation is formed locally in small, metre-wide zones distributed across the Frogmoore Granodiorite phase of the Nicola batholith. The fabric is associated with a prominent north-trending lineation, defined by elongate quartz ribbons.

granodiorite. In this study, the Bush Lake granodiorite is considered indistinguishable from, and is mapped as a component of, the LeJeune granodiorite.

Hornblende-Biotite Granodiorite (Frogmoore Granodiorite): PFgd

The Frogmoore Granodiorite underlies an area of approximately 7 km² directly east of and in intrusive contact with the LeJeune granodiorite (Figure 2.1.1). The unit is a hornblende-biotite granodiorite being composed mainly of feldspars, with plagioclase being the most abundant mineral (~ 45 %). Plagioclase occurs as large 2-3 cm (long) phenocrysts and as a groundmass mineral. Plagioclase displays lamellar twinning and concentric zoning. Potassic feldspar constitutes only about 10% of the total volume. Quartz, which displays undulose extinction, constitutes approximately 30-35 modal %. Hornblende and biotite combined constitute less than 10 % of the rock. Secondary epidote is also present in minor amounts (3-5%) and trace amounts of titanite are closely associated with the mafic minerals. Generally, the unit is not strongly deformed; however a well developed foliation is formed locally in small, metre-wide zones distributed across the entire extent of the unit within the mapped region (Photo 2.2.13). The fabric is defined by both biotite and hornblende and is observed to wrap around large feldspar phenocrysts. This planar fabric is associated with a prominent north-trending lineation, defined by elongate quartz ribbons. This observation suggests that quartz has deformed ductilely in relatively higher strain zones. A U/Pb zircon date of 64.5 +/- 0.1 Ma has been obtained for the granodiorite (Moore et al., 2000).

2.4 Volcanic Facies and Depositional Environment

According to Fisher and Schmincke (1984), the products of ancient volcanoes can be divided into three facies based on the relative proximity of the deposits to the volcanic center. These are the near-source, intermediate-source and distant-source facies. For arc assemblages in particular, these three facies have been recognized as a central

eruptive center (near-source facies), flanked by fans, aprons, or shelves (intermediate-source facies) and a basinal facies, such as trench, fore-arc basins and back-arc basins (intermediate- to distant-source facies) (Dickinson, 1974). From lithological observations summarized below, it is interpreted that Nicola Group rocks underlying the Kamloops region can be divided into at least two distinct volcanic facies, an intermediate (fan or apron) facies and a distant, back-arc basin facies. These facies were deposited in at least two different depositional environments: a transitional (aerial - marine) environment and a marine environment.

Intermediate-Source Facies

Southwest of the Iron Mask batholith and northeast of the Cherry Creek Tectonic Zone Nicola Group rocks are characterized by a thick sequence of massive, primary pyroclastic rocks including: plagioclase-augite porphyritic tuff, augite porphyritic lapilli tuff and volcanic breccia (Figure 2.1.1 Units 1-9). These units show little or no evidence of post-eruptive sedimentary reworking, as crystals are euhedral, fragments are sub-angular to sub-rounded with cusped boundaries, coarser fragmental units are poorly sorted and pyroclasts show evidence indicative of molten transport. Higher in the Nicola Group stratigraphic succession rocks transition to a dominantly volcanoclastic unit predominantly comprising reworked pyroclastic material. Laminated material displays sedimentary features and the fragmental volcanoclastic unit contains an abundance of heterolithic volcanic fragments and minor non-volcanic derived material (e.g. laminated mud clasts) which are interpreted to indicate reworking by sedimentary transport and resedimentation (see Section 2.2.1 for details).

Volcanoclastic material is compositionally similar to the underlying pyroclastic material and is, for the most part, compositionally and texturally immature. Grains are not rounded and sorting is poor, indicating that volcanoclastic material experienced only limited transport and was likely redeposited proximal to its source. Southeast of Jacko

Lake, fine grained tuffaceous sandstones contain an abundance of detrital carbonate material (> 30 modal %). The detrital limestone fragments are interpreted to have been derived from a nearby reefoid limestone bed within the volcanic-sedimentary rocks. The source of detritus was most likely proximal, as detrital carbonate grains are not generally transported significant distances before dissolving. Reefoid limestone is commonly observed in the western and central belts of the Nicola Group (Preto, 1979). Thus the composition and sedimentology of volcanoclastic rocks in the upper portions of the Nicola Group stratigraphic succession are consistent with derivation from equivalents of the underlying Nicola Group volcanic rocks.

According to Fisher and Schmincke (1984), intermediate-source facies include rocks deposited from pyroclastic flows, fallout processes, lava flows and their reworked equivalents. The distance between source and deposit and the amount of resedimented pyroclastic and epiclastic volcanic debris within the deposit is directly proportional. The above observations are interpreted to suggest that volcanic and volcanoclastic rocks between the Iron Mask batholith and Cherry Creek Tectonic Zone are an intermediate-source facies (Fisher and Schmincke, 1984).

Transitional Aerial to Marine Environment

South of the study area, the depositional setting of the Nicola Group has been interpreted to be transitional marine to aerial (Preto, 1979; Lefebure, 1976). Between Merritt and Princeton, Preto (1979) interpreted red and purple flows and associated red laharic breccias to be of subaerial origin, and green coloured flows, lapilli-tuff, volcanic breccias and calcareous sandstones to indicate a marine setting. Red subaerial flows and lahars are generally highly oxidized and nonmagnetic, whereas green lahars may be intercalated with lenses of limestone and water-lain sediments and were deposited in a reducing marine environment (Preto, 1979).

A similar scenario is observed in this study in the vicinity of the Iron Mask batholith. Colour variations may be used as a proxy for depositional environment of

some Nicola Group rocks. Green coloured, coarse grained pyroclastic deposits are massive and lack internal structure such as sorting or grading. This most likely reflects the shorter length of time that material fell through the water column before it was deposited. These deposits were therefore most likely deposited at shallow marine levels. Deep green to bluish green volcanogenic siltstone and mudstone contain biological material (Section 2.2.1), indicative of a marine environment. Deep green exposures of fine grained tuffaceous sandstone interlayered with marine mudstone also display soft sediment deformation features such as: ball and pillow structures, associated flame features demonstrating the perturbation of mud extending from the margins of the balls, and convolute bedding. These features indicate rapid deposition of material such as in underwater debris flows, where the underlying beds become unstable and are hence internally deformed. This type of deformation could have taken place along slopes in the marine environment.

Capping the Nicola Group succession are laharic debris flows and probable reworked sedimentary equivalents: red plagioclase-rich sandstone, siltstone and volcanic conglomerate. Although some lahars may have flowed into the ocean, lahars at the top of the Nicola Group with a red hematitic ash matrix, similar to those to the north of the IMB (Logan and Mihalynuk, 2005), are interpreted to have been deposited in a subaerial environment. A transition from rocks deposited in a dominantly marine environment in the basal portions of the Nicola Group stratigraphy to rocks deposited in an aerial environment at the top of the group is therefore interpreted.

Distant-Source Facies

Directly northeast of the IMB there is an abrupt transition to the Nicola Group sedimentary facies. Rocks consist of finely laminated mudstone and siltstone, massive mudstone and minor basalt of the Dome Hills succession (Beatty, 2003). Volcaniclastic rocks are generally not coarser than coarse sandstone. According to Fisher and

Schmincke (1984), within the distant-source facies, lava flows and pyroclastic flows are absent, as they cannot travel such distances. Fall-out tephra and isolated ash deposits is most often observed, as are isolated ash deposits. Layers are generally thin and well sorted.

The above observations are therefore interpreted to indicate that the succession was deposited in a basin that was relatively distant from volcanic centers (e.g. distant-source facies: Fisher and Schmincke, 1984).

Marine Depositional Environment

Thick sequences of mudstone were most likely deposited at somewhat deeper marine levels, however thick sequences of mud may also accumulate during tectonically and magmatically quiet periods. Intervals of laminated mudstone probably reflect slow and steady deposition and minor basaltic flows may have been extruded along the sea floor. Although no limestone intervals are observed in the study area, Beatty (2003) documents rare limestone interbeds, some of which form massive linear bodies within the Dome Hills succession, approximately 14 km north and east of the city of Kamloops. Because Nicola Group sediments in the study area are correlated with rocks of the Dome Hills succession (Beatty, 2003) (see Section 2.2.1), the observations of Beatty (2003) further support the interpretation that mudstone and laminated mudstone and siltstone of the Dome Hills succession within the study area most likely reflect deposition in a marine environment as apposed to being deposited during a period of no tectonic activity. Marine sediments of the Dome Hills succession are interpreted to have been deposited east of the Nicola volcanic arc in a distal back arc basin setting (distant facies). Later faulting occurred along a northwest striking fault system, juxtaposing the marine facies rocks and rocks deposited in the transitional aerial-marine environment. Hence the fault system presently separates the two distinct facies. Evidence supporting fault juxtaposition of these disparate successions is discussed in detail in chapter 5, Section 5.5.1.

2.5 References

- Beatty, T.W. 2003. Stratigraphy of the Harper Ranch Group and tectonic history of the Quesnel terrane in the area of Kamloops, British Columbia. M.Sc. thesis, Simon Fraser University, Burnaby, B.C. 213 p.
- Dickinson, W.R. 1974. Sedimentation within and beside ancient and modern magmatic arcs; In Modern and ancient geosynclinal sedimentation, Dott, Jr., R.H. and Shaver, R.H., Editors. Soc. Econ. Paleont. Mineral. Sp. Publ. **19**: 230-239.
- Ewing, T.E. 1980. Paleogene tectonic evolution of the Pacific Northwest. *Journal of Geology* 88: 619-638.
- . 1981. Regional stratigraphy and structural setting of the Kamloops Group, south-central British Columbia. Mem. 249 *Geological Survey of Canada*. 164 p.
- Fisher, R.V. and H.-U. Schmincke. 1984. Pyroclastic Rocks. Springer-Verlag, Berlin Heidelberg New York Tokyo.
- Ghosh, S. 2003. Petrology. Geochemistry, Geochronology and Tectonic History of the Nicola Horst, B.C. M.Sc. thesis, Simon Fraser University, Burnaby, B.C.
- Lefebure, D.V. 1976. Geology of the Nicola Group in the Fairweather Hills, B.C. M.Sc. thesis. Queen's University, Kingston, Ontario.
- Logan, J.M., and M.G. Mihalynuk. 2005. Porphyry Cu-Au Deposits of the Iron Mask Batholith Southeastern British Columbia: In Geological Fieldwork 2004. *British Columbia Geological Survey Branch, Paper 2005-1*.
- . 2006. Geology of the Iron Mask Batholith. Open File Map 2006-11. *British Columbia Geologic Survey Branch*.
- McMillan, W.J., Armstrong, R.L. Harakal, J. 1981. Age of the Coldwater Stock and Nicola Batholith, near Merritt (92H). *British Columbia Department of Mines and Petroleum Resources, Geological Fieldwork*: 102-105.
- Monger, J.W.H., and W.J. McMillan. 1984. Bedrock geology of Ashcroft (92 I) map area. Geological Survey of Canada.

- Moore, J.M., J.E. Gabites, and R.M. Friedman. 2000. Nicola Horst: toward a geochronology and cooling history. In Cook, F. and Erdmer, P. (Compilers). Slave-Northern Cordillera Lithospheric Evolution (SNORCLE) Transect and Cordillera Tectonic Workshop Meeting, February 25-27.2000. *University of Calgary*, no. Lithoprobe Report No. 72: 177-185.
- Moore, J.M. and A.R. Pettipas. 1990. Geological studies in the Nicola Lake region (92 I/SE); Part A. In Nicola Lake region geology and mineral deposits. *British Columbia Geological Survey Branch, Open File 1990-29*.
- Preto, V.A. 1979. Geology of the Nicola Group between Merritt and Princeton, British Columbia. *British Columbia Ministry of Energy, Mines and Petroleum Resources*, no. Bulletin 69: 90.
- Schmid, R. 1981. Descriptive nomenclature and classification of pyroclastic deposits and fragments: Recommendations of the IUGS Subcommittee on the Systematics of Igneous Rocks. *Geology* 9: 41-43.
- Snyder, L.D. and Russell, J.K. 1993. Field Constraints on the diverse igneous processes in the Iron Mask batholith (92L/9); in Geological Fieldwork 1992, BC Ministry of Energy, Mines and Petroleum Resources, Paper 1993-1: 281-286.
- . 1994. Petrology and stratigraphic setting of the Kamloops Lake picrite basalts, Quesnellia Terrane, south-central B.C. (92I/9, 15 and 16); in Geological Fieldwork 1993, BC Ministry of Energy, Mines and Petroleum resources, Paper 1994-1: 297-311.
- Stanley, C.R. 1994. Geology of the Pothook alkali copper-gold porphyry deposit, Afton Mining Camp, British Columbia; Unpublished M.Sc. thesis, The University of British Columbia, Vancouver, British Columbia, 192 pages.
- Stanley, C.R., Lang, J.R. and Snyder, L.D. (1994): Geology and mineralization in the northern part of the Iron Mask batholith, British Columbia (92I/9, 10); in Geological Fieldwork 1993, BC ministry of Energy, Mines and Petroleum

Resources, Paper 1994-1: 269-274.

Villani, M.G., L.L. Allee, A. Diaz, and P.S. Robbins. 1999. Adaptive strategies of edaphic arthropods. *Annual review of Entomology* 44: 233-256.

Willis, and Roth. 1962. Soil and moisture relations of *Scaptocoris divergins* Troeschner (Hemiptera: Cynidae). *Annals of the Entomological Society of America* 55: 21-32.

Chapter 3: Metamorphism

3.1 Introduction

Rocks of the Nicola Group are variably but generally weakly metamorphosed. Most rocks within the study area are massive and lack tectonic fabric. Original igneous textures are typically preserved and rocks appear to be fresh or only weakly altered. Variations in the degree of metamorphism can be observed locally near intrusions or at major shear zones, where minerals indicative of higher grades can be found and secondary fabrics are developed.

Fresh, unaltered basaltic flows and fragmental units contain zoned augite and plagioclase crystals. Close to the margin of the Iron Mask batholith, rocks can be hornfelsed. In these samples, actinolite has completely replaced augite phenocrysts and plagioclase laths have been saussuritized.

Metre-wide, hornblende porphyritic dykes intrude the volcanoclastic unit of the Nicola Group (Location 2*). Hornblende phenocrysts commonly define trachytic texture in the dykes. The unit is dioritic in composition with plagioclase and hornblende phenocrysts commonly being 1-2 mm in size. The dykes are interpreted to be part of the Sugarloaf diorite, the youngest intrusive phase of the Iron Mask batholith (e.g. Stanley, 1994; Stanley et al., 1994). Sugarloaf dykes are radially oriented around Sugarloaf Hill, which Snyder and Russell (1993) interpreted as a volcanic neck and intrusive center. In this study, a similar radial arrangement of metre-wide dykes was observed southeast of a large, northwest trending lenticular body (~ 1 km x 500 m) of Sugarloaf rocks directly south of the Ajax East deposit (Figure 2.1.1) (Location 3*). This intrusive body may therefore represent another volcanic center. Volcanic rocks in contact with or near the margins of the Sugarloaf diorite dykes are metamorphosed and recrystallized to a greenschist-facies mineral assemblage of epidote, actinolite and chlorite.

North of the Iron Mask batholith and South of the Cherry Creek Tectonic Zone rocks bear mineral assemblages indicative of greenschist-amphibolite and

amphibolite facies conditions respectively. Metamorphic fabrics resulting from regional metamorphism are present in rocks underlying these regions. The following section will describe the metamorphic assemblages and fabrics formed within rocks underlying these regions.

3.2 Analytical Methods

In order to estimate the peak metamorphic grade of meta-Nicola Group rocks, quantitative mineral compositional data was collected from carbon coated thin sections using the JEOL 8900 electron microprobe at the University of Alberta. Wavelength dispersive spectroscopy (WDS) analyses were conducted at an accelerating voltage of 15k eV with a 15 nA beam and a spot size of 3-5 μm . Standards used for calibration are listed in appendix 1. Data reduction was done using the $\phi(\rho Z)$ correction (Armstrong, 1995). The composition of secondary standard was reported within error margins that were defined by counting statistics, therefore the calibration was considered successful.

3.3 Rocks South of the Cherry Creek Tectonic Zone: Domain [3]*

South of the Cherry Creek Tectonic Zone (CCTZ: Figure 2.1.1) meta-Nicola Group rocks bear the mineral assemblage plagioclase-amphibole-biotite-chlorite-epidote-clinozoisite. Rocks in this domain appear to be more strongly deformed and metamorphosed than those directly north of the CCTZ (Plate 3.3.1). Major element compositions of representative minerals are displayed in tables 3.3.1 a,b. Phenocrysts of calcic amphiboles and the majority of groundmass amphibole contain the following proportion of cations: $(\text{Na} + \text{K}) < 0.5$, $\text{Ca} > 1.5$, $7.5 > \text{Si} > 6.5$. According to Deer et al. (1992) these amphiboles are hornblende, and because $\text{Mg}/(\text{Mg}+\text{Fe}^{2+}) > 0.5$, the name magnesiohornblende is more appropriate according to recommendations by Leake et al. (1997). One analysis of a hornblende porphyroclast showed a rim of actinolite, which is interpreted to represent retrograde metamorphic mineral growth. Analysis of

an amphibole grain within the groundmass determined the amphibole to be actinolite. It is uncertain, however, whether the analysis represented the entire grain or whether the analysis also represents a rim of retrograde mineral growth.

Plagioclase composition of individual grains ranges from An_{23} – An_{46} , indicating the coexistence of both oligoclase and andesine. The presence of calcic plagioclase with magnesiohornblende would indicate that the sample was metamorphosed at amphibolite facies conditions, whereby the transition from greenschist to amphibolite facies is defined by the replacement of the (actinolite + albite) pair to the (hornblende + calcic plagioclase) pair (e.g. Bucher and Frey, 2002). These changes occur as metamorphic temperatures approach 500°C (e.g. Bucher and Frey, 2002), indicating that these rocks have most likely seen temperatures of this degree or slightly higher. The presence of epidote within rocks south of the CCTZ places an upper limit on peak temperature and pressure, as the stability of epidote is pressure sensitive. At intermediate pressures, epidote will persist to higher temperatures and at lower pressures epidote persists at a lower temperature, giving rise to the epidote amphibolites facies (Figure 3.3.1). Thus, compositional and petrological data constrain peak metamorphism in the footwall of the CCTZ to be approximately $3.0 < P \text{ (kbar)} < 11$ and $500^\circ < T \text{ (}^\circ\text{C)} < 650^\circ$. This is consistent with thermobarometry results reported by Ghosh (2003), in which the author estimated peak metamorphic conditions to be $\sim 3.1 < P \text{ (kbar)} < 3.7$ and $475^\circ < T \text{ (}^\circ\text{C)} < 525^\circ$.

Minerals of the peak metamorphic assemblage – biotite and hornblende – define a pervasive schistosity in meta-Nicola Group rocks. A penetrative mineral lineation (defined by biotite and aligned hornblende) associated with the planar fabric is indicative of general non-coaxial shear. The disparity in metamorphic grade and intensity of tectonic fabrics developed strongly supports a tectonic juxtaposition of Nicola Group rocks on either side of the CCTZ.

Sample 827 Amphibole analysis
weight %

	Hbl (GM)	Act (GM)	Hbl (Core)	Hbl (Core)	Hbl (Rim)	Act (Rim)	Hbl (Core)	Act (GM)
SiO2	50.15	53.45	48.56	49.35	51.94	53.24	52.92	52.33
TiO2	0.51	0.25	0.36	0.36	0.10	0.20	0.25	0.12
Al2O3	7.60	4.23	8.32	7.51	4.70	4.18	4.62	5.43
FeO	9.56	8.36	10.58	10.40	9.31	8.56	8.78	8.59
MnO	0.24	0.18	0.19	0.18	0.22	0.18	0.18	0.22
MgO	15.69	17.73	15.12	15.77	17.19	17.55	17.61	16.85
CaO	12.45	12.74	11.94	12.54	12.59	12.61	12.63	12.34
Na2O	0.66	0.36	1.09	0.84	0.55	0.41	0.43	0.54
K2O	0.43	0.18	0.55	0.51	0.19	0.19	0.22	0.17
Cl	0.01	0.00	0.01	0.02	0.01	0.02	0.00	0.02
Total	97.32	97.47	96.75	97.46	96.81	97.17	97.67	96.64
Number of ions based on 23 Oxygen								
Si	7.190	7.569	7.060	7.118	7.461	7.569	7.445	7.501
Ti	0.055	0.026	0.039	0.039	0.011	0.021	0.021	0.027
Al	1.284	0.705	1.426	1.276	0.796	0.701	0.878	0.772
Fe	1.147	0.990	1.286	1.254	1.119	1.018	1.033	1.041
Mn	0.029	0.022	0.023	0.022	0.027	0.021	0.024	0.022
Mg	3.353	3.743	3.278	3.391	3.681	3.720	3.663	3.721
Ca	1.913	1.932	1.860	1.938	1.938	1.920	1.943	1.918
Na	0.183	0.098	0.307	0.235	0.154	0.114	0.122	0.119
K	0.079	0.033	0.101	0.093	0.035	0.034	0.046	0.039
Cl	0.002	0.000	0.003	0.005	0.003	0.005	0.004	0.000
Total	15.237	15.118	15.386	15.370	15.224	15.126	15.179	15.162

Table 3.3.1a: Representative microprobe analyses of amphibole grains in biotite-amphibole schist unit south of the Cherry Creek Tectonic Zone. See text for details.

Sample 827 Plagioclase analysis

	And		Olig		And		Olig		And		And		And		Olig		And		Lab		And	
	Weight %		Weight %		Weight %		Weight %		Weight %		Weight %		Weight %		Weight %		Weight %		Weight %		Weight %	
SiO2	56.44	60.91	57.52	60.83	56.04	56.22	55.92	55.99	56.43	62.30	60.23	52.85	59.68									
TiO2	0.00	0.02	0.01	0.00	0.02	0.01	0.00	0.00	0.00	0.03	0.02	0.02	0.00									
Al2O3	28.44	25.38	27.69	25.08	28.10	27.87	28.11	28.57	28.55	24.57	25.48	30.46	25.68									
FeO	0.08	0.13	0.10	0.19	0.11	0.15	0.16	0.12	0.12	0.13	0.01	0.00	0.01									
MnO	0.00	0.03	0.04	0.01	0.02	0.00	0.00	0.00	0.00	0.02	0.00	0.01	0.01									
MgO	0.02	0.00	0.02	0.00	0.01	0.01	0.04	0.00	0.00	0.00	0.02	0.02	0.00									
CaO	9.24	5.96	8.48	5.66	9.33	9.20	9.45	9.71	9.43	4.84	6.39	12.13	6.62									
Na2O	6.07	8.20	6.50	8.33	6.25	6.25	6.12	6.06	6.20	8.84	7.92	4.45	7.71									
K2O	0.07	0.09	0.10	0.13	0.08	0.08	0.06	0.08	0.06	0.08	0.10	0.03	0.08									
Total	100.37	100.71	100.53	100.29	99.99	99.79	99.88	100.57	100.80	100.83	100.17	100.00	99.79									
Number of ions based on 8 Oxygen																						
Si	2.521	2.688	2.560	2.696	2.517	2.529	2.515	2.502	2.514	2.738	2.674	2.389	2.662									
Ti	0.000	0.001	0.000	0.000	0.001	0.000	0.000	0.000	0.000	0.001	0.001	0.001	0.000									
Al	1.497	1.320	1.452	1.310	1.488	1.477	1.490	1.505	1.499	1.272	1.333	1.623	1.349									
Fe	0.003	0.005	0.004	0.007	0.004	0.006	0.006	0.004	0.005	0.005	0.000	0.000	0.000									
Mn	0.000	0.001	0.001	0.000	0.001	0.000	0.000	0.000	0.000	0.001	0.000	0.001	0.000									
Mg	0.001	0.000	0.002	0.000	0.001	0.000	0.002	0.000	0.000	0.000	0.001	0.001	0.000									
Ca	0.442	0.282	0.404	0.269	0.449	0.443	0.455	0.465	0.450	0.228	0.304	0.587	0.316									
Na	0.525	0.701	0.561	0.716	0.544	0.545	0.534	0.525	0.536	0.753	0.681	0.390	0.666									
K	0.004	0.005	0.006	0.007	0.004	0.005	0.003	0.004	0.003	0.005	0.005	0.002	0.004									
Total	4.994	5.004	4.994	5.009	5.013	5.007	5.008	5.008	5.006	5.004	5.001	4.995	4.999									
%An	45.7	28.6	41.9	27.3	45.2	44.9	46.1	47.0	45.7	23.2	30.8	60.1	32.2									

Table 3.3.1b: Representative microprobe analyses of plagioclase grains in biotite-amphibole schist unit south of the Cherry Creek Tectonic Zone. See text for details.

P-T Diagram Showing the Principal Metamorphic Facies

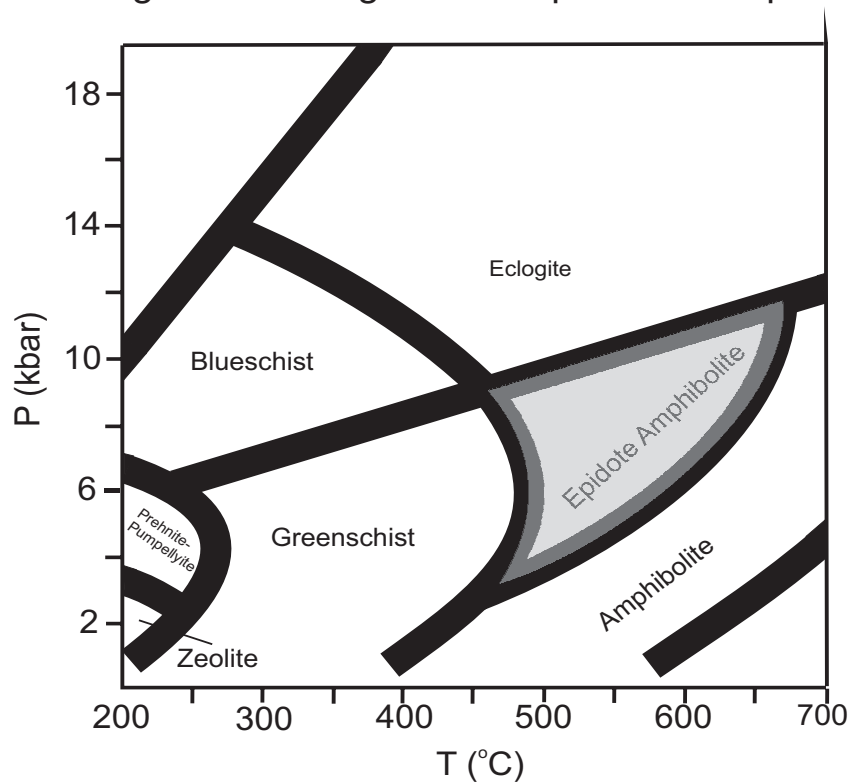


Figure 3.3.1: Diagram showing the principle metamorphic facies for metabasite rocks. The shaded region represents the region in P-T space where rocks of typical mafic composition would have been metamorphosed under epidote-amphibolite conditions (ie: such as those south of the Cherry Creek Tectonic Zone). See text for details (Figure modified from Spear, 1993).

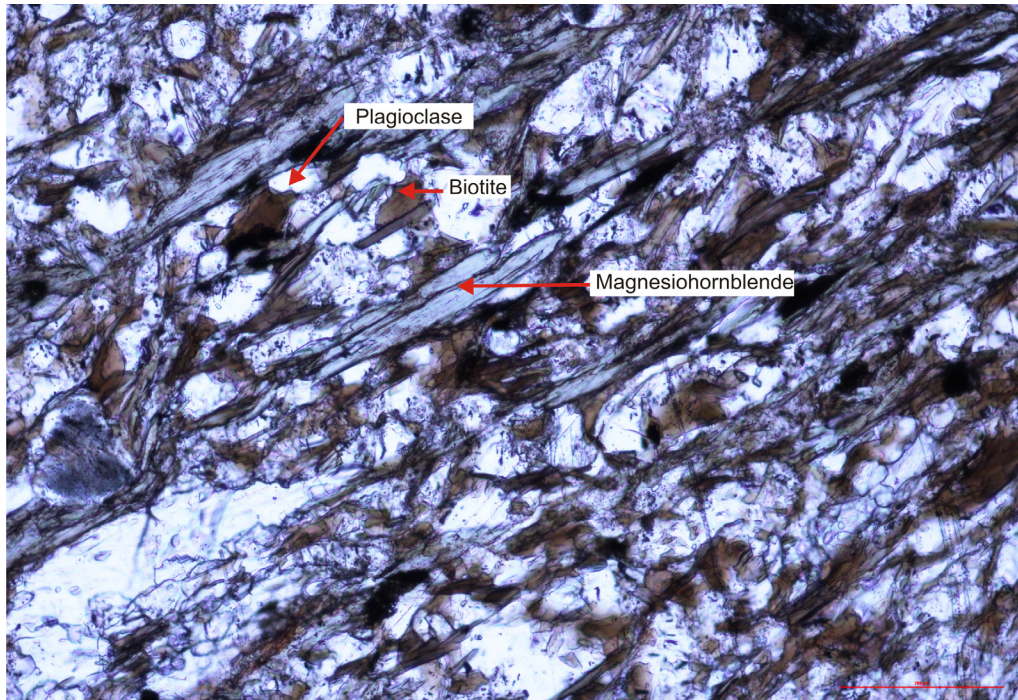


Plate 3.3.1: Photo displaying amphibolite grade mineral assemblage and metamorphic fabric in hornblende-biotite schist, meta-Nicola Group (Sample sw-827).

3.4 Rocks North of the Iron Mask Batholith: Domain [2]*

North of the Iron Mask batholith, meta-sedimentary rocks of the Dome Hills succession contain the mineral assemblage plagioclase-amphibole-epidote-clinozoisite-carbonate. Meta-sedimentary rocks are not penetratively deformed and, as such, primary sedimentary structures have been preserved. It is apparent from field and thin section petrographic observations, that rocks of the Dome Hills succession have undergone low grade metamorphism (Plate 3.4.1). Quantitative data for amphibole and plagioclase grains in a representative sample (sample 164-sw) of the Dome Hills succession are summarized in tables 3.4.1 a,b. Unlike rocks south of the CCTZ, plagioclase is significantly less calcic ($< 10\% \text{An}$) and thus dominantly albitic (Table 3.4.1b). One analysis of a single plagioclase grain in sample 164-sw yielded an andesine composition (An_{34}). The coexistence of grains of albite ($\text{An}_2 - \text{An}_9$) and andesine (An_{34}) can be explained due to the existence of miscibility gaps along the plagioclase solid-solution series. Due to these “gaps”, at upper greenschist facies, albite will not continuously change its composition along the albite-anorthite binary (e.g. Evans, 1964; in Miyashiro, 1994). Two compositionally distinct calcic amphiboles are also present. Amphibole, identified quantitatively as hornblende, has $\text{Ca} > 1.5$, $7.5 > \text{Si} > 6.5$, and Al_2O_3 ranges from 7-12 wt%. The hornblendes are dominantly magnesiohornblendes on the basis of $\text{Mg}/(\text{Mg}+\text{Fe}^{2+}) > 0.5$. Actinolite has relatively higher Si (>7.5) and lower Al_2O_3 (3-5 wt%) than coexisting hornblende (Table 3.4.1a).

The coexistence of dominantly calcium poor plagioclase (albite) and calcium rich plagioclase (andesine) together with the presence of two Ca-amphiboles, suggest that rocks of the Dome Hills succession were most likely metamorphosed near the greenschist-amphibolite facies transition, whereby incomplete replacement of Act + Ab (defining greenschist facies) to Hbl + Pl (defining amphibolite facies) has occurred. It is hypothesized that perhaps if a larger sample set of the Dome Hills succession were analyzed a greater number of plagioclase grains with higher calcic compositions

(oligoclase and andesine) would be observed. At relatively low pressures, the upper limit of temperature of the greenschist facies is approximately 400°- 450°C where at intermediate pressures it does not occur until temperatures of ~ 500°C (Spear, 1993).

The absence of chlorite has two possible explanations: (1) either chlorite has been entirely consumed via the following prograde metamorphic reaction:



or (2) the bulk composition (e.g. low Al content or high FeO/MgO ratio) of the rocks was such that chlorite was not stable despite the favorable metamorphic conditions. The latter is preferred, due to the fact that the anorthite component of plagioclase (produced in reaction (1)) is minor, relative to albite, indicating that this reaction has not gone to completion.

Sample 164 Amphibole analysis										Sample 164 Plagioclase analysis									
weight %										weight %									
Mineral	Hbl	Hbl	Hbl	Act	Act	Hbl	Hbl	And	Albite	Albite	Albite	Albite	Albite	Albite	Albite				
SiO2	44.99	46.09	47.45	50.79	51.37	48.59	48.59	59.60	66.62	64.18	66.97	66.94	66.1	66.1	66.1				
TiO2	0.39	0.35	0.21	0.12	0.10	0.18	0.18	0.00	0.01	0.04	0.00	0.00	0.0	0.0	0.0				
Al2O3	11.98	11.60	9.01	4.73	3.14	7.88	7.88	26.15	20.98	21.79	20.96	21.28	21.1	21.1	21.1				
FeO	17.33	16.94	15.97	15.61	15.02	16.08	16.08	0.07	0.13	1.26	0.14	0.17	0.0	0.0	0.0				
MnO	0.35	0.33	0.39	0.41	0.33	0.39	0.39	0.00	0.01	0.04	0.02	0.02	0.0	0.0	0.0				
MgO	9.34	9.47	10.99	12.80	13.59	11.41	11.41	0.01	0.03	0.59	0.03	0.11	0.0	0.0	0.0				
CaO	11.82	11.65	12.06	12.28	12.16	12.10	12.10	6.77	1.29	1.88	1.06	1.26	1.3	1.3	1.3				
Na2O	1.02	0.95	0.66	0.35	0.28	0.60	0.60	7.38	10.74	9.92	10.90	10.74	10.6	10.6	10.6				
K2O	0.26	0.24	0.26	0.13	0.09	0.19	0.19	0.12	0.04	0.05	0.07	0.08	0.1	0.1	0.1				
Cl	0.00	0.00	0.00	0.00	0.03	0.03	0.03	100.18	99.86	99.81	100.16	100.61	99.4	99.4	99.4				
Total	97.49	97.63	97.00	97.23	96.11	97.48	97.48												
Number of ions based on 23 Oxygen										Number of ions based on 8 Oxygen									
Si	6.706	6.823	7.044	7.479	7.625	7.164	7.164	2.647	2.923	2.841	2.928	2.916	2.91	2.91	2.91				
Ti	0.044	0.038	0.024	0.013	0.011	0.020	0.020	0.000	0.000	0.001	0.000	0.000	0.00	0.00	0.00				
Al	2.105	2.023	1.576	0.821	0.549	1.369	1.369	1.368	1.085	1.137	1.080	1.092	1.09	1.09	1.09				
Fe	2.160	2.097	1.982	1.921	1.864	1.982	1.982	0.003	0.005	0.047	0.005	0.006	0.00	0.00	0.00				
Mn	0.044	0.041	0.048	0.051	0.041	0.049	0.049	0.000	0.000	0.002	0.001	0.001	0.00	0.00	0.00				
Mg	2.076	2.090	2.431	2.810	3.007	2.507	2.507	0.001	0.002	0.039	0.002	0.007	0.00	0.00	0.00				
Ca	1.887	1.848	1.918	1.937	1.933	1.911	1.911	0.322	0.060	0.089	0.050	0.059	0.06	0.06	0.06				
Na	0.294	0.271	0.190	0.101	0.081	0.170	0.170	0.635	0.914	0.852	0.924	0.907	0.90	0.90	0.90				
K	0.050	0.045	0.049	0.025	0.017	0.036	0.036	0.007	0.002	0.003	0.004	0.004	0.00	0.00	0.00				
Cl	0.000	0.000	0.001	0.000	0.009	0.006	0.006	4.986	4.992	5.012	4.995	4.994	4.99	4.99	4.99				
total	15.367	15.279	15.263	15.159	15.139	15.221	15.221	33.7	6.2	9.5	5.1	6.1	6.	6.	6.				

Table 3.4. 1a: Representative microprobe analyses of amphibole grains in meta-sediments of the Dome Hills succession. See text for details.

Table 3.4. 1b: Representative microprobe analyses of plagioclase grains in meta-sediments of the Dome Hills succession. See text for details.

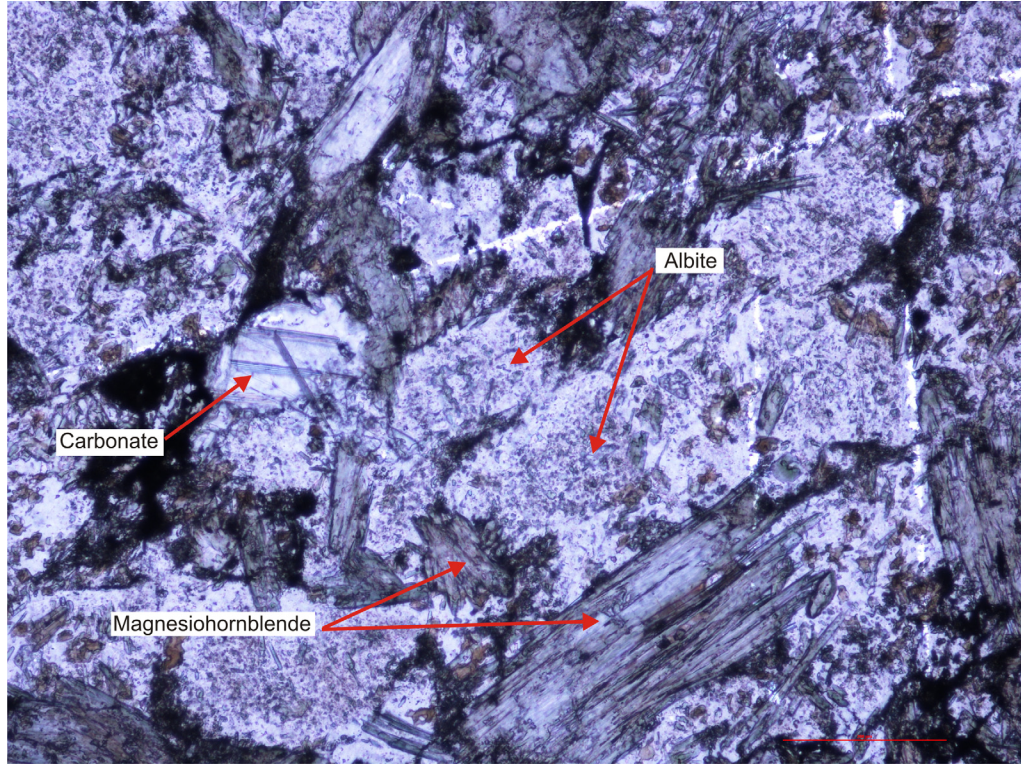


Plate 3.4.1: Photo displaying low-grade metamorphic mineral assemblage of the Dome Hills succession, Nicola Group (Sample sw-164).

3.5 References

- Armstrong, J.T. 1995. A Package of Correction Programs for the Quantitative Electron Microprobe X – ray Analysis of Thick Polished Materials, Thin Films, and Particles. *Microbeam Analysis*, **4**: 177 – 200.
- Bucher, K., M. Frey. 2002. *Petrogenesis of Metamorphic Rocks*. 7th ed. Springer-Verlag Berlin Heidelberg New York.
- Deer, W.A., R.A. Howie, J. Zussman. 1992. *An Introduction to The Rock-Forming Minerals*. 2nd ed. Prentice Hall, Harlow, England.
- Evans, B.W. 1964. Coexisting albite and oligoclase in some schists from New Zealand. *American Mineralogist* **49**: 173-179.
- Leake, B.L., A.R. Woolley, C.E.S. Arps, W.D. Birch, M.C. Gilbert, J.D. Grice, F.C. Hawthorne, A. Kato, H.J. Kisch, V.G. Krivovichev, K. Linthout, J. Laird, J.A. Mandarino, W. V. Maresch, E.H. Nickel, N.M.S. Rock, J.C. Schumacher, D.C. Smith, N.C.N. Stephenson, L. Ungaretti, E.J.W. Whittaker, G. Youzhi. 1997. Nomenclature of amphiboles: report of the subcommittee on amphiboles of the international mineralogical association, commission on new minerals and mineral names. *Canadian Mineralogist*. **35**: 219-246.
- Miyashiro, A. 1994. *Metamorphic Petrology*. UCL Press, London.
- Snyder, L.D. and Russell, J.K. (1993). Field Constraints on the diverse igneous processes in the Iron Mask batholith (92L/9); in *Geological Fieldwork 1992*, BC Ministry of Energy, Mines and Petroleum Resources, Paper 1993-1: 281-286.
- Spear, F.S. 1993. *Metamorphic Phase Equilibria and Pressure-Temperature-Time Paths*. Mineralogical Society of America, Washington, DC.
- Stanley, C.R. 1994. *Geology of the Pothook alkali copper-gold porphyry deposit, Afton Mining Camp, British Columbia*; Unpublished M.Sc. thesis, The University of British Columbia, Vancouver, British Columbia, 192 pages.
- Stanley, C.R., Lang, J.R. and Snyder, L.D. (1994): *Geology and mineralization in*

the northern part of the Iron Mask batholith, British Columbia (92I/9, 10);
in Geological Fieldwork 1993, BC ministry of Energy, Mines and Petroleum
Resources, Paper 1994-1: 269-274.

Chapter 4: Geochronology of LeJeune Granodiorite

4.1 Introduction

In the southern portion of the map area (south of the Cherry Creek Tectonic Zone-CCTZ), Nicola Group rocks possess penetrative metamorphic fabrics and mineral assemblages indicative of the amphibolite facies (Chapter 3). As discussed in Section 3.3 these rocks have been deformed at relatively lower crustal levels than rocks directly north of the CCTZ and south of the Iron Mask batholith (IMB). A sample of the undeformed LeJeune granodiorite, which was observed to cross-cut a west-northwest striking foliation in meta-Nicola Group rocks, was collected for age dating to determine a minimum age of the fabric in the footwall of the CCTZ (Location 4*).

In sample 776-sw, biotite constitutes approximately 7% of the total minerals present in the sample. Feldspars constitute approximately 50% -55%, with potassic feldspar comprising about 5%. The feldspars occur as phenocrysts and within the equigranular groundmass. Quartz constitutes about 30% and also occurs as a groundmass mineral. Concentrically zoned, igneous titanite occurs as an accessory mineral. Individual crystals of igneous titanite range on average from 1 – 2 mm in length. Some biotite grains are altered to chlorite and epidote. A planar fabric was not observed in this sample.

4.2 Methods and Analytical Techniques

Modern application of laser ablation-multiple collector- inductivity coupled plasma-mass spectrometry (LA-MC-ICP-MS) enables affordable and rapid acquisition of a reasonably accurate and precise isotopic age from a number of accessory minerals (Simonetti et al., 2005). Although less precise than traditional isotope dilution techniques, LA-MC-ICP-MS offers several clear advantages including: (1) procedures for sample preparation are simpler, (2) high spatial resolution for measurements of isotopic ratios, (3) rapid analysis and (4) low cost relative to other techniques such as SHRIMP (sensitive high resolution ion microprobe) or ID-TIMS (isotope dilution-thermal ionization mass

spectrometry). This study uses a modification of the LA-MC-ICP-MS analytical protocol to date zircon *in situ* from a standard petrographic thin section, which is possible by the unique design of a modified collector block containing a combination of Faraday collectors and 3 ion detectors (Simonetti et al., 2006). The modified collector block configuration measures very low Pb ion signals at high precision, allowing ablation to be performed successfully with smaller sample volumes, whereby a standard 30 second laser ablation analysis will produce a pit $< 15\mu\text{m}$ (Jackson et al., 2004; Jeffries et al., 2003).

The study was carried out at the University of Alberta's Radiogenic Isotope Facility using a Nu Instruments Nu Plasma MC-ICP mass spectrometer coupled with a New Wave Research UP213 laser ablation system. The MC-ICP-MS has a collector consisting of 12 Faraday buckets and 3 ion counters allowing for simultaneous measurement of ^{238}U , ^{235}U , ^{207}Pb , ^{206}Pb , ^{205}Tl , ^{204}Hg , ^{204}Pb , ^{203}Tl , and ^{202}Hg (Simonetti et al., 2006). Four zircon grains were analyzed *in situ* from a petrographic section cut from sample 776-sw of the LeJeune granodiorite.

Before analyzing the sample zircons, a 30 second background measurement was performed in order to subtract from sample measurements any ambient signal at mass 204. In this procedure, a 1 ppb solution of Tl is added to the plasma so that the measured $^{205}\text{Tl}/^{203}\text{Tl}$ ratio can be used to correct the measured Pb isotopic ratios for instrumental mass bias subsequent to the ablation process. In house standard zircon LH94-15 was measured before analyzing sample 776-sw in order to normalize the measured U and Pb ratios. A beam diameter of 30 microns was used where zircons were large enough, however several analyses were run with a 20 micron beam. Each laser ablation measurement (spot) lasts approximately 30 seconds and is followed by a similarly short waiting period in order to clear the chamber of the sample cloud and prepare for the next analysis. The sample is carried by He gas to a torch where it is ionized before being directed to the mass spectrometer.

4.3 Results

Table 4.3.1 summarizes the data collected from 6 analyses on 4 zircon grains in sample 776-sw. The analyses that gave the most reliable results are the two ablation runs conducted at 30 microns on grain number 5. The calculated concordia age, based on analysis 1 of grain 5, is 144.8 ± 5.9 Ma (2 sigma confidence level) (Figure 4.3.1). The analysis is 6% discordant. A weighted mean 206/238 age of 144.7 ± 4.3 Ma was also calculated for the two analyses for grain 5 (2 sigma level). Regressing a discordia line through the two points and zero results in a less precise upper intercept age of 162 ± 22 Ma (2 sigma level). It is therefore concluded that the 144.8 ± 5.9 Ma age is in fact reliable. It should also be noted that all the other 206/238 ages are within error of this preferred age (Table 4.3.1).

Some zircons within sample 776-sw were relatively small ($< 30\mu\text{m}$) and hence small spot diameters ($20\mu\text{m}$) were chosen for the analyses of these zircons. Zircons with smaller spot diameters ($20\mu\text{m}$) had fewer Pb counts (due to smaller volume of material being analyzed), resulting in a larger error and consequently less reliable ages. Discordant results may be due to lead loss. Reversely discordant results may possibly be due to Pb gain or U loss.

776

sample 776 Grain#	spot size um	206Pb cps	206Pb/204Pb	238U/206Pb	2s error	207Pb/206Pb	2s error	rho'	207Pb/206Pb Age (Ma)	2s error	206Pb/238U Age (Ma)	2s error	% discord.
776 -3	30	68805	infinite	46.9380	1.9025	0.0498	0.0012	0.859	184	55	136	6	26.2
776 -5-1	30	106112	infinite	44.1434	1.8705	0.0491	0.0006	0.955	154	30	144	6	6.4
776 -5-2	30	92245	infinite	43.9348	1.9493	0.0495	0.0007	0.944	173	35	145	6	16.1
776 -6	20	35756	infinite	47.1069	2.0720	0.0489	0.0014	0.834	141	67	135	6	3.7
776 -6-2	20	43661	infinite	45.9241	1.8559	0.0485	0.0007	0.940	122	34	139	6	-13.9
776 -2	20	27198	infinite	47.5798	2.3414	0.0487	0.0012	0.888	132	59	134	7	-1.8

Table 4.3.1: Summary of data collected from 6 analyses on 4 zircon grains in a sample of the undeformed Lejeune granodiorite (sample 776-sw).

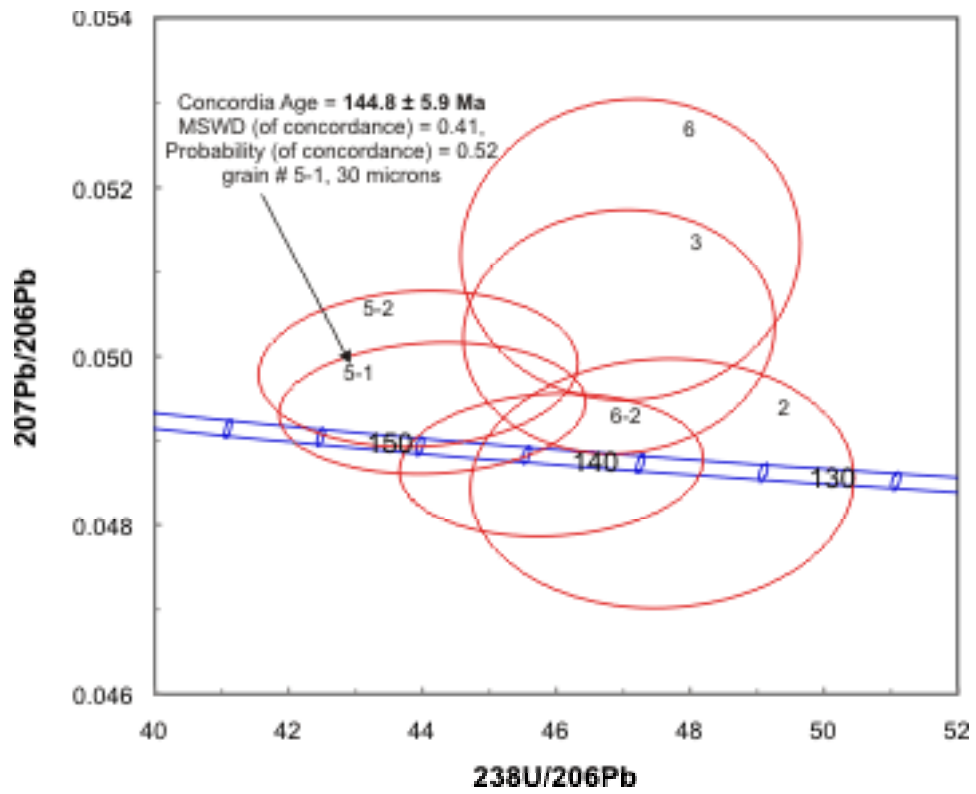


Figure 4.3.1: Tera-Wasserburg diagram. The calculated concordia age, based on analysis #1 of grain 5, is 144.8 ± 5.9 Ma. Analyses shown in Table 4.3.1.

4.4 References

- Jackson, S.E., N.J. Pearson, W.L. Griffin and E.A. Belousova. 2004. The application of laser ablation-inductively coupled plasma-mass spectrometry to in situ U/Pb zircon geochronology. *Chemical Geology*. **211**: 47 – 69.
- Jeffries T.E., J. Fernandez-Suarez, F. Corfu and G. Gutierrez- Alonso. 2003. Advances in U-Pb geochronology using a frequency quintupled Nd:YAG based laser ablation system ($\lambda = 213$ nm) and quadrupole based ICP-MS. *Journal of Analytical Atomic Spectrometry*. **18**: 847–855.
- Simonetti, A., L.M. Heaman, R.P. Hartlaub, R.A. Creaser, T.G. MacHattie and C. Bohm. 2005. U-Pb zircon dating by laser ablation-MS-ICP-MS using a new multiple ion counting Faraday collector array. *Journal of Analytical Atomic Spectrometry*. **20**: 677 – 686.
- Simonetti, A., L.M. Heaman, T. Chacko and N.R. Banerjee. 2006. In situ petrographic thin section U-Pb dating of zircon, monazite, and titanite using laser ablation-MC-ICP-MS. *International Journal of Mass Spectrometry*. **253**: 87 – 97.

Chapter 5: Structural Geology

5.1 Introduction

Rocks of the Nicola Group, in the vicinity of the Iron Mask batholith (IMB), predominantly display brittle deformation features such as fracturing, faulting and jointing, indicating that Nicola Group rocks were deformed in a high level environment. Exceptions occur immediately south of the Cherry Creek Tectonic Zone (CCTZ), as the zone marks an abrupt transition to highly foliated Nicola Group rocks. North of the Iron Mask batholith, mudstone and siltstone of the Dome Hills succession (Nicola Group) are observed to be folded and rocks display cleavage. Dominant structural panels are defined by northwest striking faults and northwest trending folds and these structures have been disrupted by later northeast striking faults and possible folds. It is interpreted, from structural data collected and map relations, that the Nicola Group has been subjected to multiple deformation episodes, with southwest directed compressional features being the earliest recognizable structures. Thrust faults are later reactivated and northwest trending folds and faults are disrupted during later extension. The following section will first describe structural data collected during the 2007 field season (Sections 5.2 - 5.4), while Section 5.5 describes the division of the map area into northwest trending structural domains, defined on the basis of their distinctive lithological and structural characteristics.

5.2 Folds and Associated Foliations

For the most part, rocks of the Nicola Group in the vicinity of the Iron Mask batholith (IMB) display brittle deformation features such as fracturing, faulting and jointing, indicating that Nicola Group rocks were deformed in a high crustal level, brittle environment. South of the IMB and north of the Cherry Creek Tectonic Zone (CCTZ), bedding attitudes indicate, however, that Nicola Group rocks are folded (Figure 5.2.1). These macroscopic folds are asymmetric, with a limb length ratio of $\sim (1:7)$. Folds are

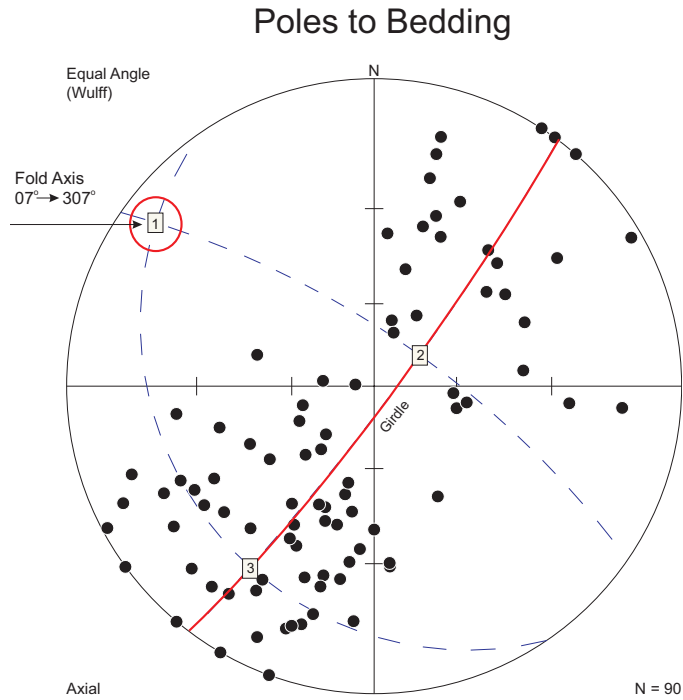


Figure 5.2.1: Stereonet showing pole-to-bedding measurements within Nicola Group rocks south of the Iron Mask Batholith and north of the Cherry Creek Tectonic Zone.

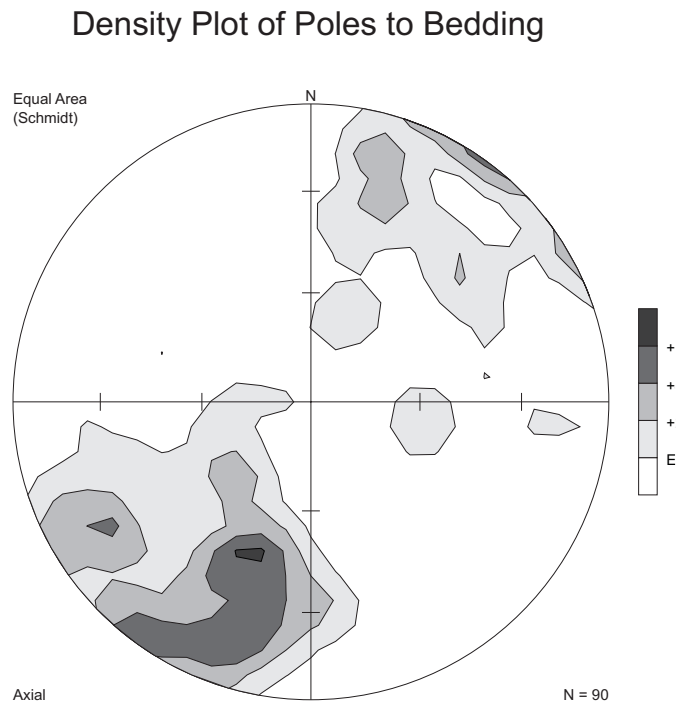


Figure 5.2.2: Density plot of the pole-to-bedding measurements. Asymmetry suggests vergence towards the southwest. See text for details.

defined by the reversal of bedding orientations; outcrop-scale folds were not observed. Folds are upright and plunge very shallowly toward the northwest (Figure 5.2.1). In map view, the reversal of bedding orientations is abrupt occupying a very narrow region in map space (< 30 metres). This indicates angular, northwest trending hinge zones, which are traceable across the entire map area. Because the structures (hinges) are relatively narrow, folding leads to no significant thickening of Nicola Group strata in the hinge zones and structural repetition of stratigraphic horizons is not evident. The macroscopic folds have close interlimb angles ranging from 50° to 70°, and their chevron style is consistent with deformation at higher levels in the crust. Three areas within the hinge zone display bedding measurements that dip northwest, indicating that folds are box fold, or kink fold structures (e.g. Location 5*). The long limb of the angular folds dips steeply to the northeast, with an average length of approximately 2 km. The southwest dipping limb has an average length of less than 300 m. A density stereoplot of poles to bedding displays this asymmetry and shows vergence toward the southwest (Figure 5.2.2). These structures are of only a local scale and so Nicola Group strata form an upright, east-facing, steeply tilted succession of volcanic and volcanoclastic rocks.

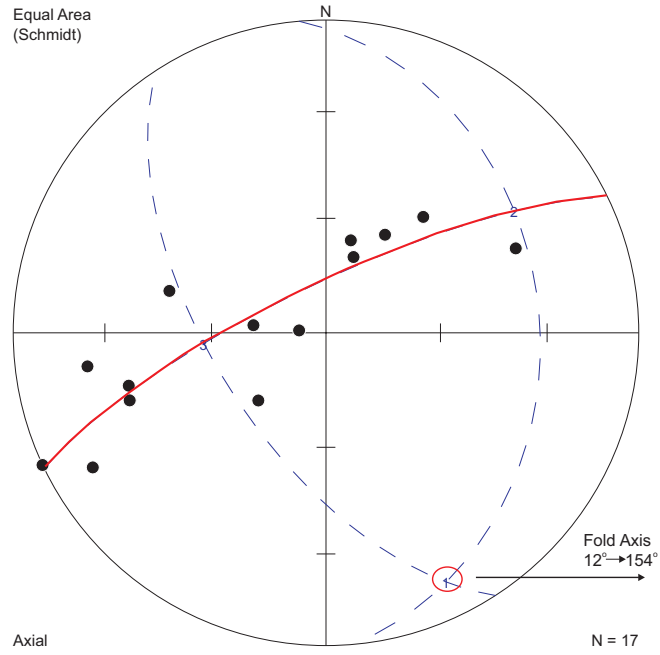
North of the Iron Mask batholith, laminated mudstone and siltstone of the Dome Hills succession is also folded. Folds are symmetrical, upright, and are subhorizontal to gently southeast plunging (Figure 5.2.3). The folds have close to tight interlimb angles and anticline-syncline pairs can range in wavelength from tens to hundreds of metres. Outcrop-scale parasitic folds are also observed (Photo 5.2.1). A regional metamorphic event is associated with the deformation. A mineral assemblage of actinolite, hornblende, plagioclase, epidote, and carbonate is indicative of greenschist-amphibolite facies metamorphism (Chapter 3).

Rocks with cleavage are rare in the Nicola Group, and south of the IMB there is no axial planar fabric associated with the northwest trending asymmetric folds. Cleavage, however, has formed within sedimentary rocks of the Dome Hills succession



Photo 5.2.1: Small cm-scale southeast plunging folds formed within the Nicola Group sedimentary rocks northeast of the IMB.

Poles to Bedding in the Nicola Sedimentary Facies



● Poles to bedding

Figure 5.2.3: Stereonet showing poles-to-bedding measurements within rocks of the Dome Hills succession of the Nicola Group.



Photo 5.2.2: Cleaved Nicola Group rocks. Cleavage planes are northwest striking and dip steeply to the northeast.

Axial Planar Cleavage

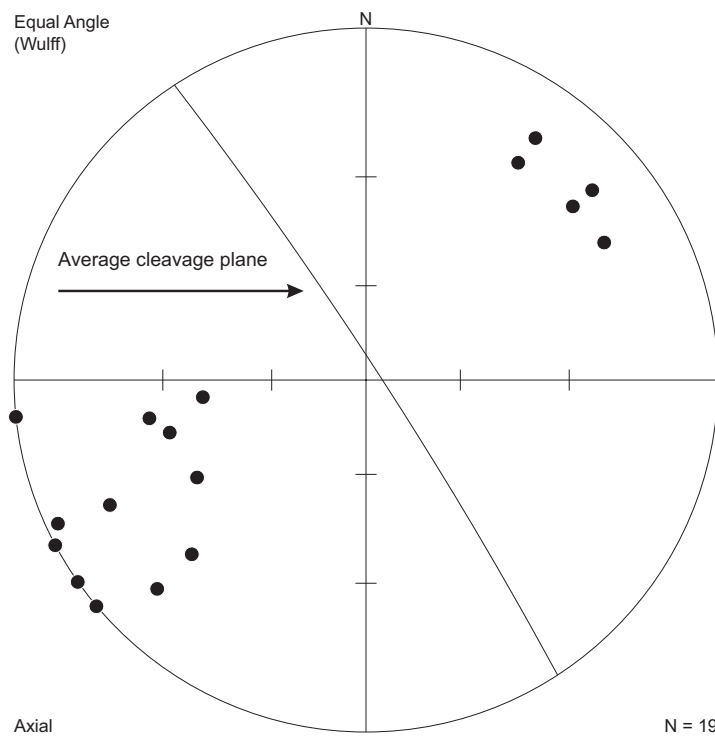


Figure 5.2.4: Cleavage formed within rocks of the Dome Hills succession of the Nicola Group. Cleavage is consistent with an axial planar cleavage to northwest trending asymmetric folds south of the IMB and northwest trending symmetric folds north of the IMB.

(Photo 5.2.2). Cleavage planes dip steeply toward the northeast or are vertical (Figure 5.2.4). Rocks can be strongly cleaved in approximately one metre-wide zones, with a transition to non-foliated rocks, across and along strike being abrupt. This indicates a highly heterogeneous distribution of strain throughout this portion of the Nicola Group. This could result from either (1) a heterogeneous stress field during compression or (2) differing rheological properties between parallel beds whereby lithologically differing layers would have responded differently to deformation. Because sedimentary rocks of the Dome Hills succession comprise layers of varying lithologies the latter is most likely involved in generating the observed strain heterogeneity, although the former has most likely also contributed. The cleavage is consistent with an axial planar relationship to the upright folds formed in Nicola Group rocks both south and north of the IMB, although foliation fabrics have not formed within the axial planar region of southeast plunging folds.

Foliation is also present within the IMB, however fabrics are not pervasive. Because foliation fabrics occur locally at intrusive contacts and within shear zones and are not of a consistent orientation across the batholith, it is interpreted that the foliations are not related to a large-scale, regional deformation event that would have affected the entire map area.

5.3 Foliated Rocks: South of the Cherry Creek Tectonic Zone

5.3.1 Nicola Group Rocks

As stated in previous sections, rocks in the study area are penetratively deformed immediately south of the Cherry Creek Tectonic Zone (CCTZ), a northwest striking fault zone marking an abrupt transition from non-foliated to strongly schistose Nicola Group volcanic and sedimentary rocks (see Section 2.2.1: Unit LTrNu). This transition also corresponds to an equally abrupt decrease in magnetic response, generating a strong vertical gradient that is recognized to roughly correspond with the mapped trace

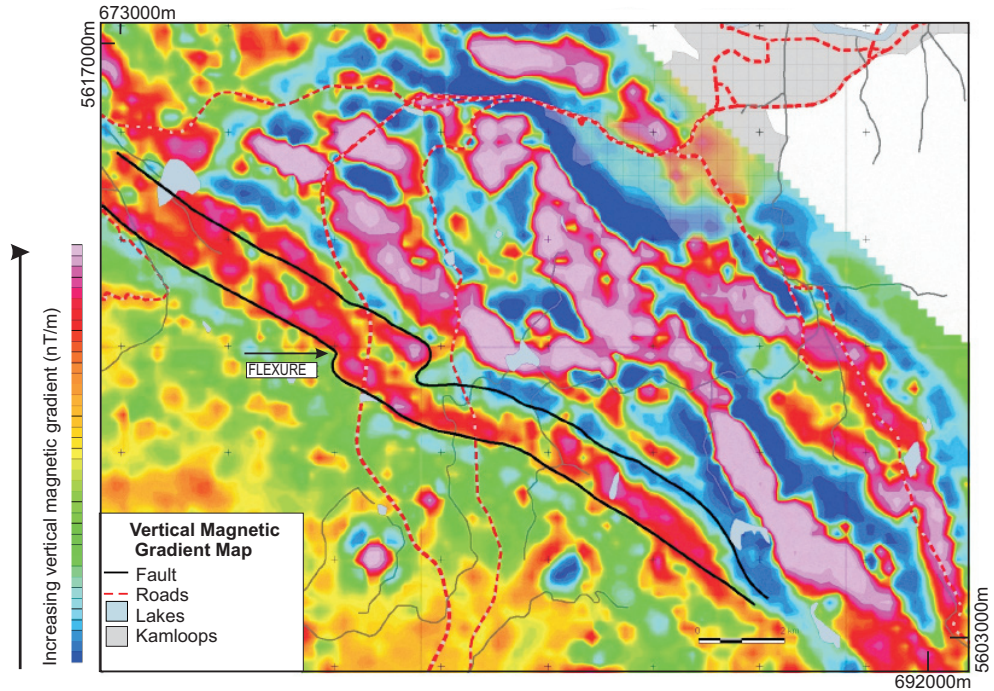


Figure 5.3.1: Vertical gradient aeromagnetic map of the Iron Mask batholith (Modified from Logan et al., 2005). Survey is from a subset of data from the 1995 airborne geophysical survey of the Iron Mask batholith covering Parts of NTS 92I/08NW; 92I/09SW; 92I/10; 92I/15SE (Shives, and Carson, 1995)

Tectonic Fabrics South of the CCFZ

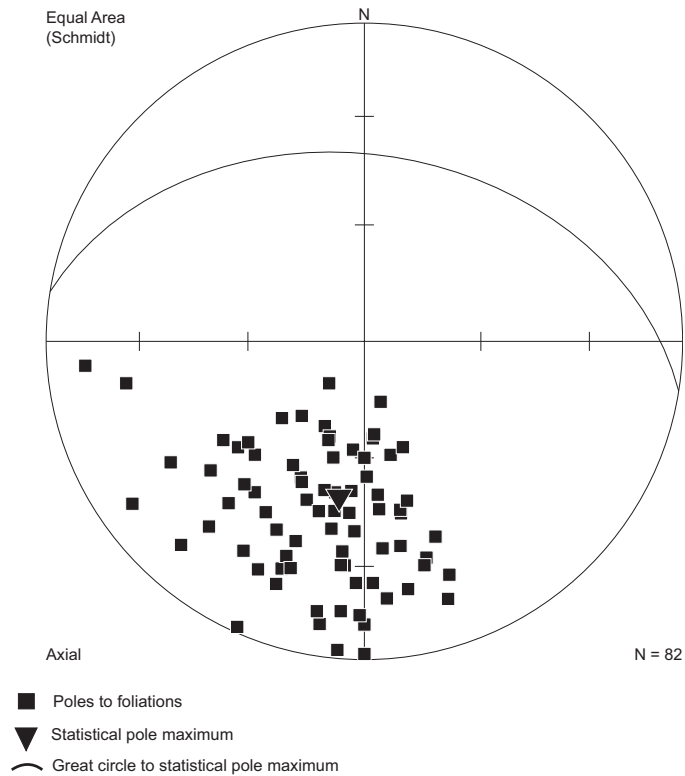


Figure 5.3.2 West-northwest striking tectonic fabric, south of the CCTZ.

of the Cherry Creek Tectonic Zone (Figure 5.3.1). This abrupt decrease in magnetic response of the exposed volcanic rocks is thought to result from magnetic destruction during fabric development (Logan and Mihalynuk, 2005). A pervasive schistosity that envelopes pyroxene and feldspar porphyroclasts and flattened pyroclasts has been described by Logan and Mihalynuk (2005). The foliation generally strikes west-northwest and dips north-northeast (Figure 5.3.2). The tectonic fabric is associated with a mineral lineation that plunges approximately 25°-30° and consistently trends southeast along west-northwest striking foliation surfaces. The mineral lineation is defined by biotite in schistose rocks and by aligned hornblende crystals that have pseudomorphed augite in tectonized porphyry (Figure 5.3.3). In fragmental units, porphyritic fragments can be stretched into prolate shapes. Foliation surfaces along the western edge of the foliated zone were observed to dip steeply toward the west - striking approximately 200°. Here the strong, stretching lineation, plunging 35° towards 355°, is defined by stretched augite porphyritic fragments (Photo 5.3.1). In a couple of localities along the western margin of the foliated zone the fabric is entirely lineated (L-tectonite), and planar fabrics are not observed.

One kilometre southwest of the Afton tailings pond, in the footwall of the CCTZ (Figure 2.1.1), strain in meta-Nicola Group rocks is distributed inhomogeneously. This is most likely a function of the mechanical heterogeneity within the unit. Competent rock types such as augite porphyritic, volcanic breccia are boudinaged and deformation is partitioned into incompetent, mica-rich domains that have behaved plastically, wrapping and deforming readily around the competent rock types. Shear bands are produced within the mica-rich domains (slip along (001) planes) and a layer parallel mineral lineation, plunging moderately towards the southeast, is associated with the shear planes. Within boudinaged fragments, tension gashes have formed (Photo 5.3.2). Approximately 1.2 km south of Goose Lake (Figure 2.1.1), sheared rocks are mylonitic and foliation surfaces are schistose. The schistosity is defined by the alignment of biotite and hornblende.

Stretching Lineations Along Main Shear Zones

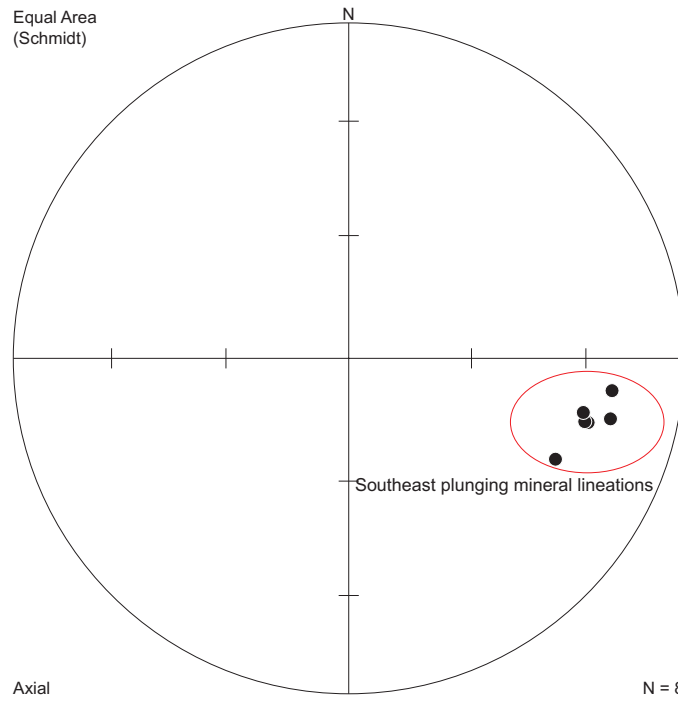


Figure 5.3.3: Southeast trending mineral lineations along west-northwest striking foliations.



Photo 5.3.1: Strong stretching lineation, defined by stretched augite porphyritic fragments, plunging 34° towards 356° .



Photo 5.3.2: Tension gashes formed in deformed Nicola Group footwall rocks south of the Afton tailings pond. See text for details.

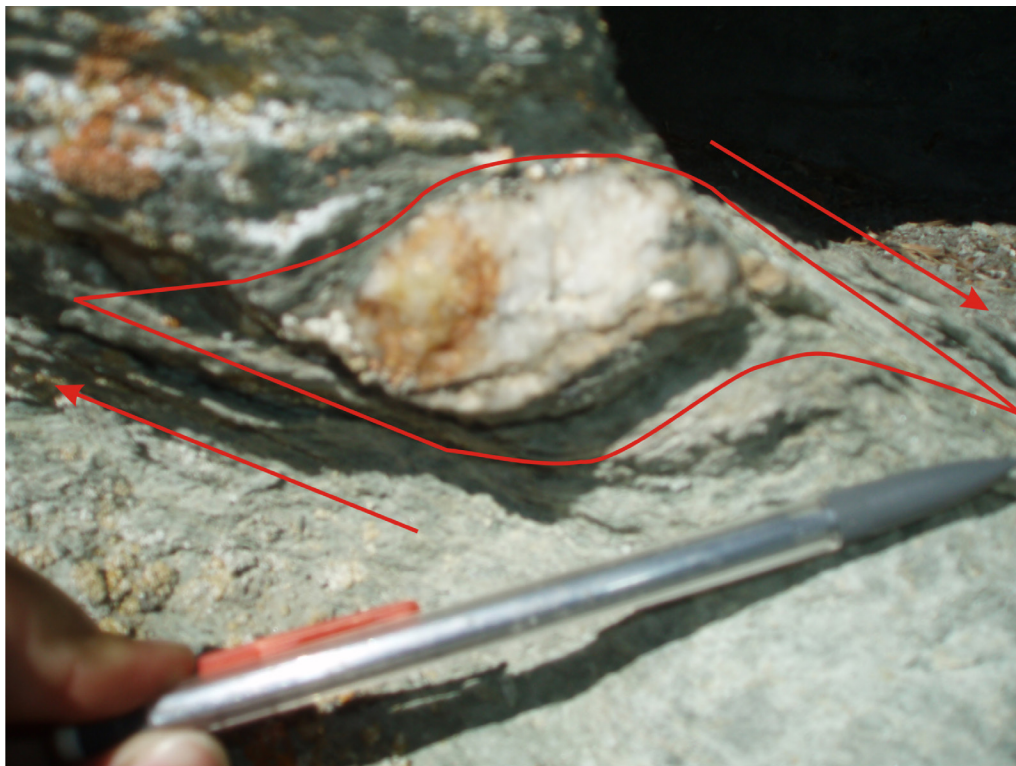


Photo 5.3.3: Schistose fabric is deflected by ridged aggregates of quartz to form asymmetric tails around the porphyroclasts that indicate a top-to-the-east sense of rotation of the clast.

Shear surfaces are associated with a southeast trending, moderately plunging, penetrative mineral lineation (defined by biotite). Interlayered within schistose rocks are layers of more competent lithologies (tectonized porphyries) and the southeast plunging lineation in porphyritic layers is defined by the alignment of hornblende. Shear fabrics, such as C-S fabric, are observed and consistently indicate a top-to-the-east sense of shear along the southeast trending mineral lineation. Ridged aggregates of quartz form porphyroclasts that are observed to be “floating” in the finer grained, ductily deformed matrix. The schistose fabric is deflected by the ridged grains and forms asymmetric tails around the porphyroclasts that indicate a top-to-the-east sense of rotation of the clast. Asymmetric folded veinlets of quartz are also consistent with a top-to-the-east sense of shear (Photos 5.3.3; 5.3.4).

Foliated Nicola Group rocks can be traced southward for approximately 3-4 km, until they are intruded by rocks of the Nicola batholith (Section 2.3). The northwest striking foliation is cut by the 144.8 +/- 5.9 Ma LeJeune granodiorite (see Chapter 4). The fabric is therefore older than Early Cretaceous and younger than Late Triassic, the age of the host Nicola Group. Schistose rocks of the Nicola Group can be traced as far south as Nicola Lake (Schau, 1968). The zone of foliated rocks is bounded to the north by the northwest striking Cherry Creek Tectonic Zone and to the west by the Clapperton Fault (Monger and McMillan, 1989).

The schistosity is observed to be folded by multiple generations of folds and has been crenulated subsequently. The dominant folds are of metre- to centimetre-scale amplitude and wavelength and are close to tight, plunging moderately toward the northwest. South of the Afton tailings pond (Figure 2.1.1), northwest trending folds have amplitudes ranging from 0.5-2 metres, with wavelengths being approximately 1-3 metres. The folds are upright, with axial surfaces dipping toward the northwest and fold hinges plunging moderately toward the northwest (Photo 5.3.5). In the Rush Lake area (Figure 2.1.1) the folds are significantly smaller, with amplitudes and wavelengths of



Photo 5.3.4: Asymmetric folded veinlets of quartz indicating a top-to-the-right (east) sense of shear.



Photo 5.3.5: Northwest trending folds with northwest striking axial surfaces. The folds located south of the Afton tailings pond are upright.

only a couple of centimetres. The folds in the Rush Lake area are chevron and overturned to the southeast and also have moderate to steep northwest-west dipping axial surfaces and northwest plunging fold axes (Figure 5.3.4). A crenulation cleavage is axial planar in northwest plunging chevron folds (Photo 5.3.6). The cleavage strikes southeast and dips moderately toward the west-northwest, and forms an intersection lineation on foliation surfaces (Photo 5.3.7). Northwest trending, open folds also fold the schistosity in the area just south of Rush Lake. These folds are small (centimetre-scale) with the wavelength being 2 to 3 times greater than amplitude height.

Northeast trending, asymmetric folds that consistently trend 75° - 80° and plunge at approximately 25° also fold the schistosity. These folds are of centimetre-scale. In most localities, it is difficult to determine the relative chronology of these minor folds.

5.3.2 Foliated Zones within the Frogmoore Granodiorite

As previously stated, foliated Nicola Group rocks south of the Cherry Creek Tectonic Zone were cut by intrusive phases of the Nicola batholith after formation of the metamorphic foliation. Locally, however, a strong foliation, defined by the alignment of biotite and hornblende, has formed within the Frogmoore granodiorite (Location 6*). These foliated zones are observed to be of similar composition to the main pluton, but have experienced a higher degree of strain in comparison with the relatively unstrained state of the Frogmoore granodiorite. These small, high strain zones form metre-wide, north-south trending lenses within the pluton (Photo 5.3.8). Foliation surfaces strike north and are vertical or dip steeply toward the east. Associated with the foliation surfaces is a lineation defined by stretched quartz ribbons. This lineation plunges moderately north at approximately 20° . Where observed, the foliation is consistently oriented across the entirety of the batholith and is sub-parallel to the general north-south trend of the elongate Nicola batholith. The fabric is observed not to continue into Nicola Group strata. As such, these minor shear zones are interpreted to be syn-intrusive in origin.

Northwest Trending Tilted Folds

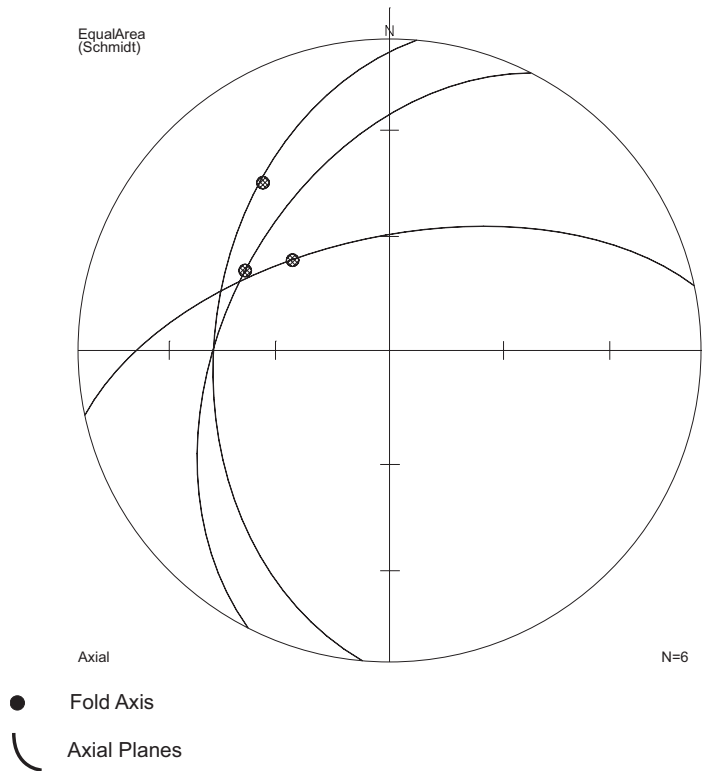


Figure 5.3.4: Northwest plunging, tilted folds formed within meta-Nicola Group rocks south of the Cherry Creek Tectonic Zone. See text for details.



Photo 5.3.6: Northwest trending folds with west dipping axial surfaces. South of Rush Lake chevron folds are overturned



Photo 5.3.7: Crenulated tectonic fabric formed in meta-Nicola Group rocks south of the Cherry Creek Tectonic Zone. See text for details



Photo 5.3.8: Small, meter-wide shear zone within the Frogmoore granodiorite phase of the Nicola batholith.

5.4 Faults and Shear Zones

The structure of the Nicola Group is typically dominated by brittle deformation features and is characterized by northerly (Preto, 1977; Preto, 1979) and northwest striking fault systems. In the Iron Mask region, northwest striking faults are the dominant control on the map pattern.

5.4.1 Northwest Striking Fault Zones

Cherry Creek Tectonic Zone

The Cherry Creek Tectonic Zone (CCTZ: Logan and Mihalynuk, 2005) is located approximately 3-4 kilometres from the southwest margin of the Iron Mask batholith (IMB) and runs sub-parallel to the elongate northwest-southeast trend (in map view) of the batholith (Figure 2.1.1). The zone strikes northwest-southeast, and as such parallels the dominant structural and stratigraphic trends in the Kamloops region.

The northwest striking CCTZ marks an abrupt transition from non-foliated rocks of the Nicola Group (north of the fault) to schistose Nicola Group volcanic rocks (south of the fault), over a strike-normal distance of approximately 200 m (Location 7*). The tectonic zone is not exposed at surface and its location, projected to surface, can only be approximated due to overburden. Its location is defined as the prominent structural break separating metamorphic rocks in the footwall and non-metamorphic volcanic rocks in the hanging wall.

The Iron Mask Batholith

Emplacement of the Iron Mask batholith (IMB) is interpreted to have been controlled by a major, northwest striking fault system (Logan and Mihalynuk, 2005). Various phases of the IMB have been intruded along the fault system that has also been interpreted by earlier authors to be part of a deep-seated system of north to northwest striking faults that have been active as early as the mid-Triassic (Campbell and Tipper, 1970; Preto 1977). The batholith is an elongate body, trending northwest-southeast in

map view, and its orientation is sub-parallel to the northwest striking Cherry Creek Tectonic Zone and as such follows the dominant structural and stratigraphic trends in the region. The batholith coincides with an important depositional and structural boundary, marking the transition from a volcanic facies (displaying upper crustal brittle deformation features: Domain [1], Section 5.5.1) in the south, to a sedimentary facies (ductilely deformed and regionally metamorphosed to a lower greenschist facies: Domain [2], Section 5.5.1) in the north. This would suggest that the batholith may have intruded along a northwest striking fault zone (that has been proposed by Logan and Mihalynuk (2005)). Before intrusion, displacement along the fault zone juxtaposed rocks deformed at differing structural levels. Presently the Iron Mask batholith plugs this structural contact. This fault zone is discussed in more detail in Section 5.5 and Chapter 6.

5.4.2 North Striking Fault Zone

Clapperton Fault

The Clapperton Fault lies south of the CCTZ and along the western margin of the zone occupied by highly foliated Nicola Group rocks. In the vicinity of the Iron Mask batholith (IMB), the structure is not exposed at surface and its existence is implied by the distribution of rocks that are interpreted to have been deformed at differing structural levels. The fault strikes north-south and is delineated by the north-south trending zone separating schistose rocks to the east of the fault with non-schistose Nicola Group rocks to the west of the fault. The fault zone is spatially associated with the western margin of the Nicola batholith. North of the CCTZ, there are no schistose rocks and the Clapperton Fault does not offset the northwest striking CCTZ, indicating that the Clapperton Fault is most likely truncated by the CCTZ.

5.4.3 Northeast Trending Faults

In the northeast portion of the map area (Location 8*) late, northeast striking

faults offset the northwest trending stratigraphic sequence of Nicola Group rocks and the Iron Mask batholith (IMB). The faults dip about 60 degrees toward the southeast and extend for at least 2.5 kilometres in length along strike. The faults displace Nicola Group strata and intrusive phases of the Iron Mask batholith in a left-lateral sense, with strike separations being on the order of 50 to 100 metres. To the northeast of the IMB, these faults juxtapose cleaved Nicola Group rocks with undeformed mudstones of the Dome Hills succession, indicating that these faults are younger than the dominant northwest trending structures within the region. Northwest striking faults and intrusive contacts within the IMB are also truncated by the northeast striking set of faults. The faults have been previously recognized to displace various phases of the Iron Mask batholith along its eastern margin (e.g. Logan and Mihalynuk, 2006). This study has further traced displacement along these faults into Nicola Group strata, in which a basalt marker is offset in a left-lateral sense with a strike separation of approximately 50 m (Location 9*). Slickenlines along an exposed fault surface indicate almost pure left-lateral strike-slip motion, plunging 05° towards 072°, or dip-slip motion, plunging 46° towards 093°, recording possible multiple episodes of displacement.

5.5 Discussion: Three Structural Domains

On the basis of structural and lithological variations, the map area can be divided into three northwest elongate domains, (Figure 5.5.1). Domains [1] and [3] are separated by the northwest trending Cherry Creek Tectonic Zone, while domains [1] and [2] are separated by the elongate, northwest trending Iron Mask batholith. The following section interprets the structural elements found within each domain.

5.5.1 Domain [1] and Domain [2]

Domain [1] is underlain by augite + plagioclase volcanic and volcanoclastic rocks (see Section 2.2.1: units 1-9). This domain is located between the elongate Iron Mask

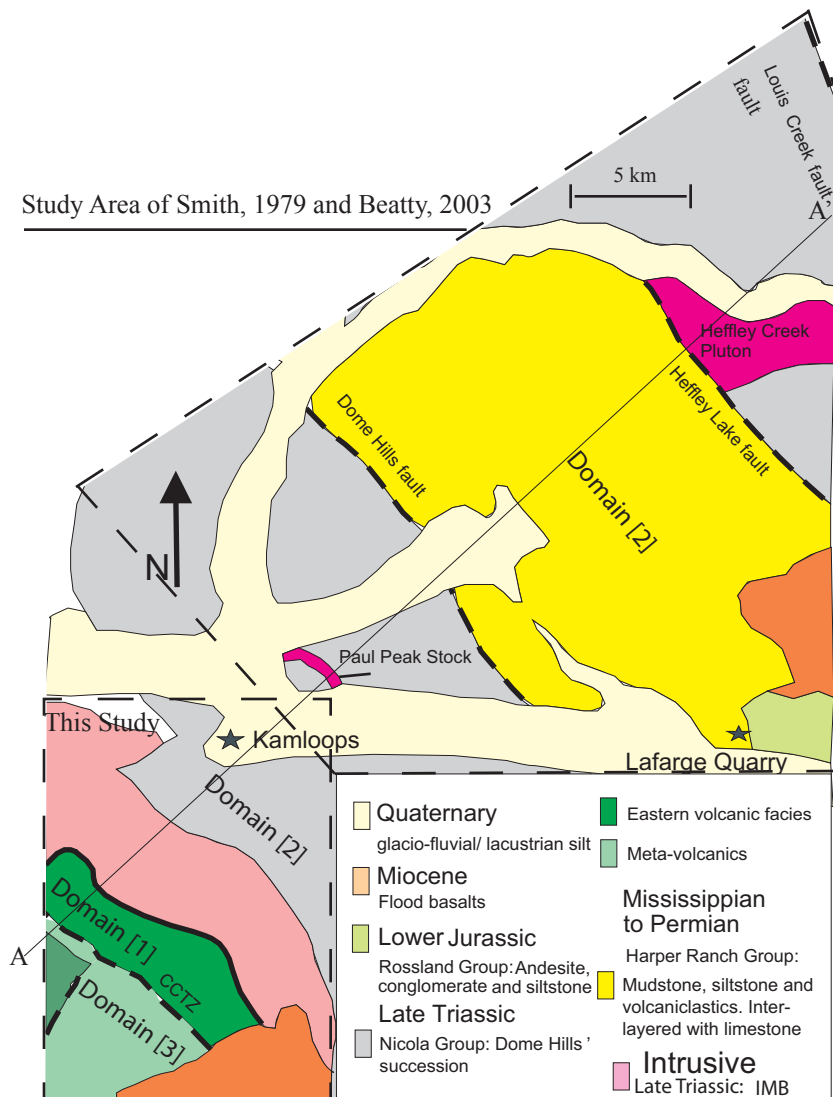


Figure 5.5.1: Location map depicting three northwest trending domains defined on the basis of structural and lithological variations between each (Modified from Beatty, 2003).

batholith and Cherry Creek Tectonic Zone (Figure 5.5.1) and the dominant structural elements within the domain are northwest trending, asymmetric folds (Figure 5.2.1). The asymmetry suggests vergence to the southwest and it is interpreted that a southwest directed compressional event generated these southwest verging folds. Because these structures are relatively small, it is evident that southwest directed compression mainly tilted the strata. The structures in domain [1] are interpreted to have formed at upper crustal levels in the brittle regime. Characteristics of the domain that lead the writer to suggest this are as follows: (1) Rocks do not display ductile deformation observable in the field, (2) in outcrop, rocks display brittle deformation features such as fractures, joints and faults, (3) folds are angular (kink folds), (4) Nicola Group strata is dominantly tilted (hinge zones are relatively small structures), (5) there is no associated fabric development with the asymmetric kink folds and (6) there is no associated metamorphism with the deformation event. The mechanism of folding is interpreted to be flexural slip, whereby flow and internal deformation within layers was not important and movement was most likely along discrete bedding planes. The style of brittle deformation within the Iron Mask batholith indicates that the batholith may have been strained at similar crustal levels as the volcanic rocks underlying domain [1].

Later deformation, following southwest directed compression is interpreted from the observation that the dominant northwest trending stratigraphy appears to be disrupted and possibly folded by northeast trending cross-folds. Compressive stresses would have been oriented, northwest-southeast or perpendicular to stresses that generated the dominant structural trends (Figure 2.1.1).

Domain [2] is entirely underlain by rocks of the Dome Hills succession of the Nicola Group. The dominant structural features are southeast trending mesoscopic and macroscopic folds and an associated steeply dipping, northwest striking axial planar cleavage. Because of the strong structural conformity within domains [1] and [2], with

both domains being dominantly controlled by northwest-southeast trending, southwest directed structures, it is interpreted that congruent structures within both domains were generated by the same deformation event. A 180° reversal in fold trends between domain [1] (northwest trending) and [2] (southeast trending) is observed. A reversal from northwest to southeast trends could be due to a later cross-folding event or due to minor rotation of the folds along northwest striking faults. Late northeast trending cross-folds are not observed in outcrop but may be interpreted from structural data, as the orientations of bedding and layering vary from northwest striking to west striking. This observation leads to the interpretation that the dominant northwest trending stratigraphy is disrupted/folded by a late southeast-northwest trending cross-folding event (Figure 2.1.1). It seems more likely however, that faulting may have reversed fold trends. This interpretation is drawn from the fact that folds within domain [2] consistently plunge southeast, suggesting that all folds within the fault block were rotated together. If a cross-folding event reversed trend orientations it would follow that both northwest and southeast trending folds would be observed within the same fault block and this, however, is not the case.

If cleavage within the Dome Hills succession of domain [2] represents an axial planar cleavage to southwest-verging folds in both domains [1] and [2], there is the question as to why a cleavage was not formed in volcanic rocks of domain [1]. Two possibilities are presented here. Lithologically, rocks within domain [1] and domain [2] are quite different. Volcanic rocks underlying domain [1] are more competent than the predominantly sedimentary rocks underlying domain [2] and as such most likely deformed more readily. Another possibility is that rocks of domain [2] were deformed at deeper crustal levels with respect to rocks underlying domain [1] and as such may have responded differently to or experienced different stresses. The fact that the rocks within the sedimentary domain show ductile deformation at the outcrop-scale, display a consistent northwest striking cleavage, and have undergone pervasive greenschist-

amphibolite grade metamorphism supports the theory that these rocks were deformed at deeper crustal levels than rocks within domain [1]. Both factors, however, were most likely variables in generating an axial planar cleavage. Domains [1] and [2] are therefore interpreted to have been deformed at differing structural levels, and subsequent southwest directed thrust faulting has brought relatively lower crustal rocks of domain [2] to the current structural position. The position of the Iron Mask batholith is along the approximate surface trace of the structural boundary representing the interpreted fault zone and as such it is interpreted that the Iron Mask batholith may have been intruded along the fault system that accommodated uplift of domain [2].

Domain [1] is separated from both domains [2] (to the east) and [3] (to the west) by major northwest striking fault zones. Because of the structural uniformity of major folds and faults across the study area, the major bounding fault zones are also interpreted to have been derived from the same southwest directed compressional event generating northwest trending folds of domains [1] and [2] and this deformation episode was the last significant phase of deformation affecting Nicola Group rocks in the map area. Interpretations about movement along northwest trending faults separating domain [1] from domain [2] is speculative, however juxtaposition of belts deformed at differing structural levels (with lower crustal rocks (domain [2]) north of upper crustal rocks (domain [1]), is consistent with southwest directed thrusting. Faults related to asymmetric folds are slightly younger, as faults juxtapose rocks of varying structural levels (e.g. domains were deformed/folded before juxtaposition).

Late northeast striking faults offset northwest striking cleavage planes within domain [2] (Figure 2.1.1). The northeast directed plunge of slickenlines and apparent strike separation indicate that these faults were the locus of normal dip-slip during a later extensional event, with extension oriented northwest-southeast.

Boundary Between Domain [1] and Domain [2]

A lateral facies transition, from an eastern volcanic assemblage to an eastern sedimentary facies, has been recognized by Monger (1985) and Monger and McMillan (1989). In some areas along the Nicola arc, the facies domains are structurally juxtaposed (Preto, 1977; Preto 1979), while grading depositionally into one another in other areas (Schau, 1968; Monger and McMillan, 1984; Mortimer, 1987). Easternmost volcanic rocks are observed to interfinger eastwards with sedimentary rocks and rocks of the eastern sedimentary facies are observed to overlie the eastern volcanic facies. In the study area the transition from Domain [1] (eastern volcanic facies) to Domain [2] (eastern sedimentary facies) is abrupt and due to the abrupt change in lithology and metamorphic grade across the width of the IMB, the boundary is interpreted to be a fault (above, Section 5.5.1). It is unclear whether this fault controlled Late Triassic distribution of the Nicola Group rocks in the study area, whereby an eastern sedimentary basin would have been bounded to the west by a normal growth fault. This fault may have accommodated subsidence during accumulation of sediments derived further west (volcanic facies). It can be said that if this fault did control the deposition of Nicola Group sediments that it has later been reactivated (during southwest directed thrusting) because structurally deeper level rocks are currently exposed east of the fault.

5.5.2 Domain [3]

Domain [3] is underlain by meta-volcanic Nicola Group rocks (Section 2.2.1: Unit 11) and occupies the southern portion of the map area, bounded by the Cherry Creek Tectonic Zone to the north and Clapperton Fault along its western margin (Figure 5.5.1). Uplift and exhumation of this lower crustal block is interpreted to have occurred during the Eocene, as a white mica Ar-Ar cooling date of 53-54 Ma has been obtained from the meta-Nicola Group rocks (M. Mihalynuk personal communication, 2007). The fabric, which is cut by a relatively undeformed pluton of Late Jurassic-Early Cretaceous age

(144.8 +/- 5.9 Ma: Chapter 3), is interpreted to be older than Eocene uplifting and not generated by it. The formation of secondary, cross-cutting fabrics and later folds indicate multiple episodes of deformation within this belt.

Folds

Within domain [3], the schistosity has been folded during multiple deformation episodes. Folds vary in shape, tightness and orientation (Section 5.3.1). The relative timing of events is difficult to determine, as cross-cutting fabrics are rare and folds of varying orientations are rarely observed in the same locality.

Because folds were not developed within the hanging wall of the CCTZ, (and the CCTZ truncates fold axes) the episodes of compression that generated both northwest and northeast trending folds within domain [3] most likely took place before uplift of the footwall block to its current structural position.

Because axial surfaces and hinges of northwest trending folds are both inclined toward the northwest, folds may have been tilted to the northwest during later faulting along the CCTZ. It is assumed that when the folds are initially formed, the structures would generally be subhorizontal and therefore later tilting is interpreted.

Folds are found only in footwall rocks within a few hundred metres of the Cherry Creek Tectonic Zone. Potential explanations are: (1) exposure near and within the tectonic zone is better than all other areas of domain [3], and more exposure leads to more structural control, or (2) folds may be directly related to movement along the fault zone. Because the orientation of the folds is such that they cannot be directly related to compression along the CCTZ (e.g. fold axes truncated by CCTZ), the former is preferred.

5.5.3 Bounding Faults of the Ductily Deformed Footwall

It is clear from structural data (Section 5.3) and quantitative mineral analyses (Section 3.3) that footwall rocks south of the CCTZ and east of the Clapperton fault were

deformed at lower crustal levels relative to rocks within the hanging wall. It is interpreted that this crustal block (bounded by both faults) was uplifted to its current structural position by displacement along both the CCTZ and Clapperton fault. Because of the interpreted orientation of the CCTZ (steeply northeast dipping-originally accommodating southwest directed compression: Section 5.5.1) these faults would have been normal faults, with the footwall (foliated rocks) moving up relative to the hanging wall block (non-foliated). Uplift and exhumation of this lower crustal block is interpreted to have occurred during the Eocene (Section 5.5.2). During the Eocene extensional tectonics was prevalent throughout the southern portion of the Intermontane (e.g. Ewing, 1980), further supporting that these bounding faults are normal, with hanging wall down relative to footwall.

Field data (Section 5.3) suggest that footwall rocks along the western portion of the fault zone were deformed within a brittle-ductile regime and those along the eastern portion of the CCTZ under purely ductile conditions. As such, displacement on the CCTZ may decrease to the west from a maximum magnitude south of Goose Lake (e.g. differential uplift along the CCTZ).

Bounding faults are interpreted as steep, dominantly dip-slip faults, where most of the displacement was in the normal sense. Because rocks north of the Cherry Creek Tectonic Zone and west of the Clapperton fault have not been regionally metamorphosed to a greenschist facies, the rocks probably saw temperature of no more than 200°C. Assuming an average geothermal gradient of 35°C/Km, the rocks were at a depth of no more than ~ 6 km prior to uplift. Temperature constraints derived from petrological data (Section 3.3) suggest that footwall rocks, south of the Cherry Creek Tectonic Zone, have seen temperatures of at least 500°C. Assuming an average geothermal gradient of 35°C/km, these rocks were buried to a depth of at least 15 km. It is therefore interpreted that throw on the faults must have been at least 9 km in order to explain the difference in metamorphic grade across the faults (Chapter 3). There is no evidence for significant

strike-slip motion along either of the faults, but it cannot be ruled out. Strike-slip motion along the Clapperton fault is negligible, as the CCTZ truncates the fault and has not been displaced by it. The Clapperton fault however, may be related to the fault system that appears to have controlled the distribution of intrusive phases of the Nicola batholith, as the batholith follows a north-south trend, hinting at some form of structural control.

5.5.4 Reactivation of the Cherry Creek Tectonic Zone

The CCTZ, has most likely seen multiple deformation episodes, both compressive and extensional, therefore being inverted at least once in its geologic history. Its orientation suggests that it could have accommodated southwest directed shortening associated with the generation of southwest verging folds formed within domains [1] and [2]. Later extensional movement along the fault zone is more readily interpreted because of the significantly higher grade footwall rocks. The following chapter will discuss the timing and regional implications of these proposed deformation events.

Folds within the footwall suggest northeast directed compressional events before uplift of the footwall to its current structural position. Rocks within the hanging wall are not folded (into northeast vergent folds), suggesting either that compression occurred before final uplift or only footwall rocks were deformed/folded during compression. The vergence of minor northwest trending folds suggests eastward directed compression and as such are most likely not related to motion along the CCTZ, and the former interpretation is preferred.

5.6 References

- Beatty, T.W. 2003. Stratigraphy of the Harper Ranch Group and tectonic history of the Quesnel terrane in the area of Kamloops, British Columbia. M.Sc. thesis, Simon Fraser University, Burnaby, B.C. 213 p.
- Campbell, R.B. and H.W. Tipper. 1970. Geology and mineral exploration potential of the Quesnel Trough, British Columbia. *British Columbia Institute of Mining and Metallurgy Bulletin* 63: 785-790.
- Ewing, T.E. 1980. Paleogene tectonic evolution of the Pacific Northwest. *Journal of Geology* 88: 619-638.
- Logan, J.M. and M.G. Mihalynuk. 2005. Porphyry Cu-Au Deposits of the Iron Mask Batholith Southeastern British Columbia: In Geological Fieldwork 2004. *British Columbia Geological Survey Branch, Paper 2005-1*.
- . 2006. Geology of the Iron Mask Batholith. Open File Map 2006-11. British Columbia Geologic Survey Branch.
- Monger, J.W.H. 1985. Structural evolution of the southwestern Intermontane belt, Ashcroft and Hope map areas, British Columbia; in Current Research, Part A. *Geologic Survey of Canada, Paper 85-1A*: 349-358.
- Monger, J.W.H., and W.J. McMillan. 1984. Bedrock geology, Ashcroft, British Columbia (92 I). Geological Survey of Canada.
- . 1989. Bedrock geology, Ashcroft, British Columbia (92 I). Geological Survey of Canada, Map 42.
- Mortimer, N. 1987. The Nicola Group: Late Triassic and Early Jurassic subduction-related volcanism in British Columbia. *Canadian Journal of Earth Sciences* 24: 2521-2536.
- Preto, V.A. 1977. The Nicola Group: Mesozoic volcanism related to rifting in Southern British Columbia. *Geological Association of Canada*, no. Special paper 16: 39-57.
- . 1979. Geology of the Nicola Group between Merritt and Princeton, British Columbia.

British Columbia Ministry of Energy, Mines and Petroleum Resources, no.
Bulletin 69: 90.

Schau, M.P. 1968. Geology of the Upper Triassic Nicola Group in south-central British Columbia. University of British Columbia; Unpubl. Ph.D. thesis.

Shives, R. B. K. and J.M. Carson. 1995. Airborne geophysical survey, Iron Mask Batholith. *British Columbia, Geological Survey of Canada*, Open File 2817, 1:150,000 scale, 61 pages, 18 maps.

Chapter 6: Discussion of Tectonic History

6.1 Basement of Quesnellia

In the southern Canadian Cordillera there is debate as to the nature of the basement of the Quesnel Terrane, which can be more objectively referred to as Quesnellia or the Quesnel arc*. One interpretation involves Quesnellia being formed atop ancient oceanic crust, as an intraoceanic island arc, far from the continental margin. During Jurassic time the foreign crust is hypothesized to have drifted eastward and accreted onto ancient North American continental crust (Monger et al., 1982). Alternative models proposed that Quesnel arc basement may comprise Precambrian continental crust, whereby the arc developed atop a rifted fragment of the North American craton (Okulitch, 1984; Struik, 1987). These authors suggested that episodes of Proterozoic to mid- Paleozoic extension caused differential thinning of the continental crust at the Cordilleran margin. Sedimentary basins were formed, separated by “horsts” or less thinned crust, where the most westerly fragment was overlain by volcanic arc rocks of Quesnellia. In the southern Canadian Cordillera, recent studies have offered considerable evidence for a coherent stratigraphic relationship between Quesnellia and ancient North America (Erdmer et al., 2002; Unterschütz, 2002) and suggest thin stratigraphic cover atop this western continental high (Erdmer et al., 2002; Thompson et al., 2006). The observation that deformation appears to be less intense in Quesnellia (Quesnellia is relatively undeformed with respect to the adjacent Omineca and Coast Plutonic belts and is dominated by brittle faults and fractures) may be explained in terms of a possible continental basement. Supracrustal rocks, including the Nicola Group, that overlie the continental high were spared intense east-west compression because the crust they overlie was an old, thick and strong “ribbon” of continental crust (Oxburgh, 1982; Struik, 1987; Thompson et al., 2006). This continental basement could perhaps be the controlling factor behind the systematic orientations of deep-seated faults and fractures, controlling the

locations of volcanic centers in Quesnellia. A better understanding of the basement to Quesnellia would aid in modeling the structure of the Nicola arc.

6.2 Backfolds and Associated Backthrusts

6.2.1 Introduction

Following the deposition of arc-related successions of southern Quesnellia, the Permian and Triassic assemblages have witnessed several pulses of east verging contraction. Northwest striking thrust faults and foliations, interpreted to be axial planar to northwest-southeast trending folds, dip steeply northeast suggesting that the last significant phase of compressive deformation in the region had southwest vergence.

Southwest verging compressional features have been documented along the length of the Canadian Cordillera. Because of the predominance of northeast verging folds and thrusts in the Canadian Cordilleran orogen, southwest verging structures have been termed “backfolds” or “backthrusts” (Monger and Price, 1979). These structures generally verge away from a “point” of structural divergence, generating fan shaped fold and thrust complexes within highly deformed rocks of the Omineca Belt (e.g. Selkirk fan and Kootenay arc). A number of hypotheses for how these structures are generated have been proposed. Those based on accretionary tectonics include: (1) formation of the axis of divergence directly above a singularity point S (the point where oceanic lithosphere is subducted beneath continental lithosphere), based on mathematical models of Malavieille (1984) and Willet (1993) (Brown et al., 1993), and (2) tectonic wedging of an allochthonous terrane (in this case, composite terrane I (Monger et al., 1982)) between the cratonic basement and the overlying miogeocline (Price, 1986). More recently Thompson et al. (2006) have proposed that such structures could result from entrapment of continental margin basins and the attenuated crust beneath them, between thicker, stronger continental crustal blocks. In this model an outboard (of the miogeocline) continental high is hypothesized, as the authors propose that Permian and Triassic arc

assemblages were deposited on an incompletely rifted block or “ribbon” of continental crust that converged eastward relative to autochthonous North America during Jurassic-Paleogene deformation. In all models described above, backfolds and backthrusts form during initial mountain-building stages, occurring prior to eastward propagation of deformation.

6.2.2 Latest Triassic - Earliest Jurassic Deformation

Northwest trending, southwest verging structures are the main structural elements of the Iron Mask batholith region. These southwest directed folds and associated thrust faults give rise to the area’s map pattern, as northwest striking faults separate and bound northwest trending structural-stratigraphic panels. These structures are the oldest recognizable structures in the Kamloops region. Because of the strong structural conformity, southwest verging structures within domains [1] and [2] are interpreted to be generated during the same deformation episode D1, however the style of deformation varies between the belts, as reflected in the different class/shape of F1 folds, presence or absence of foliation fabrics, and the varying degree of metamorphism experienced by rocks within each belt (see Chapter 5 for details). These differences can be explained by the interpretation that these belts were deformed during the same southwest directed compressional event, but were at different structural levels during deformation. Following deformation, reverse faulting generated by continued southwest directed compression occurred. Relative motion along the structural boundary between the sedimentary facies and volcanic facies of the Nicola Group is inferred to be reverse or southwest side down relative to the northeast side, as indicated by the vergence of associated folds and axial planar foliations and the juxtaposition of deeper crustal rocks north of rocks deformed at higher crustal levels.

The Iron Mask batholith is coincident with the lithological and structural boundary zone that marks the abrupt transition from the eastern Nicola Group

metasedimentary facies to the eastern Nicola Group volcanic facies. As such, it is likely to have intruded along this major, northwest striking thrust fault. A key question is the timing of intrusion with respect to motion on this fault (details of fault zone in Section 5.5.1).

Southwest Vergent Structures: Kamloops Region

Southwest vergent structures have been documented in Nicola Group rocks lying approximately 14 kilometres northeast of the city of Kamloops. In an area bounded by the junction of the North Thompson and South Thompson Rivers to the west, and the Louis Creek fault to the east, Smith (1979) carried out a study of Harper Ranch Group and Nicola Group rocks. He described a pair of northwest trending folds, the Paul Ridge anticline and the Paul Ridge syncline, in mudstone and siltstone of the Dome Hills succession directly west of the Dome Hills fault (Figure 5.5.1). Smith (1979) also noted the absence of axial planar foliation in the hinge zones of these map-scale folds.

Similar to the northwest bounding faults that define structural and stratigraphic panels southwest of Kamloops (this study), major northwest striking faults have been recognized northeast of Kamloops (Figure 5.5.1). Smith (1979) noted that the Harper Ranch and Nicola groups are separated by a steep, northwest trending fault, termed the Dome Hills fault (Beatty, 2003). Beatty (2003) observed that folds of the scale of the Paul Ridge anticline and syncline were not formed in Harper Ranch Group rocks and suggested that folding of the Nicola Group may have resulted from thrust emplacement of the relatively competent Harper Ranch Group strata over the relatively incompetent Nicola Group along the Dome Hills fault. His interpretation is based on the vergence of folds and their associated steep, east dipping axial planar foliations. Similarly, northwest-southeast trending F1 folds, associated with a northwest striking, axial planar cleavage, occur within the laminated mudstone and siltstone of the Dome Hills succession mapped in this study. The orientation of these F1 folds and axial surfaces is consistent with southwest directed compression. F1 folds formed in the Dome Hills succession in this

study are therefore correlated with those of Beatty (2003).

Sub-Jurassic Unconformity

The key to understanding the timing of deformation, generated by southwest directed compression, may be located in rocks occupying the northeast corner of the Ashcroft map sheet in the Kamloops region (Monger and McMillan, 1989). Underlying this region are three unconformity bound successions of arc affinity: the Late Paleozoic Harper Ranch Group, the Late Triassic Nicola Group, and the Jurassic Rossland Group (Beatty, 2003). The stratigraphic and structural relations imply a period of regional uplift and erosion of both the Harper Ranch and Nicola groups following Late Triassic deformation, and prior to renewed arc volcanism in the Jurassic, represented by the Rossland Group (Beatty, 2003). In summary, stratigraphic relations in the Kamloops area reported in Beatty (2003) constrain southwest vergent thrusting and F1 folding to have occurred after deposition of the Late Triassic (Carnian to Norian) Nicola Group and prior to eruption of the Early Jurassic Rossland Group.

Plutonism: Pre-, Syn-, or Post-Deformational?

To further constrain the timing of D1 deformation, cross-cutting relationships of plutonic rocks have been examined. The Iron Mask batholith is an example of a weakly strained intrusive body of Late Triassic age that intruded Nicola Group rocks in the study area. U-Pb dates for various phases of the Iron Mask batholith, excluding the younger Sugarloaf diorite, are 204 ± 3 Ma (latest Norian to Rhaetian age; Mortensen et al., 1995). This places the timing of intrusion within the Upper Triassic, within or slightly younger than the time span in which D1 deformation has taken place. Lack of penetrative fabrics or well developed deformation features makes it difficult to determine whether the batholith was intruded pre-, syn-, or post- latest Triassic-earliest Jurassic deformation. D1 tectonic structures within domain [1] are limited to angular conjugate, and chevron type folds that occupy a relatively narrow, northwest trending zone (10's of metres) in

map space and can only be recognized by the reversal of bedding measurements. Because the country rocks demonstrate little evidence of appreciable strain, it is likely that the far more massive and competent Iron Mask batholith would show minimal or no signs of strain if it experienced the same episode of deformation D1.

The Heffley Creek pluton and the Paul Peak stock, Alaskan-type mafic-ultramafic igneous bodies, intrude rocks of the Nicola Group sedimentary facies northeast of the study area (Figure 5.5.1). Both intrusive bodies are interpreted to be Upper Triassic in age, where the Heffley Creek pluton has been dated at 208 ± 6 Ma (U/Pb zircon; Friedman et al., 2002) and the Paul Peak stock, although undated, is inferred to be coeval with the Heffley Creek pluton on the basis of shared lithological similarities, syn-eruptive deformation, and stratigraphic position (Beatty et al., 2006). A study by Friedman et al. (2002) documented that dikes related to the pluton strike northeasterly, and are structurally controlled by a-c fractures formed during F1 folding. A small degree of folding of the dykes is also observed, and S1 foliations, axial to F1 folds, locally transect these dykes. Friedman et al. (2002) noted that the pluton lacks S1 cleavage, except locally along the pluton margins. The above observations suggest syndeformational intrusion of the pluton (Friedman et al., 2002). The deformation event which generated F1 folds and greenschist metamorphism is therefore interpreted to have occurred at circa 208 ± 6 Ma: the crystallization age of the Heffley Creek pluton (Friedman et al., 2002).

Both the Iron Mask batholith and the Heffley Creek pluton are elongate bodies and occupy the boundaries between lithologically dissimilar successions. The Heffley Creek pluton appears to have intruded along the Harper Ranch- Nicola Group unconformity (Ray and Webster, 2000), while the Iron Mask batholith clearly separates eastern volcanic facies rocks from eastern sedimentary rocks of the Dome Hills succession. The contact between these two successions of the Nicola Group is interpreted in this study as a major fault (Section 5.5.1), as the belts have been deformed at different structural levels prior to their juxtaposition.

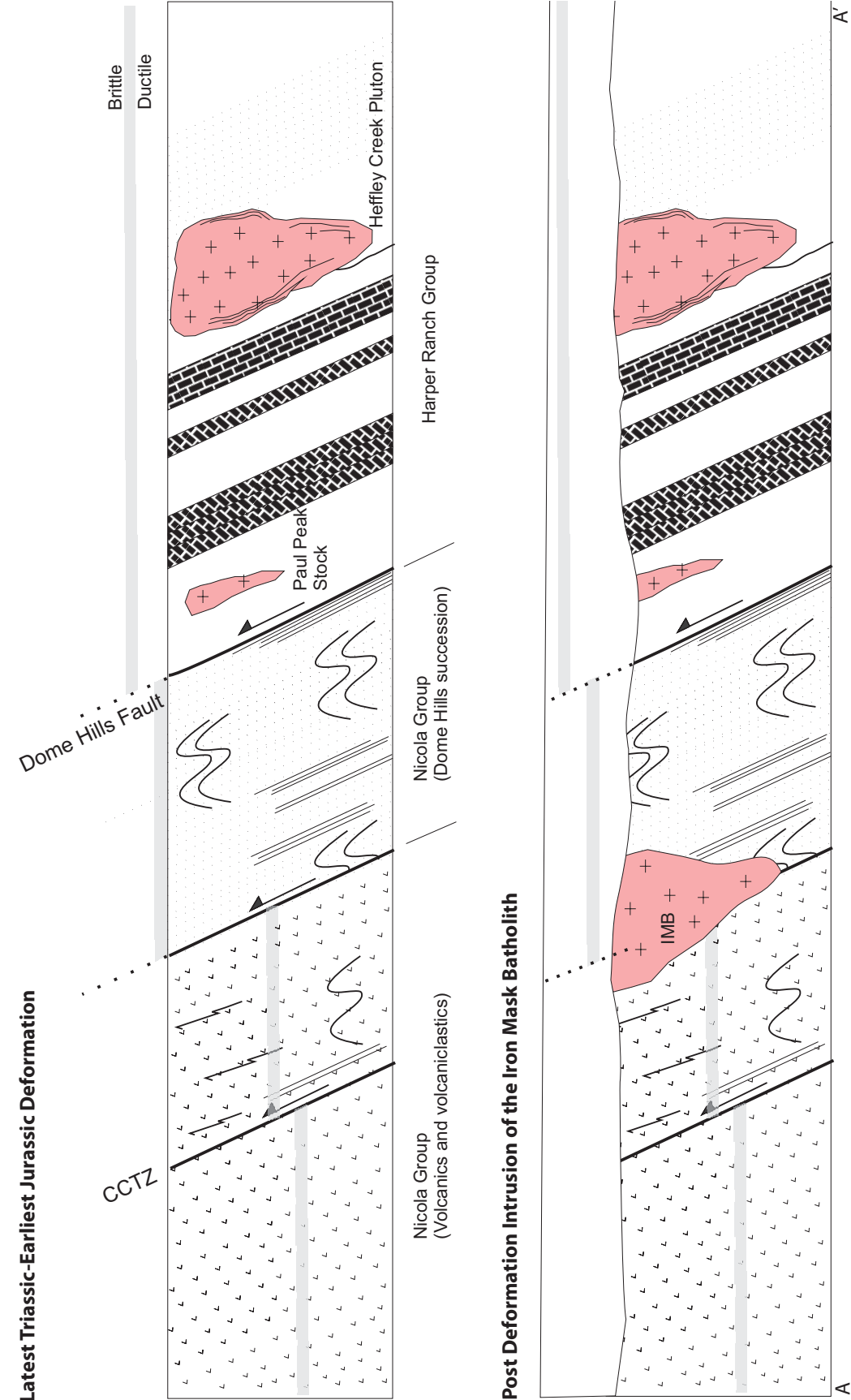


Figure 6.2.1a: Schematic section depicting latest Triassic-earliest Jurassic deformation. Note post deformation emplacement of the Iron Mask batholith (IMB). In this interpretation the IMB was intruded along pre-existing northwest trending fault. Figure 3.5.1 is a reference map for these schematic sections which run southwest-northwest along A-A'.

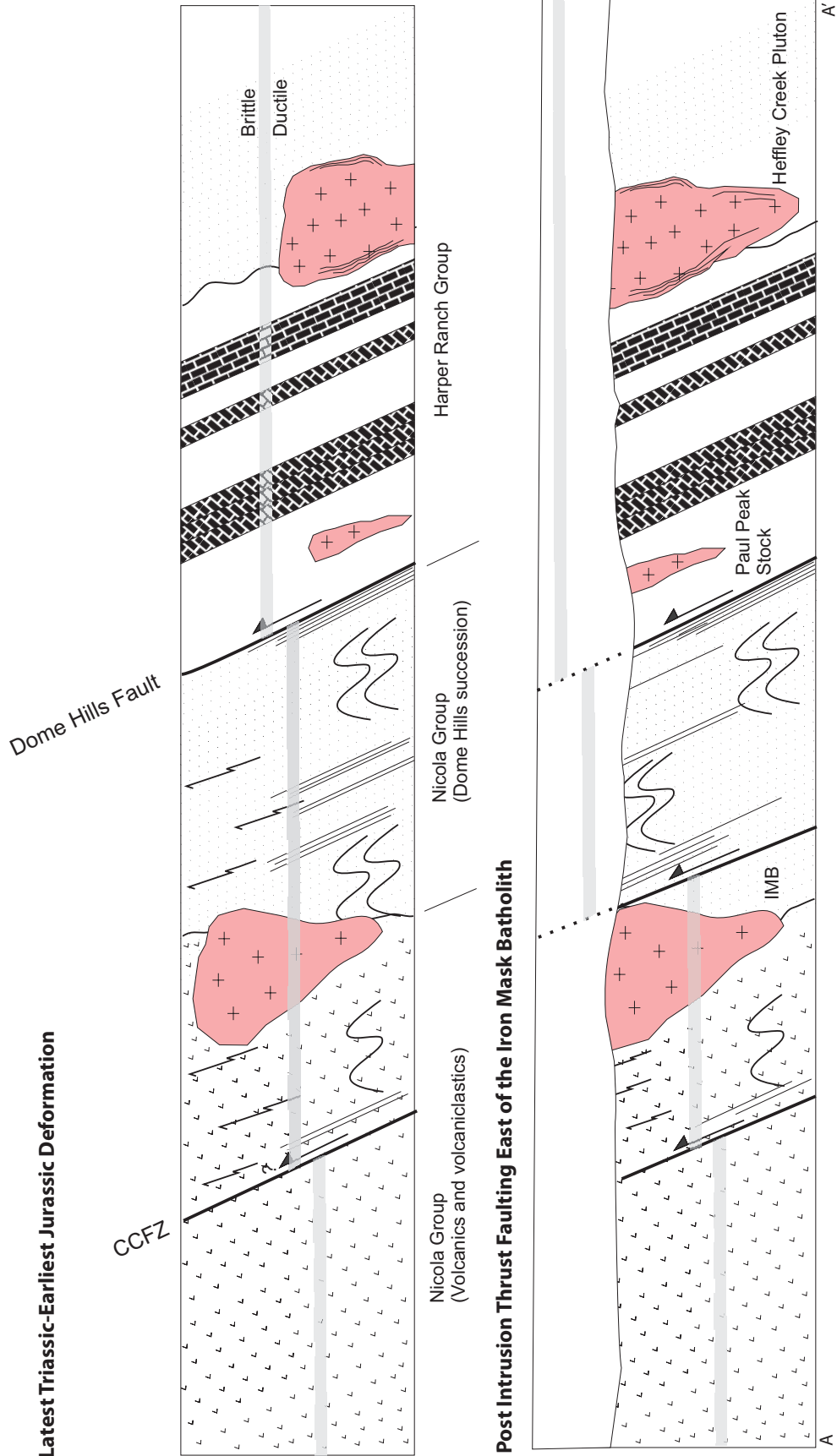


Figure 6.2.1b: Schematic section depicting latest Triassic-earliest Jurassic deformation. In this interpretation the IMB is intruded pre- or syn-deformation. Later, southwest directed thrust faulting occurs east of the Iron Mask batholith

The 204 ± 3 Ma zircon date from the Iron Mask batholith (Mortensen et al., 1995) overlaps, within error, with the crystallization age of the Heffley Creek pluton (208 ± 6 Ma: Friedman et al., 2002) interpreted to have been emplaced during F1 folding and associated greenschist metamorphism of Nicola sedimentary rocks. Along the southern portion of the batholith, the IMB separates the sedimentary facies from the volcanic facies, however in the north rocks of the volcanic belt lie both north and south of the batholith. Because the Iron Mask batholith appears to be undeformed, a few assumptions can be made. (1) Either the batholith was emplaced along the pre-existing northwest striking fault (at least along the southern portion of the fault) and was therefore intruded later than the proposed timing of deformation D1 (Figure 6.2.1a), or (2) the batholith intruded prior to or during D1 but did not undergo observable strain because of the rheological contrasts and deformation style in the upper crustal structural panel (Figure 6.2.1b). D1 has mainly generated an east facing, steeply tilted package of volcanic and volcanoclastic rocks and it is likely that if the IMB has experienced D1, it too would have been tilted steeply to the northeast.

It has been suggested by Logan and Mihalynuk (2005) that the batholith may be folded into a kilometre-scale synform, in which three zones of subvertical faulting, along the northeast and southwest margins and a zone within the body of the batholith, form sheared limbs of the fold. This interpretation is based on the idea that the picrite unit can be used as a marker horizon that is folded into a kilometre scale synform (Logan and Mihalynuk, 2005). Mapping from this study did not support evidence of such folding. The new data suggest that the batholith may be passively tilted to the northeast together with its host stratigraphy.

6.2.3 Southwest Vergent Structures: Omineca Belt

Northeast of Kamloops, Monger and McMillan (1989) reported that southwesterly overturned structures and associated greenschist metamorphism appear to be related

to the tectonic evolution of the adjacent Omineca belt. In that area, the Omineca belt lies immediately east of the Louis Creek fault, which divides the Omineca belt from Intermontane belt to the west (Figure 5.5.1). Nearing the northwest striking Louis Creek fault from the south, Intermontane rocks show strong penetrative foliation and upper greenschist-facies metamorphism (Gabrielse et al., 1991). Within the Omineca belt, north of the fault, similar rock types occur at the same metamorphic grade. Gabrielse et al. (1991) suggested that the structures are congruent with westerly directed, syn-metamorphic structures in metamorphic rocks of the Shuswap region (Brown and Read, 1983) and west verging structures in the Adams Plateau area to the northeast (Schiarizza and Preto, 1987). In the Adams Plateau area, Schiarizza and Preto (1987) interpreted the west vergent structures to be linked to a second phase of deformation that post-dates pre-metamorphic, easterly directed thrust faults. Schiarizza and Preto (1987) interpreted that the west verging deformation event gave rise to the dominant megascopic structure of the area, which relates to northeast dipping thrust faults that separate the major structural and stratigraphic panels. These thrust faults, inferred to have formed in conjunction with the syn-metamorphic folds, appear to post-date most southwest verging folds (Schiarizza and Preto, 1987). Data from this study, linking southwest directed structures in the vicinity of the Iron Mask batholith with congruent structures northeast Kamloops also support earlier proposals that structures within the eastern Intermontane and western Omineca may be congruent.

Structures within the Omineca belt in the Adams Lake region, however, have been attributed to Middle Jurassic deformation (Monger and McMillan, 1989). In the Shuswap region of the Omineca belt, structures have also been assigned a Middle Jurassic age (171-164 Ma) and are presumed to have been formed following the accretion of the Intermontane Superterrane (Brown and Read, 1983). North of Kamloops, in the Quesnel Lake region, east directed thrusting in late Early Jurassic time is recognized, followed by west vergent folding and thrust faulting in the Middle Jurassic (Brown et al., 1986;

Rees, 1987). A similar scenario of east directed imbrication and emplacement followed by west directed folding and thrust faulting is documented just east of Bonaparte Lake map sheet (Schiarizza, 1983), however that author interpreted a Permian –Triassic age of deformation. Field relations between the Permian Harper Ranch Group, Triassic Nicola Group and overlying Jurassic Rossland Group northeast of Kamloops suggest a Late Triassic-earliest Jurassic age for southwest verging structures. Although structures and metamorphic grade appear to be congruent with those of the adjacent Omineca belt, previous studies do not uniformly support coeval formation. Friedman et al. (2002), have recently interpreted that deformation immediately northeast of Kamloops is Late Triassic (208-187 Ma; Section 6.2.1); however they also interpreted the structures as possibly being related to the docking of Quesnellia onto rocks of ancient North America. Alternatively, Beatty (2003) attributed Triassic-Jurassic deformation to the eastward migration of the axis of Nicola magmatism. Thus, despite similarities in structural style, structural attitudes and metamorphic grade, deformation in the southern Intermontane belt is likely older than in the adjacent Omineca belt. One possible explanation for these observations is that southwest directed thrusting was diachronous, whereby the deformation propagated northeastward.

This can be explained in terms of oblique convergence following Late Paleozoic asymmetrical back-arc spreading (Thompson et al., 2006). Thompson et al. (2006) described the possibility that late Paleozoic extension succeeded in cracking the attenuated continental crust but failed to open a bonafide ocean basin in the southern Canadian Cordillera resulting in a dramatic southward narrowing of the Slide Mountain ocean. Accordingly, the return of rifted terranes and the accompanying deformation would have propagated northward throughout the Triassic.

6.3 Tertiary Deformation

Within the study area, the most prominent manifestation of extensional tectonic

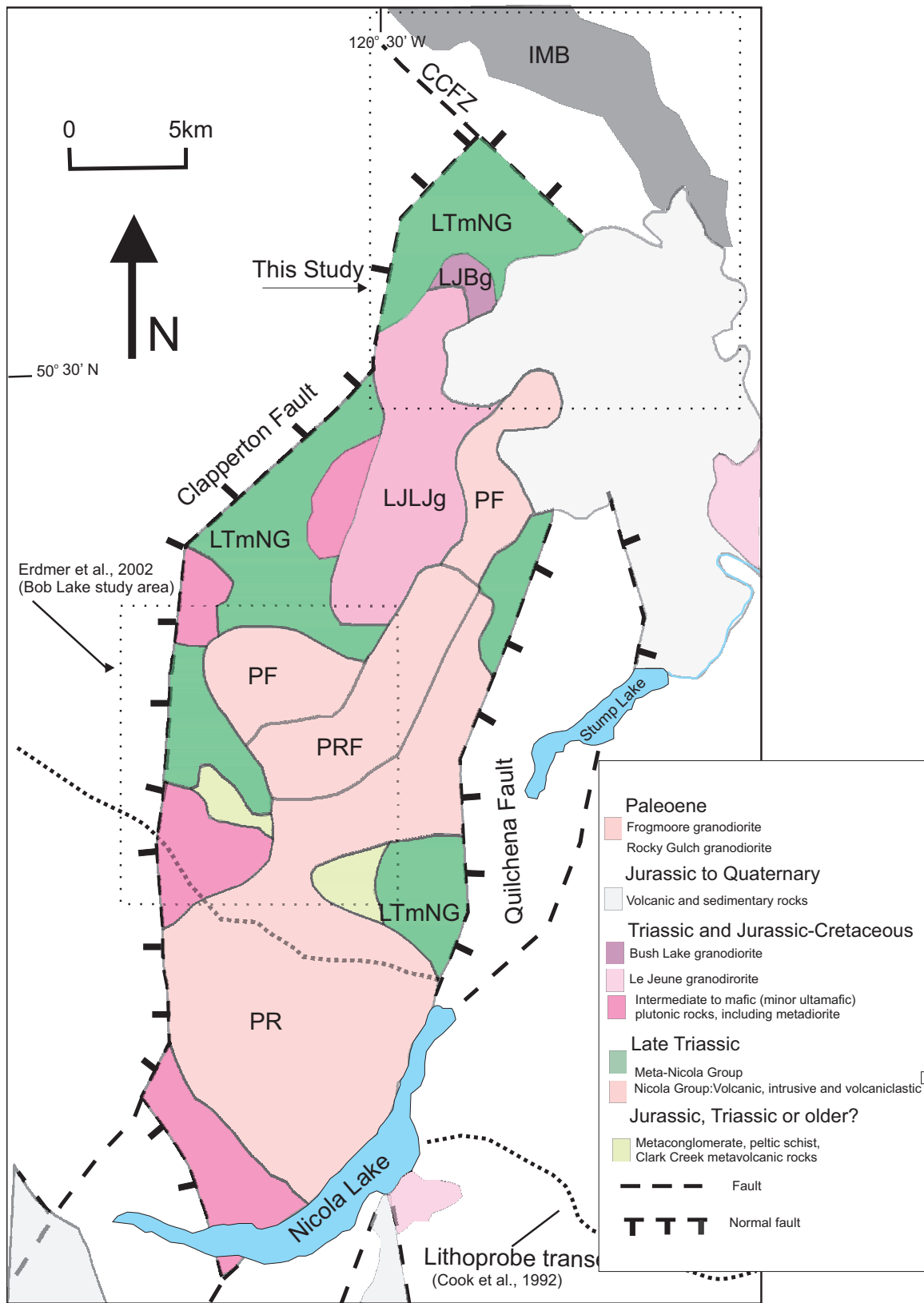


Figure 6.3.1: Geological map of the Nicola horst (modified from Erdmer et al., 2002 and Ghosh, 2003).

activity is demonstrated by the uplift of a block of highly deformed Nicola Group rocks, and younger intrusive phases, from mid-crustal levels. This block is interpreted to be the northern extent of the Nicola horst, a north trending crustal block approximately 40 km in length and bound by Tertiary normal faults (Figure 6.3.1). Ewing (1980) first interpreted the horst as a metamorphic core complex (see Coney et al., 1979).

Early K-Ar thermochronology conducted by Preto et al., (1979), suggested that the Nicola batholith is of Paleocene age. A Rb-Sr study by McMillan et al. (1981), however, suggested that at least some of the intrusive phases are Early Jurassic or older, and concluded that the younger dates most likely represented new magmatic material intruded into older parts of the batholith. McMillan et al. (1981) did, however, state that these dates might possibly represent remobilized older material. Subsequently, Monger and McMillan (1984) concluded that the early Tertiary K-Ar dates and the early Mesozoic (Rb-Sr) dates were most likely a reflection of resetting of the isotopic systems because of depth of burial in early Tertiary time.

In the southern portion of the map area the uplifted block is bounded to the north by the northwest striking Cherry Creek Tectonic Zone and along its western extent by a Clapperton fault. Schistose rocks within the horst can be traced as far south as Nicola Lake, where the north-south striking Clapperton and Quilchena faults bound the horst along its western and eastern margins, respectively. Farther to the south, the bounding faults of the horst have been interpreted to be related to the same deep-seated, regional north and northwest trending fault systems that controlled deposition of Nicola Group volcanic and related sedimentary rocks (Preto, 1977). Preto (1977) recognized that all structures formed within the volcanic and intrusive rocks are dominated by the same northerly trend, which he ascribed to the long-lived system of deep-reaching crustal fractures. If these systems aided in controlling the deposition of Nicola Group strata, these fault systems have been active since at least the Upper Triassic, and have been reactivated to accommodate extensional uplift of the Nicola horst in early Tertiary time.

The elongate, north-south trending shape of the Nicola batholith, also hints at a strong element of structural control.

Monger (1985) attributed development of the Nicola horst to right lateral wrench faulting along the Fraser River Fault system, with the orientations of both the Quilchena and Clapperton faults paralleling the maximum stress direction that can be deduced from the fault geometry near Fraser River. From the map pattern, he predicted that the northwest striking Cherry Creek Tectonic Zone should have both dextral strike-slip and north-block-down reverse fault movements. This study does not support this interpretation and cannot attribute the formation of the horst to motion along the Fraser River fault system. The Cherry Creek Tectonic Zone is interpreted as a normal fault and it therefore seems most likely that this fault and other faults bounding the horst are part of a regional extensional system (Ewing, 1980; Monger and McMillan, 1989; Moore and Pettipas, 1990) as opposed to being directly related to right lateral movements along the Fraser River Fault System.

From the perspective that the highly deformed Nicola Group rocks south of the Cherry Creek Tectonic Zone are in fact part of the Nicola horst it becomes clear as to why there could have been differential uplift along the CCTZ (Section 5.5.3). The original field observations suggest that footwall rocks along the western portion of the CCTZ (south of Afton tailing pond) were deformed within a brittle-ductile regime and those along the eastern portion of the CCTZ (south of Goose Lake) under purely ductile conditions (Section 5.3). Figure 6.3.1 displays the bounding faults of the horst, with the Clapperton fault marking the western boundary of the horst and only the eastern portion of the CCTZ bounding the horst to the north. The original observations, pointing toward differential uplift along the fault (CCTZ), are therefore consistent with greatest displacement along the portion of the fault that accommodated uplift of the central horst.

Tectonic fabrics within the Nicola Horst

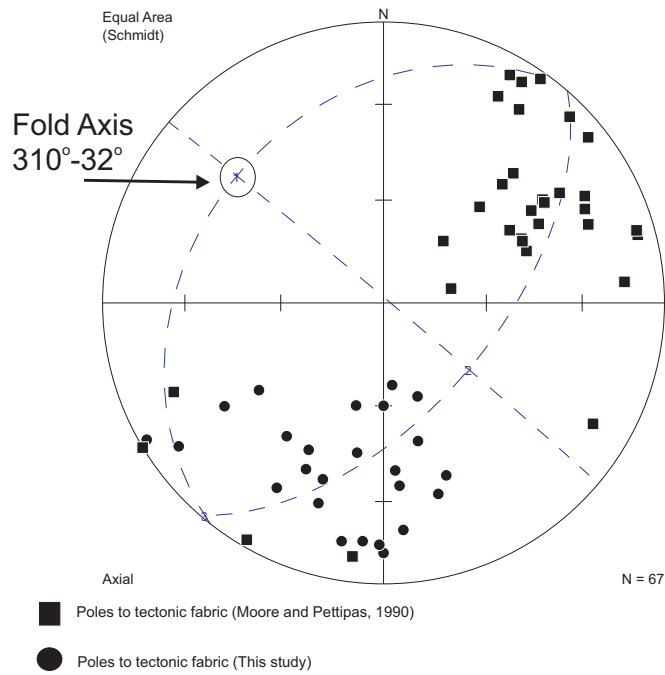


Figure 6.3.2: Stereonet displaying a best fit girdle through poles-to-foliation. The data demonstrates that the tectonic fabric may be folded into kilometre-scale, northwest plunging folds. Data displayed is from this study and that of Moore and Pettipas (1990). See text for details.

Rotation of Lineation to the Horizontal

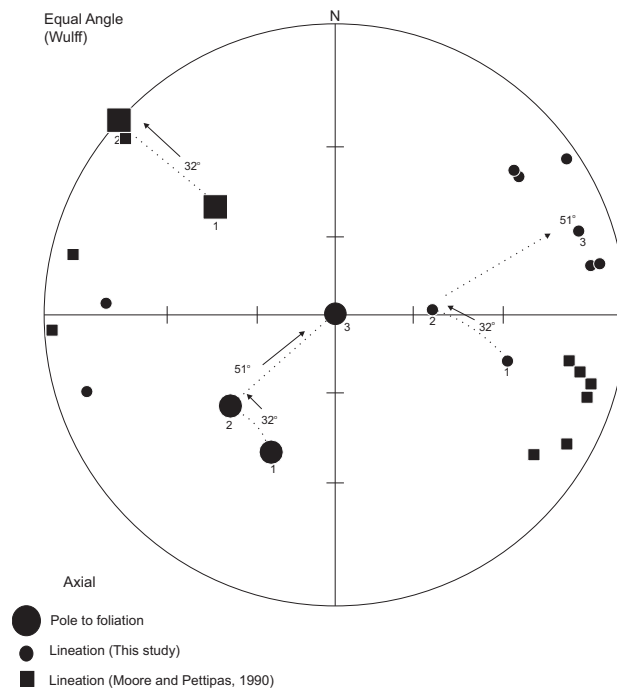


Figure 6.3.3: Stereonet displaying restoration of mineral lineations such that the tectonic fabric they lie parallel to is horizontal (or restored). The figure demonstrates a general east-west orientation of shear along a Late-Jurassic shallow dipping shear zone. Data displayed is from this study and that of Moore and Pettipas (1990). See text for details.

Fabrics within the Nicola Horst: A Tectonic Window

It is clear from structural relationships and radiometric dating of intrusive phases, that the fabrics formed in the Nicola Group rocks within the Nicola horst are older than Tertiary and therefore predate the generation of the horst. Previous workers, including Moore and Pettipas (1990) and Erdmer et al. (2002), have agreed that ductile deformation within the horst (Bob Lake area) is older, predating Tertiary extension, as boundary faults cut the penetrative structural trends (Moore and Pettipas, 1990) that are consistent in orientation across the width of the horst therefore predating its generation (Erdmer et al., 2002). Penetrative ductile fabrics within the study area are correlated with strain fabrics formed in rocks underlying the Bob Lake area due to consistency in the style of deformation. Within the Bob Lake area, Late Triassic metatonalite, meta-Nicola Group rocks and rocks of the Bob Lake assemblage are strongly deformed with respect to the relatively undeformed cross-cutting plutons. In the study area, the northwest striking planar fabric is cross-cut by the 144.8 +/- 5.9 Ma LeJeune granodiorite and the 65 Ma Frogmoore granodiorite (Moore et al., 2000). The D2 deformation episode, generating the strong tectonic fabric, is therefore younger than Late Triassic (age of meta-Nicola Group) but older than the Late Jurassic-Early Cretaceous LeJeune granodiorite and can therefore be constrained to the Jurassic. It should be noted that a younger fabric exists in the Bob Lake area whereby Erdmer et al. (2002) observed that similarly oriented ductile fabrics are formed within a 158-155 Ma feldspar metaporphry and also within a 64 Ma leucogranite. The 64 Ma and 65 Ma plutons (Rocky Gulch and Frogmoore intrusions) however, are not affected.

Previous studies, involving geological mapping of outcrop exposures within the horst, have not recognized large-scale folding of tectonic fabrics (Moore and Pettipas, 1990; Erdmer et al., 2002). The present study, however, has presented evidence that there may in fact be a folding event that has deformed Nicola Group rocks into kilometre-scale northwest plunging folds (Figure 6.3.2). Fabrics vary in orientation along the horst. In the

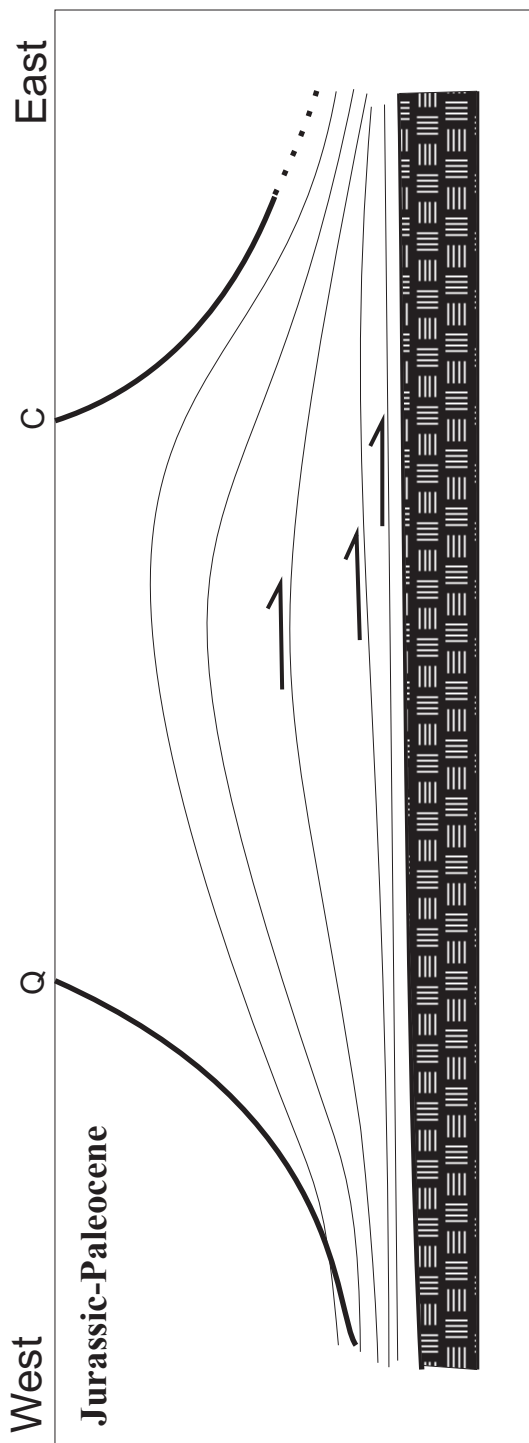


Figure 6.3.4.a



Figure 6.3.4.b

Figure 6.3.4 a,b: (a): Schematic section running east-west through the Nicola horst. The section shows Late Jurassic east directed compression, generating a broad shear zone within middle crustal rocks of the Nicola Group (Q = Quilchena Fault; C = Clapperton Fault). Protracted east-directed compression during Jurassic-Paleocene Cordilleran deformation generated kilometre scale folding (F3) of the shear zone by thrust stacking of middle crustal rocks below the arched reflectors. (b): Schematic section running east-west through the Nicola horst. Tertiary extension generated uplift of the Nicola Horst. The section displays reactivation of brittle Tertiary faults bounding the horst to accommodate uplift. Faults cross-cut Mesozoic compressional fabrics (Figure modified from Cook et al., 1992: See text for details).

Bob Lake region, southwest dipping foliations associated with a west plunging lineation are formed within meta-Nicola Group rocks across the width of the horst (Moore and Pettipas, 1990; Erdmer et al., 2002).

Using data from this study and Moore and Pettipas (1990) it can be shown that the fabric folds about a shallow, northwest plunging axis, and the layer parallel lineation rotates about the same axis (Figure 6.3.3). By “unfolding the fold” the lineation should lie somewhere near (or on) the primitive when the tectonic fabric is restored. The rotations are demonstrated in figure 6.3.3. The lineation lies closely in an east-west orientation, although there is some spread. Several factors can contribute to spread in the data. (1) The orientation of the fold axis chosen for the rotation may not be accurate. (2) The lineation is not parallel with the fabric everywhere, or is not consistently oriented. (3) The shear surface was not originally planar. (4) Paleocene faulting has reoriented tectonic fabrics. Previous workers have suggested that tectonic fabrics in the horst may represent an originally shallow dipping ductile shear zone (Erdmer et al., 2002) therefore the folded shear zone may have been originally sub-horizontal to shallow dipping with movement oriented east-west. In the study area shear sense indicators demonstrate a consistent east directed (compressional: top-to-the-east) sense of shear, however further south studies show a mix of shear senses (Erdmer et al., 2002, Moore and Pettipas, 1990). Moore and Pettipas (1990) noted that a mix of shear senses and strong flattening is consistent with a compressional regional stress field.

Large-scale folding within the Nicola horst has been interpreted from seismic reflection data. Cook et al. (1992) presented a crustal profile through the central Nicola horst and noted that the horst is characterized by an overall antiformal pattern of reflections. In the interpretation of the seismic data Cook et al. (1992) depicts the surfaces as compressional structures, with associated bounding faults of the horst truncating the folded reflectors.

Moore (2000) suggested that early strain features and the presence of slices of

exotic rocks between Nicola facies belts suggest significant early contraction in the horst. In the Bob Lake region, Erdmer et al. (2002) interpret the fabrics to represent an originally shallow dipping ductile shear zone. The original fabric may represent a (mid?) Jurassic broad ductile shear zone, formed during eastward translation of the Nicola arc during D2. Continued contraction (D3), during eastward tectonic convergence, most likely generated kilometre scale folding (F3) of the shear zone by imbrications of thrust sheets below the arched reflectors (Figure 6.3.4a,b). West of Kamloops, there is evidence of east directed thrusting within rocks of the Ashcroft Formation. This thrusting has been suggested to have taken place in the Middle Jurassic (Travers, 1978). The younger fabric, observed in the Bob Lake area (Erdmer et al., 2002), may represent relatively narrow Paleocene shear zones that overprint small zones throughout the broad Jurassic shear zone. It is interpreted that the deformation event that generated this younger fabric was not the main deformation event generating the strong penetrative fabrics seen throughout the horst as Late Jurassic-Early Cretaceous LeJeune and Paleocene Frogmoore plutons remain relatively undeformed (e.g. not affected by D2).

Fabric near the CCTZ is observed to be folded into both F3a northwest and F3b northeast trending folds. The F3a,b folds have varied orientations and their relative chronology could not be determined for lack of cross-cutting features. Folding in the footwall of the CCTZ occurred prior to uplift of the Nicola horst (D4) because Nicola Group rocks in the hanging wall are not folded. The geometry of the F3a,b folds produced at Rush Lake and south of the Afton tailings pond have orientations that suggest tilting following folding (see Section 5.5.2 for details). By removing the plunge from the folds a general orientation of the maximum compression direction during (D3?) can be determined. It is interpreted that a general east-west directed compression event most likely generated the F3a,b folds that have later been tilted. Because of their close proximity to the CCTZ, it is interpreted that D4 Tertiary uplift, along the CCTZ most likely tilted and reoriented the folds. The relationship of these smaller folds to large-scale

regional folds is unclear.

6.4 References

- Beatty, T.W. 2003. Stratigraphy of the Harper Ranch Group and tectonic history of the Quesnel terrane in the area of Kamloops, British Columbia. M.Sc. thesis, Simon Fraser University, Burnaby, B.C. 213 p.
- Beatty, T.W., M.J. Orchard, and P.S. Mustard. 2006. Geology and tectonic history of the Quesnel terrane in the area of Kamloops, British Columbia. In: M. Colpron, J. Nelson (Editors), *Paleozoic Evolution and Metallogeny of Pericratonic Terranes at the Ancient Pacific Margin of North America. Geological Association of Canada, Special Paper 45: 483-504.*
- Brown , R. L., C. Beaumont, and S.D. Willett. 1993. Comparison of the Selkirk fan structure with mechanical models: Implications for interpretation of the Southern Cordillera. *Geology* 21: 1015-1018.
- Brown , R. L., J.M. Journeay, L.S. Lane, D.C Murphy, and C.J. Rees. 1986. Obduction, backfolding and piggyback thrusting in the metamorphic hinterland of the southeastern Canadian Cordillera. *Journal of Structural Geology* 8, no. 3/4: 255-268.
- Brown, R. L., and P.B. Read. 1983. Shuswap terrane of British Columbia: A Mesozoic “core complex”. *Geology* 11: 164-168.
- Colpron, M., J.L. Nelson, and D.C Murphy. 2006. A tectonostratigraphic framework for the pericratonic terranes of the northern Canadian Cordillera. In: M. Colpron, J. Nelson (Editors), *Paleozoic Evolution and Metallogeny of Pericratonic Terranes at the Ancient Pacific Margin of North America. Geologic Association of Canada, Special Paper 45: 1-24.*
- Coney, P.J. 1979. Tertiary evolution of Canadian metamorphic core complexes, in Armentrout, J.M., Cole, M.R., TerBest, H., Jr, Editors, *Cenozoic paleogeography of the western United States: Pacific section*, Soc. Econ. Paleontol. Mineral., Sacramento CA.: 14-28.

- Cook, F.A., J.L. Varsek, R.M. Clowes, E.R. Kanasewich, C.S. Spencer, R.R. Parrish, R.L. Brown, S.D. Carr, B.J. Johnson and R.A. Price. 1992. Lithoprobe crustal reflection cross section of the southern Canadian Cordillera, 1, foreland thrust and fold belt to Fraser River fault. *Tectonics*, **11**, no.1: 12-35.
- Erdmer, P., Moore, J.M., L. Heaman, R.I. Thompson, K.L. Daughtry, and R.A. Creaser. 2002. Extending the ancient margin outboard in the Canadian Cordillera: record of Proterozoic crust and Paleocene regional metamorphism in the Nicola horst, southern British Columbia. *Canadian Journal of Earth Sciences* 39: 1605-1623.
- Ewing, T.E. 1980. Paleogene tectonic evolution of the Pacific Northwest. *Journal of Geology* 88: 619-638.
- Friedman, R., G. Ray, and I. Webster. 2002. U-Pb zircon and titanite dating of intrusive rocks in the Heffley Lake area, south-central British Columbia, in Geological Fieldwork. *B.C. Ministry of Energy and Mines, Paper 2002-1*: 109-118.
- Gabrieise, H., J.W.H. Monger, D.J. Tempelman-Kluit, and G.J. Woodsworth. 1991. *Part C. Intermontane Belt (Chapter 17) Gabrielse, H. and Yorath, C.J., Editors, Geology of the Canadian Orogen in Canada: Geological Survey of Canada, Geology of Canada, no. 4.*
- Logan, J.M., and M.G. Mihalynuk. 2005. Porphyry Cu-Au Deposits of the Iron Mask Batholith Southeastern British Columbia: In Geological Fieldwork 2004. *British Columbia Geological Survey Branch, Paper 2005-1.*
- McMillan, W.J., Armstrong, R.L. Harakal, J. 1981. Age of the Coldwater Stock and Nicola Batholith, near Merritt (92H). *British Columbia Department of Mines and Petroleum Resources, Geological Fieldwork*: 102-105.
- Malavieille, J. 1984. Modelisation experimentale des chevauchements imbriques: Application aux chaines de montagnes: Societe Geologique de France, Bulletin, ser. 7-26.
- Monger, J.W.H. 1985. Structural evolution of the southwestern Intermontane belt,

- Ashcroft and Hope map areas, British Columbia; in Current Research, Part A. *Geologic Survey of Canada, Paper 85-1A*: 349-358.
- Monger, J.W.H., and W.J. McMillan. 1989. Geology, Ashcroft, British Columbia (92 I). Geological Survey of Canada, Map 42.
- Monger, J.W.H., and R.A. Price. 1979. Geodynamic evolution of the Canadian Cordillera-Progress and problems. *Canadian Journal of Earth Sciences* 16: 770-791.
- Monger, J.W.H., R.A. Price, and D.J. Tempelman-Kluit. 1982. Tectonic accretion and the origin of the two major metamorphic and plutonic belts in the Canadian Cordillera. *Geology* 10: 70-75.
- Moore, J.M. 2000. Nicola Horst, southern British Columbia: window into the pre-Triassic margin of North America. *Geological Survey of Canada. Current Research 2000-A16*: 6 p.
- Moore, J.M., and A.R. Pettipas. 1990. Geological studies in the Nicola Lake region (92 I/SE); Part A. In Nicola Lake region geology and mineral deposits. *British Columbia Geological Survey Branch, Open File 1990-29*.
- Moore, J.M., J.E. Gabites, and R.M. Friedman. 2000. Nicola Horst: toward a geochronology and cooling history. In Cook, F. and Erdmer, P. (Compilers). Slave-Northern Cordillera Lithospheric Evolution (SNORCLE) Transect and Cordillera Tectonic Workshop Meeting, February 25-27.2000. *University of Calgary*, no. Lithoprobe Report No. 72: 177-185.
- Mortensen, J.K., D.K. Ghosh, and F. Ferri. 1995. U-Pb geochronology of intrusive rocks associated with copper-gold porphyry deposits in the Canadian Cordillera; In Porphyry Deposits of the Northwestern Cordillera of North America, Schroeter, T.G., Editor. *Canadian Institute of Mining, Metallurgy and Petroleum Special Volume 46*: 142-158.
- Okulitch, A.V. 1984. The role of the Shuswap metamorphic complex in Cordilleran

- tectonism: a review. *Canadian Journal of Earth Sciences* 21: 1171-1193.
- Oxburgh, E.R. 1982. Heterogeneous lithosphere stretching in early history of orogenic belts, in Hsu, K.J., editor, *Mountain Building Processes*: Academic Press, London: 85-93.
- Preto, V.A. 1977. The Nicola Group: Mesozoic volcanism related to rifting in Southern British Columbia. *Geological Association of Canada*. Special paper 16: 39-57.
- . 1979. Geology of the Nicola Group between Merritt and Princeton, British Columbia. *British Columbia Ministry of Energy, Mines and Petroleum Resources*, no. Bulletin 69: 90.
- Price, R.A. 1986. The southeastern Canadian Cordillera: Thrust faulting, tectonic wedging, and delamination of the lithosphere. *Journal of Structural Geology* 8: 239-254.
- Ray, G.E., and I.C.L. Webster. 2000. The Heff Prospect at Heffley Lake, South-Central B.C.(09INE096): An unusual example of a mafic-ultramafic-related Cu-Au-Ree-bearing magnetite skarn: in *Geological Fieldwork 1999*. *British Columbia Geological Survey Branch, Paper 2000-1*.
- Rees, C.J. 1987. The Intermontane-Omineca belt boundary in the Quesnel Lake area, east-central British Columbia: tectonic implications based on geology, structure and paleomagnetism. Ph.D thesis, Carlton University.
- Schiarizza, P. 1983. Geology of the Barriere River-Clearwater area; British Columbia Ministry of Energy, Mines and Petroleum Resources, Preliminary Map. 53.
- Schiarizza, P., and V.A. Preto. 1987. Geology and mineral deposits of the Adams Plateau-Clearwater-Vavenby area. *British Columbia Ministry of Energy, Mines and Petroleum Resources*. Paper 1987-2: 88 p.
- Smith, R. 1979. Geology of the Harper Ranch Group and Nicola Group northeast of Kamloops, British Columbia. University of British Columbia; M. Sc. thesis.
- Struik, L.C. 1987. The ancient western North America margin: An alpine rift model for

the east-central Canadian Cordillera. *Geologic Survey of Canada, Paper 87-15*: 19.

Thompson, R.I., P. Glombick, P. Erdmer, L. Heaman, and Y. Lemieux. 2006. Evolution of the ancestral Pacific margin, southern Canadian Cordillera: Insights from new geologic maps. In: M. Colpron, J. Nelson (Editors), *Paleozoic Evolution and Metallogeny of Pericratonic Terranes at the Ancient Pacific Margin of North America. Geologic Association of Canada, Special Paper 45*: 433-482.

Travers, W.B. 1978. Overturned Nicola and Ashcroft strata and their relations to the Cache Creek Group, southwestern Intermontane Belt, British Columbia. *Canadian Journal of Earth Sciences* **15**: 99-116.

Unterschutz, J., R.A. Creaser, P. Erdmer, R.I. Thompson, and K.L. Daughtry. 2002. North America margin origin of Quesnel terrane strata in the southern Canadian Cordillera: inferences from geochemical and Nd isotopic characteristics of Triassic metasedimentary rocks. *Geological Society of America Bulletin* **114**: 462-475.

Willett, S.D., C. Beaumont, and P. Fullsack. 1993. mechanical model for the tectonics of doubly vergent compressional orogens. *Geology* **21**: 371-374.

Chapter 7: Conclusions

- 1.) Upper Triassic Nicola Group rocks underlying the Kamloops region can be divided into at least two distinct volcanic facies, an intermediate (fan or apron) facies and a distant, back-arc basin facies. These facies were deposited in at least two different depositional environments respectively: (1) A transitional submarine to subaerial environment, dominated by fine to coarse grained pyroclastic units and reworked equivalents and (2) a relatively deeper marine basin characterized by mudstone, laminated mudstone and siltstone, fine grained sandstone and minor basaltic flows.
- 2.) Rocks of the Nicola Group are largely unmetamorphosed. Contact metamorphism occurs in host Nicola Group rocks along the margins of Jurassic plutons/dykes and metamorphic fabrics are formed locally along shear zones. Exceptions occur in the Nicola horst and north of the Iron Mask batholith (IMB) within the Dome Hills succession of the Nicola Group. Rocks are penetratively deformed south of the Cherry Creek Tectonic Zone and rocks are regionally metamorphosed to an amphibolite facies south of the CCTZ and to a greenschist-amphibolite transitional facies north of the IMB.
- 3.) At least four deformation episodes are recognized in the Kamloops region:
 - a. Late Triassic-Early Jurassic (D1): D1 deformation generated southwest directed F1 folds, S1 axial planar foliations and associated thrust faults. These structures give rise to the area's map pattern, as northwest striking faults separate and bound northwest trending structural-stratigraphic panels. This deformation period was followed by a period of uplift and exhumation prior to deposition of the Jurassic Rossland Group.
 - b. (Mid?) Jurassic (D2): A Middle Jurassic broad shear zone is interpreted

to have formed by east-directed translation of the Nicola arc during contractional tectonics inboard of an east dipping subduction zone.

- c. Jurassic-Paleocene (D3): Protracted east-directed compression during Jurassic-Paleocene deformation generated kilometre scale folding (F3) of the shear zone. This deformation may have generated F3a,b folds, where tectonic fabric is folded by northwest and northeast plunging folds. These folds may be related to kilometre-scale F3 folding in the Nicola horst.
- d. Tertiary (D4): The Cherry Creek Tectonic Zone marks the northern extent of the Nicola horst, the most prominent manifestation of Tertiary extension in the region. In the study area the horst is bounded by the Clapperton fault along its western margin and the Cherry Creek Tectonic Zone marks its northern extent. Uplift was accommodated by reactivation of pre-existing faults to form a regional extensional system. Tectonic and erosional exhumation was succeeded by deposition of Miocene continental flood basalts.

4.) The Nicola Group is dominated by deep-seated north and northwest striking faults that have been active at least since pre- Late Triassic, as they control deposition of the Nicola Group and intrusive phases of the IMB. These faults, including the Cherry Creek Tectonic Zone, have been reactivated multiple times in their geologic history, during episodes of Mesozoic compression (D1) and Tertiary extension (D4).

5.) The IMB plugs the boundary between rocks deposited in two distinct depositional environments (see (1)). It also marks the boundary between rocks that have been deformed at different structural levels. As such it is interpreted to plug a northwest striking fault system that has juxtaposed the lithologically and structurally

dissimilar belts. This fault system has most likely accommodated southwest directed compression during D1, and as such is interpreted as a thrust fault.

- 6.) Data collected in this study do not support the hypothesis of kilometre-scale folding of the Iron Mask batholith. Its host Nicola Group rocks have dominantly been tilted into an east-facing, steeply dipping monocline during Late Triassic-Early Jurassic deformation. If the batholith “saw” the D1 episode, it would most likely have been tilted steeply to the east, along with its host strata.
- 7.) During D4, there was at least 9 km of vertical displacement along bounding faults (CCTZ and Clapperton fault) of the Nicola horst in order to explain the difference in metamorphic grade across these faults.
- 8.) Uplift of the Nicola horst was accommodated by differential uplift along the CCTZ, whereby displacement on the CCTZ may decrease to the west from a maximum magnitude south of Goose Lake.

Appendix 1

Element	Standard	Locality	Block	Source		Bgds BG – BG+
Na Ka	Albite	Casadero, California	639	U of A collection		0 3
Al Ka	Anorthite	Great Sitkin Island, Al	EPS1	Smithsonian Inst.	Jarosewich , 2002	0 2
S Ka	Barite		639	U of A collection		-2 2
Ca Ka	Diopside	Wakefield, Quebec	639	U of A collection		-2 3
Mg Ka	Fo93		EPS1	U of A collection		0 3
Fe Ka	Hematite	Elba, Rio Marina Mine, Italy	639	U of A collection		-2.6 1.5
Ti Ka	Ilmenite	Ilmen Mnts., Russia	EPS1	Smithsonian Inst.	Jarosewich , 2002	-2 2
Si Ka	Plagioclase	Lake City, Oregon	EPS1	Smithsonian Inst.	Jarosewich , 2002	0 3
K Ka	Orthoclase		EPS1	U of A collection		-2 2
Cl Ka	Tugtupite		639	U of A collection		-2 2
Mn Ka	Willemite	Frankline Furnace, OH, USA	639	U of A collection		0 1.5

Standards used for electron microprobe calibration

